NTNU – Trondheim
Norwegian University of
Science and Technology

Estimation of Z-R relationship and comparative analysis of precipitation data from colocated rain-gauge, vertical radar and disdrometer

Isabel Cyr

Civil and Environmental Engineering (2 year)
Submission date: June 2014
Supervisor: Knut Alfredsen, IVM
Co-supervisor: Yisak Abdella, SINTEF Energy Research
Kolbjørn Engeland, NVE

Norwegian University of Science and Technology
Department of Hydraulic and Environmental Engineering

THE NORWEGIAN UNIVERSITY FOR SCIENCE AND TECHNOLOGY (NTNU)

Department of Hydraulic and Environmental Engineering

MSc Thesis

in

Hydraulic Engineering

Candidate: **Isabel Cyr**

Topic: **Estimation of Z-R relationship and comparative analysis of precipitation data from colocated rain-gauge, vertical radar and disdrometer**

1. Background

Quantitative precipitation is not directly measured by weather radars but is estimated from measurements of radar reflectivity factor (Z), which is proportional to the energy backscattered by precipitation particles. The conversion of the radar reflectivities measured aloft to precipitation rates (R) at the ground is a complex task. Both the reflectivity measurements themselves and the process of converting them to precipitation rates are subject to errors and uncertainties. One of the main sources of error in the conversion process is the limited spatial and temporal representativeness of a fixed radar reflectivity– precipitation rate (Z–R) relationship used for conversion. The reflectivity measurements from the national network of C-band Doppler radars in Norway are operationally converted to precipitation rates using a fixed Z-R relationship which was derived from the drop size distribution measured for stratiform rain at a different geographic location. However, various studies have documented that Z-R relationships can vary geographically, with precipitation phase, with precipitation intensity, from storm to storm, and even within the same storm. Both Z and R depend on the drop size distribution (DSD) and theoretically the relationship between Z and R is not unique. There is therefore a potential for improving radar precipitation estimates by applying variable Z-R parameters that depend on precipitation events' storm types, as convective and stratiform, and precipitation phase.

2. Main questions for the thesis

The main objective of this study is to estimate storm type and precipitation phase dependent Z-R parameters from optical disdrometer (OTT Parsivel) and Micro Rain Radar (MRR) measurements which can be used to convert Z values extrapolated from C-band radar measurements. Both instruments are placed on the ground and measure DSD. Since both Z and R depend on the DSD, Z-R

parameters can be estimated from these instruments. These parameters can then be used to convert Z values from the C-band radar which have been corrected for other sources of error and extrapolated to the same elevation as the DSD measuring instrument. However, the DSD instruments are dependent on certain assumptions to derive precipitation rate from DSD measurements. In order to efficiently utilize DSD instruments for estimation of Z-R parameters, it is important to understand the differences between these instruments and other conventional rain-gauges. In view of this, a secondary objective of the study is to evaluate the quantitative precipitation values estimated from OTT Parsivel and MRR.

Measurements from the instruments installed at Risvollan and from the C- band radar mounted in Rissa will be used for the analysis. Risvollan ground station is located within the coverage of Rissa radar. The tasks included in the study are described below.

a) Define the criteria for the beginning and end of a precipitation event and divide the precipitation series at Risvollan and Meltingen into separate events.

b) Develop a method for identifying the precipitation phase at the ground stations and determine the transition temperature between liquid and solid precipitation.

c) Apply a method for classifying storm types (stratiform and convective).

d) Classify the events according to storm type, precipitation phase and season. If necessary divide each event into sub-events.

e) Estimate Z-R parameters for each class and separately for each event in each class.

f) Estimate accumulated precipitation from the OTT Parsivel and MRR.

g) Compare the accumulated precipitation values from the different instruments (OTT Parsivel, MRR and tipping-bucket rain-gauge) and analyze the characteristics of the differences and how they depend on storm type and precipitation phase.

h) Compare the reflectivity measurements from the MRR with the corresponding measurements (i.e. at the same elevation level) from the C-band radar.

3. Supervision

Formal Supervisor: Professor Knut Alfredsen, NTNU

Supervisors: Research Scientist Yisak Sultan Abdella, SINTEF

Dr. Kolbjørn Engeland, NVE

The candidate is responsible for collecting, structuring and using data. Assistance and cooperation with others should be referenced in the report.

4. Report format

Professional structuring of the report is important. Assume professional senior engineers as the main target group. The report shall include a summary, offering the reader the background, the objective of the study and the main results. The thesis report shall be using NTNU's standard layout for Thesis work. Figures, tables, etc shall be of good report quality. Table of contents, list of figures, list of tables, list of references and other relevant references shall be included. The complete manuscript should be compiled into a PDF file and submitted electronically to DAIM for registration, printing and archiving. Three hard copies, in addition to the students own copies, should be printed out and submitted. The entire thesis may be published on the Internet as full text publishing. All documents and data shall be written on a CD thereby producing a complete electronic documentation of the results from the project. This must be so complete that all computations can be reconstructed from the CD.

Finally, the candidate is requested to include a signed statement that the work presented is his own and that all significant outside input has been identified.

The thesis shall be submitted no later than **Monday 30 June, 2014**

Department of Hydraulic and Environmental Engineering, NTNU

Knut Alfredsen

Professor

PREFACE

I would like to thank my formal supervisor, Knut Alfredsen, for proposing me this project, in collaboration with SINTEF and NVE, that suited very well my study interest and academic background. He has constantly supported my work and provided data, information and advices when needed.

My grateful thanks go to my two supervisors, Yisak Sultan Abdella, research scientist at SINTEF Energy and Dr. Kolbjørn Engeland, senior researcher at NVE, section Hydrological Modelling.They have both provided me data, processing and analysis tools, adapted scripts, useful advises and proposals on data processing, adjustments and analysis, constructive comments on results reporting and conclusions, as well as encouragements and tight follow-up of all steps in the project. Their scientific and technical help and guidance through the semester, whenever it was needed, and even before I asked for it, were very appreciated.

A CD containing all required processed data used in this project, together with analysis tables and plots is attached to this report.

Isabel Cyr
Trondheim, June 30th 2014

ABSTRACT

The estimation of precipitation rates and accumulations constitutes an essential input data for distributed hydrological models and for many hydrometeorological applications, such as short term hydro-scheduling, forecasting and monitoring of river floods and inflow forecasting into a catchment, its peak flow and response time. In order to improve quantitative precipitation estimates from C-band weather radar, variable Z-R relationships that represent the local precipitation characteristics and conditions are derived from measured precipitation drop size distribution (DSD) by two ground-based instruments: vertical pointing Doppler radar MRR and the optical disdrometer OTT Parsivel. The variability and robustness of those local Z-R relationships are analyzed, as well as their level of dependency to the storm type (stratiform, convective, air mass convection), to the precipitation phase (rain, snow, mixed precipitation), to each event and to each month. Comparative analysis of the precipitation accumulations measured or estimated by three different local instruments (tipping bucket rain gauge, disdrometer OTT Parsivel, vertical pointing radar MRR) is also performed in order to assess under which conditions those instruments are able to provide reliable precipitation rates and robust local Z-R relationships.

MRR provides the most variable and uncertain local Z-R parameters that are highly dependent on the precipitation phase. This dependency leads to high event-to-event variability of DSD-measured Z-R relations and large differences in estimated precipitation rates and accumulations (especially for snow) between the local instruments and compared to precipitation values estimated from the weather radar, using the standard Z-R relationship. The optical disdrometer OTT Parsivel provides the most stable and robust Z-R parameters that are independent of the precipitation phase and the season. In the only case of rain events, both instruments derive similar local Z-R parameters that are comparable to the standard Z-R relationship. The high variability and uncertainty related to Z-R parameters concern mainly mixed precipitations. There is no evident dependency of Z-R parameters on storm type.

When comparing the three local precipitation instruments, they all provide similar rain accumulations. In cases of snow and mixed precipitation, accumulations derived from those

instruments are quite different. However, the disdrometer OTT Parsivel and the tipping bucket rain gauge agree relatively well in terms of accumulations. In addition that OTT Parsivel may provide robust local Z-R relationships for any kind of precipitation that correspond well to standard Z-R relationship, it may compensate for precipitation losses, catch deficit and low temporal resolution of the conventional rain gauge. However, long periods of instrument instability and breakdowns for the disdrometer reduce significantly the number of valid precipitation data available at any time of the year and any precipitation conditions, hence the data representativity of this instrument. In case of MRR, more investigations and possibly better measurement filtering and correction prior to the precipitation estimation may reduce the uncertainties around the MRR-derived Z-R parameters and precipitation estimates.

TABLE OF CONTENTS

LIST OF FIGURES

LIST OF TABLES

1 INTRODUCTION

1.1 Background and motivation

Precipitation events, as well as earthquakes and avalanches, constitute a relaxation process in a non-equilibrium state that may occur in a wide range of conditions (different number, type, size, intensity and duration of events) and contribute differently to the total amount of precipitation over a region. This high temporal and spatial variability of precipitation is not always totally captured and recorded by the conventional precipitation collectors, such as rain gauges. Specific weather conditions around those types of instrument (evaporation, wind-induced turbulence), their relative low sensitivity and insufficient resolution (sparse distribution over the watershed, large or irregular time interval between data capture and recording) make the analysis of light precipitation or single events quite impossible (Peters et al., 2001; Vieux, 2013; Peter et al., 2002; Dutta et al., 2012). Nonetheless, in certain contexts, such as urban or small basins, complex terrain in lower altitudes or sharp terrain gradients, water resource decision makers are constantly searching for accurate, reliable and high-resolution data on the amount, distribution and variability of precipitation events. They search for data that represent adequately the watershed and the hydrological/hydraulic characteristics of the region.

In this context of high-quality data requirements, time series of precipitation measurements or estimates (in real time or historical data series) constitute an essential input data for numerical weather-prediction modelling, distributed hydrological modelling and for many hydrometeorological applications (Chandrasekar & Cifelli, 2012; Vieux, 2013; Sanchez-Diezma et al., 2001; Dutta et al., 2012; Vieux & Bedient, 1998; Germann et al., 2006):

- for nowcasting and monitoring precipitation,
- for forecasting of inflow into a catchment and calculation of the catchment's peak flow and response time,
- for forecasting, monitoring and warning of land or river flooding and upstream flash floods,
- for short term hydro-scheduling and other hydropower operational planning,
- for model calibration,

- for water and heat balance studies.

Besides the conventional rain gauges, there are other types of instruments measuring or estimating the precipitation intensity and distribution/patterns. Today, many countries use the weather radar as the central part of an operational system providing nationwide high-resolution ground precipitation products derived from radar measurements of precipitation particles, previously corrected from a series of systematic and random errors induced by the atmospheric, terrain, precipitation and radar conditions. In addition to providing new information on the movement and evolution of the precipitating system, those radar products contribute to improve the accuracy and spatio-temporal coverage (wider area covered in a shorter period of time) of the precipitation measured from ground-based instruments as well as the precipitation forecast and hydrological effect on the terrain. Weather radar may be preferred to conventional precipitation instruments (point-measurement) for two important reasons (Dutta et al., 2012; Vieux, 2013; Chandrasekar & Cifelli, 2012; Richards & Crozier, 1983; Löffler-Mang et al., 1999; Vieux & Bedient, 1998):

1) it can cover remote and inaccessible regions where ground measurements/sampling by rain gauges are difficult, impossible or simply not sufficiently distributed, and
2) it provides 3D areal coverage (scanning volume), avoiding the need of extrapolating point measurements (local rain characteristics) over the area of interest based on the simple assumption that the precipitation amount is uniformly distributed.

In Norway, nine weather radar stations, operated by the Norwegian Meteorological Institute and located along the coast, provides automatically to the meteorologists, the industry, scientists and the public in general real-time radar products (e.g. accumulated precipitation, surface rainfall intensity, classification of precipitation) updated every 7,5 minutes (Elo, 2012; Norwegian Meteorological Institute & Norwegian Broadcasting Corporation, 2014). The operational weather radar processing system is the central computing unit able to provide spatio-temporal descriptions of the precipitation from radar measurement following those steps (Vieux, 2013; Elo, 2012; Gjertsen et al., 2003; Huang et al., 2012):

1) corrects the radar measurement (power and phase difference of the return signal) reflected by precipitation particles for different sources of errors,

2) converts this measurement to radar reflectivity (variable Z, expressed in mm^6/m^3) which corresponds to the measure of the cross section of the particles within the volume scanned by the radar,
3) extrapolates the Z-value to the ground level,
4) transforms the reflectivity (Z-values) to ground precipitation intensity (variable R, expressed in mm/h) using an empirical Z-R relationship which is predefined for the weather radar system (fixed in space and in time), and
5) assesses the performance of this reflectivity-rainfall intensity transformation (Z-R relationship) and, if needed, make adjustments to the R-values based on a comparison with precipitation accumulations measured at rain gauges in the area of interest.

The type of Z to R conversion used is not unique. The weather radar system selects the most appropriate Z-R relationship from a large number of empirical Z-R relationships available in the literature ($Z=ARb$). This variety of Z-R relationships shows the high variability of the Z-R parameters (A and b) according to the geographic location and season (climatic conditions), to the precipitation phase (different water, ice, snow composition) and intensity (storm type and drop size distribution) as well as to the variability within the same storm and from storm to storm. This selection of a single Z-R relationship increase the probability of under- or overestimating the precipitation rates or accumulations (Ulbrich & Lee, 1999; Vieux, 2013; Vieux & Bedient, 1998; Sánchez-Diezma et al., 2001). An important variability factor in the Z-R relationship is the drop size distribution (DSD), which is the spatial variability of the number and size of droplets within the sampling volume. DSD depends on the precipitation process and vary both in space and in time. Both variables Z and R are highly dependent on this drop size distribution variable within radar measurement. In a weather radar system, the variable DSD is not measured but only assumed, based on the Marshall and Palmer precipitation model developed mainly with stratiform rain events that occured at a different location (Vieux, 2013).

Such as many other countries, Norway has chosen the empirical relationship $Z=200R^{1,6}$, based on the Marshall and Palmer assumption on DSD. Besides the fact that the choice of a single Z-R relationship may create significant under and overestimation of the precipitation, it is relevant at this point to question if this unique Z-R relationship represent adequately the spatio-temporal variability of precipitation in Norway. Moreover, there remains uncertainties

around Z-R relationships deduced from DSD measurement, mainly due to the high spatio-temporal variability of DSD and to uncertainties related to the measurement.

1.2 Objectives of the project

In order to evaluate the representativeness of the standard Z-R relationship for Norway, this project aims to determine Z-R relationships from direct DSD measurement using two types of ground-based precipitation instruments: the optical disdrometer (OTT Parsivel) and the vertical pointing Micro Rain Radar (MRR). The objective of deriving and analyzing such local Z-R relationships is to improve ground precipitation measurement.

Also, in order to analyze and control the uncertainties around Z-R relationships derived locally from DSD measurements, those variable Z-R relationships can be compared for different precipitation conditions to the standard Z-R relationship used in the norwegian operational weather radar system where DSD is only assumed.

This project has two main objectives:

1) Estimate Z-R relationships based on ground-based DSD measurements from the optical disdrometer (OTT Parsivel) and the vertical pointing Micro Rain Radar (MRR), evaluate the variability of these Z-R parameters (A and b), determine if they are significantly dependent on the storm type, the ground precipitation phase and/or the season and evaluate their influence on precipitation estimates.
2) Compare the quantitative precipitation values estimated from three different ground-based instruments (optical disdrometer OTT Parsivel, the vertical pointing Micro Rain Radar and the tipping-bucket rain gauge), in order to assess under which conditions the precipitation rates measured by the rain gauge and the Z-R relationships estimated by the MRR and OTT Parsivel instruments are reliable.

To achieve these objectives, the following tasks were defined:

a) Identify separate precipitation events (starting/end times) using 15-min and 7,5-min C-band weather radar images and the 1-min MRR vertical reflectivity profile and classify them according to the storm type (stratiform, convective, air mass convection)
b) Classify each observation in terms of ground precipitation phase (rain, snow, mixed)

c) Estimate Z-R parameters for the whole time period and for each month, for each class and for each event in each class
d) Compare precipitation rate estimates using standard Marshall-Palmer Z-R parameters and estimated Z-R parameters
e) Compare precipitation from the three ground-based instruments for the whole time period.

The unique contribution of this report is to perform these analysis with datasets from Norway. The results will be essential to assess the average Z-R relationship and to improve quantitative radar precipitation estimates from the C-band weather radars by applying variable Z-R relationships according to the precipitation characteristics.

1.3 Organization of the report

This report is divided in four main chapters. The chapter 2 presents the review of litterature on the estimation of precipitation by ground-based instruments (assumptions, variability factors, instrument limitations, source of errors and correction) and the methods used to define Z-R relationships.

The third chapter presents the data and methodology used in this project. This includes the description of the study site, the time period, the different instruments with their measurements and estimates, the method for defining and identifying each precipitation event and the different steps followed to estimate the Z-R parameters and to make the comparative analysis of precipitation measurement from the different instruments.

The chapter 4 contains all results of the project, including the detected events and classified precipitation periods (sub-events), the Z-R parameters estimated for different precipitation types, events and months of the year and the compared precipitation accumulations, reflectivity and intensity measured by the different instruments.

Finally, the chapter 5 focuses on the different types of analysis and discussion around the results presented in the chapter 4. Based on the analysis of the differences in the Z-R parameters and measurements, it also presents some proposals to improve the derivation of

local Z-R relationships from the DSD instruments, the comparative analysis of precipitation measurements and the complementary use of those co-located precipitation instruments.

2 THEORY

2.1 Estimation of precipitation: assumptions and variability factors

There are many ways to measure or estimate precipitation or rainfall. Vieux (2013) and Chandrasekar & Cifelli (2012) identify three main methods based on different types of sensor: 1) precipitation measurement at rain gauge, 2) radar observations of precipitation particles from ground-based instruments (weather radar station or vertical pointing radar) and 3) remotely sensed images from satellites (radar) scanning regularly the earth's surface and its atmosphere. Concerning the radar observations, many authors (Dutta et al., 2012; Chandrasekar & Cifelli, 2012; Peters et al., 2002; Williams et al., 2005 and Vieux, 2013) recognize the advantage of using radar polarimetry (dual polarized radar signal, which means transmitting and receiving both in vertical and horizontal planes) in the estimation of precipitation. Dual polarized radar enhances the radar measurement (compared to the most commonly used single polarized radar) by giving additional information on the rainfall structure and rate, by improving the discrimination of precipitation phase (frozen or liquid particles or hydrometeors) and by being less sensitive to variations in drop size distribution (DSD) and to some errors inherent to the instrument (beam blocking and calibration bias). A fourth way to measure size and velocity of precipitation particles, represent the actual DSD variability and estimate the rainfall intensity is from ground-based optical disdrometer (Jameson & Kostinski, 2001; Löffler-Mang & Joss, 2000; Thurai et al., 2011).

As confirmed by many authors (Chandrasekar & Cifelli, 2012; Löffler-Mang & Joss, 2000; Ulbrich & Lee, 1999; Vieux & Bedient, 1998; Gjertsen et al., 2003 among others), it is a common practice, both in the context of operational precipitation processing systems and in hydrological/hydraulic studies, to apply a multi-sensor approach in the determination of the precipitation characteristics over a region, in the analysis or production of precipitation information (e.g. accumulated rainfall maps, estimation of catchment-averaged rainfall, prediction of catchment response to different precipitation events). This means that different types of instruments measuring or estimating precipitation are combined or compared for calibration or validation purpose.

While rain gauges measure directly quantitative precipitation, radar instruments estimate rainfall by indirect radar measurements (precipitation echoes detected and converted at the instrument). Two different radar instruments exist: 1) weather radar, covering in space and time a varying volume of precipitation particles, and 2) vertical pointing radar (called Micro Rain Radar or MRR), point-based instrument covering in time a fixed volume of precipitation particles at different height (from the height of the instrument antenna to few kilometers above the ground).

Norwegian weather radar stations emit microwave pulses at a specific frequency (5,64 GHz, corresponding to a C-band). The radar beam scans and samples a certain volume of air (covering an opening angle of 1^0) with a specific tilt angle (beam center located at different elevation angles or elevation PPI radar scan, from $0{,}5^0$ to $15{,}5^0$). A schematic view of the radar scanning process is showed in Figure 2.1. The precipitation particles (hydrometeors) reflects the radar signal and a part of this reflected signal is returned (or backscattered) to the weather radar station. The strength (magnitude) and phase difference of the precipitation echoes received at the radar station are measured and converted in equivalent radar reflectivity (Z_e). This variable is highly dependent on the drop size and water reflectivity of the precipitation particles present in the scanned volume of air. The rainfall rate (R) can then be derived from the equivalent radar reflectivity using a standard Z-R relationship ($Z_e=200R^{1,6}$ which is the Marshall-Palmer empirical Z_e-R relationship covering drop sizes from 1 to 3,5 mm).

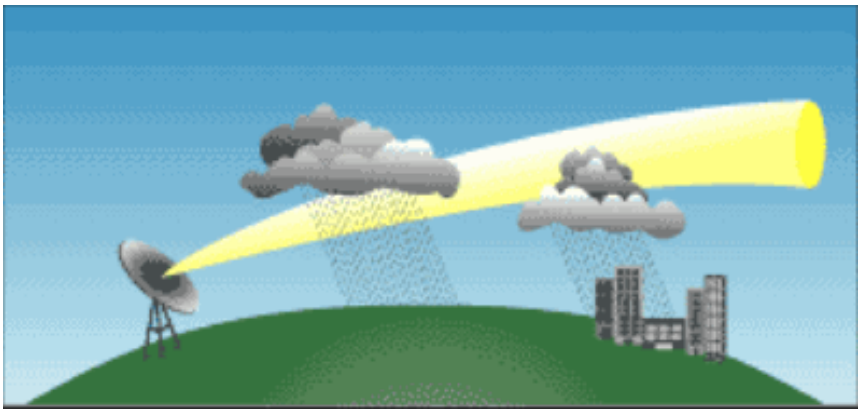

Figure 2.1 – Scanning volume of the weather radar
(extracted from www.kmvt.com/weather/blog,
written by Nick Kosir, meteorologist for KMVT and FOX 14)

At each revolution of the weather radar, the real-time pattern of the rainfall is measured and updated in space (covering a radius of 240 km, spatial resolution of 0,25 km) and in time

(every 7,5 minutes). From those radar revolutions, time series are produced and presented for example as radar images (available online at the Norwegian Meteorological Institute and Norwegian Broadcasting Corporation website yr.no). At the weather radar station, a precipitation processing system (called ProRad) is responsible for the correction of the radar signal from different sources of errors (see sub-chapter 2.2), for the removal of false radar reflectivities (from the sea, the ground or the atmosphere) and for the generation of real-time radar products, such as precipitation accumulations, classified precipitation, surface rainfall intensity (Elo, 2012). In order to improve the quality and representativity of the weather radar products, rainfall intensity estimated values are compared and adjusted to precipitation measurements at rain gauges located in the area of interest.

MRR is a Doppler radar instrument that emits vertically a microwave beam at a different frequency (24 GHz, corresponding to a K-band) than for the weather radar, measures the vertical velocity spectrum of precipitation particles located at 31 different range gates (or elevations above the ground), each gate having a 35 m of height resolution. This radar measurement can be expressed in terms of real-time drop size distribution (DSD) and precipitation reflectivity (Z) and intensity (R) can be both derived from this measured DSD. In contrary to the weather radar station which assumes the DSD variable before estimating the precipitation intensity, the MRR is considered as a DSD measurement instrument (Maahn & Kollias, 2012).

Another DSD instrument is the optical disdrometer. This instrument measures simultaneously the particle size and velocity and deduce from those measurements the precipitation reflectivity (Z) and intensity (R). By converting the disdrometer-derived Z-values to equivalent radar reflectivity factor (Z_e), the optical disdrometer Parsivel can be compared to C-band weather radar results and constitute an important interpretation and validation tool for the weather radar, especially in alpine regions where most of the precipitation particles present in the scanned volume is snow (Löffler-Mang & Joss, 2000; Löffler-Mang & Blahak, 2001).

Whatever instrument is used for the estimation of precipitation, the latter is based on a certain number of assumptions, which mainly depend on the type of instrument, measurement and

data processing system. The weather radar system makes the following assumptions for its estimated precipitation (Vieux, 2013; Jameson & Kostinski, 2001; Smith, 1984):

1) Hydrometeor distributions (DSD) defined by the Marshall and Palmer precipitation model, where the number of droplets N(D) is related to the droplet size (D) by the following equation: $N(D)=N_0e^{-\wedge D}$ where values of N_0 and $\wedge$ are given for snow and rain
2) Approximation by the Rayleigh backscattering of radiation, meaning that the size of droplets reflecting the radar signal following the Rayleigh scattering type is assumed to be much more smaller than the radar wavelength ($D<<\lambda$). In this case (weather radar frequency of 5.64 GHz), the corresponding wavelength is 5,3 cm, which means that the droplets of size D equal or lower than 3,3 mm ($D<=\lambda/16$) are expected to scatter a specific way, with dielectric properties associated to water particles. This assumption makes the equivalent reflectivity factor (Z_e) equal to the radar reflectivity Z. For precipitation drops larger than 3,3 mm and for ice particles with weak dielectric properties, this assumption represents a source of uncertainties in a sense that the droplet size can be misinterpret by the weather radar.
3) Precipitation (rain) is statistically homogeneous, which means that the concentration of drop sizes (DSD) is steady (constant over time, since its mean and variance are expected to be constant) and can then be averaged. This assumption implies that the precipitation characteristics (DSD) is fixed whereever the droplets are located in the scan volume and do not depend on the measurement process. It also implied that the drop counts (N) represent a statistically independent random variable (drop counts in the neighboring radar scan volumes are not correlated). In reality, the precipitation is statistically inhomogeneous (mean and fluctuations of droplet concentration changes as new data are measured) and the drop counts in one scan volume influence the presence and variability of droplets of various sizes in the neighboring sampling volumes (DSD varies with the location of the droplets in the sampling volume).
4) Extrapolated radar measurements from the height measuring volume to the ground are representative of the actual DSD and reflectivity vertical fluctuations
5) Precipitation characteristics are stationary within the sampling interval (15 minutes)
6) Unique Z-R relationship is suitable for every storm event.

In case of the MRR instrument, the main assumptions on the estimated precipitation are the following (Peters et al., 2005; Kneifer et al., 2011):

1) Precipitation particles backscatters the radar signal according to the Mie backscattering of radiation ($D>=\lambda$). In this case (MRR frequency of 24 GHz), the corresponding wavelength is 1,25 cm, which means that the droplets of size D around and larger than 2,5 mm ($D >= \lambda/5$) are expected to scatter according to the Mie theory (most of the drop sizes at this frequency).
2) Assumed drop size-terminal velocity relation in order to compute DSD.
3) No horizontal particle velocity and zero vertical wind (only fall velocity distributions, not influenced by horizontal or vertical movement, are measured).
4) Statistically homogeneous precipitation, which justify to convert observed Doppler vertical velocity spectra in distribution of fall speeds with averaged DSD, considered as steady.
5) Precipitation particles are mainly in liquid form.

The main assumptions for the optical disdrometer OTT Parsivel are as followed (Löffler-Mang & Joss, 2000; Richards & Crozier, 1983; Thurai et al., 2011; Battaglia et al., 2010):

1) Precipitation particles are spherical and correspond to raindrop shape falling at a certain velocity. This assumption may generate discrepancies for non-fully melted particles and for large drops with different shape.
2) Fall velocity has no horizontal component (only vertical component is considered).
3) Only one particle is passing through the laser beam at a certain time. This assumption may affect the interpretation of the particle characteristics (size, fall speed, snowflake size distribution).
4) Detected drops are at their terminal velocity. This assumption may lead to rainfall overestimates in case of downdraughts in precipitation altering.
5) Use of different mass-size relations related to different particle types. This has high influence on Z-values derived from measured DSD (high Z variability for the same DSD).

For all those ground-based instruments, including the conventional rain gauges, when they are parts of an established weather station network, the distribution of precipitation over the area

around the measurement is assumed uniform (there is no variability between the neighboring instruments of the same type).

Many variability factors influence at various degree the performance and the accuracy of the precipitation estimation. Those factors can be divided in four categories (Vieux, 2013; Chandrasekar & Cifelli, 2012; Dutta et al., 2012; Vieux & Bedient, 1998; Ulbrich & Lee, 1999; Williams et al., 2005):

1) target-related factors (precipitation characteristics),
2) measurement-related factors (type of instrument, conditions of measurements, method of calibration),
3) data processing-related factors (choice and uncertainties of the Z-R relationship, types of correction, adjustment and calibration), and
4) atmospheric and terrain conditions.

In terms of target-related factors, the drop size distribution (DSD), the precipitation phase (water reflectivity or dielectric constant of the precipitation particles), the fall velocity and rain intensity and the storm type have significant effects on the radar and DSD measurements at the ground-based instruments. For example, it is well known that snow particle type and shape cause significant differences both in radar reflectivity (Z) and disdrometer measurements and that the variable number and sizes of precipitation drops (DSD) have important effects on estimated precipitation intensity (R).

Measurement-related factors of variability in estimated precipitation include differences in sampling methods (radar measurement, laser beam shadowing, tipping bucket accumulations) and area sizes (weather radar's scanned volume, rain gauge opening orifice, MRR height range, laser beam measurement area), in temporal and spatial resolution for each measurement recorded, in detection or sensitivity capacities (size, shape and types of precipitation particles) as well as in the type of calibration performed on the instrument. An important factor of variability and possible source of errors in estimating precipitation at the ground is the measurement height. Depending of the type of instrument used and/or the measurement condition (many possible heights of measurement for the same instrument, such as the different height ranges for MRR and the variable height of the weather radar scanned volume depending of the distance to the radar), this factor shows high variability among the

instruments and measurement conditions and may influence significantly the accuracy of the precipitation estimation.

As data processing-related factors, we can name the type of correction and adjustment performed by the retrieval algorithm (removals of clutters, adjustment of anomalous propagation, correction of attenuated signal, adjustment based on mean radar to rain gauge ratio) as well as the level of thresholds applied on the reflectivity values in order to avoid the misinterpretation of noisy or contaminated data.

In terms of atmospheric and terrain factors, this category includes the air composition (presence of hail or ice, water content) and its seasonal variability, the vertical wind influence on the fall velocity of particles, the distance between the target area and the radar station (which has a direct impact on the height of measurement), the level of obstructions and types of terrain (or surface) in the measurement area (sea, mountains, trees, high structures, moving objects, etc.).

2.2 Instruments: direct/indirect measurement, limitations, sources of errors and correction

In case of the tipping bucket rain gauge, the quantitative precipitation (rainfall accumulation and intensity) is measured directly, in a sense that it collects rainfall in a funnel with a tipping bucket of 0,1 mm. The recording of measurement occurs at each tip of the bucket, which produces a single pulse. The number of pulses registered in a certain period of time is transformed to the total rainfall measurement over that period of time (Dutta et al., 2012; Ulbrich & Lee, 1999). It as assumed that direct measurement of rain gauge represent the true rainfall measurement at the ground level (Richards & Crozier, 1983).

Both the vertical pointing radar (MRR) and the optical disdrometer (OTT Parsivel) measure real-time DSD (particle concentration and size) via the relation between the measured particle fall velocity and drop size. In case of MRR, the vertical distribution of velocity is measured (velocity spectra of falling hydrometeors) and the actual DSD for each MRR height range is deduced (Löffler-Mang et al., 1999; Peters et al., 2005). From those direct measurement (DSD and velocity), the precipitation intensity and reflectivity can be indirectly calculated.

The MRR instrument measures the spectral power and from the scattering cross section of droplets calculated by applying the Mie theory, the number density of drops of a certain volume falling with a certain velocity is deduced. From this density, the precipitation rate can be calculated (Peters et al., 2001). The vertical pointing radar MRR is a Doppler radar transmitting continuous microwave at the modulated frequency (FW-CW) of 24GHz. It retrieves Doppler spectra from each range gate (height resolution of 35 m). The spectral volume reflectivity is measured considering the spectral power received from each range gate. The DSD is deduced from the ratio between the volume reflectivity and the single particle scattering cross section calculated by using the Mie theory. In order to be consistent with the weather radar measurement, the equivalent spectral radar reflectivity factor Ze using the Rayleigh approximation ($D<<\lambda$) is identical with radar reflectivity factor Z (Peters et al., 2002; Smith, 1984).

In case of the weather radar, the reflectivity of the backscattered radar signal (Z_e) is measured, while the precipitation rate (R) is indirectly obtained by the transformation of Z_e to R where DSD is assumed (using the standard Z-R relationship) (Vieux, 2013).

Each of those precipitation instruments have its own advantages related to its sampling method and conditions of measurement, but it has also limitations related to its assumptions, detection capacity and level of sensitivity to different sources of errors. The system characteristics of each instrument affect both the resolution and precision of rainfall data (Vieux, 2013).

The weather radar have a higher spatial density than rain gauge network, provides spatio-temporal patterns of rainfall but requires correction and adjustment to remove systematic errors and to minimize uncertainties leading to either under or overestimation of precipitation intensity (R). The sampling interval (7,5 minutes) is large enough to generate some misinterpretation/estimation errors on precipitation, by assuming that the precipitation field is stationary within the sampling interval (Vieux, 2013; Piccolo et al., 2005). High measurement height, due to increasing radar beam altitude with distance from the instrument, may cause serious uncertainties related to the necessary extrapolation of radar measurements to the ground level (Löffler-Mang et al., 1999).

While constant reflectivity is generally assumed between the surface and the melting layer (explained below as sources of errors and in Figure 2.2), MRR measurements provide high-resolution vertical profiles which contribute to define the vertical structure of the precipitation and to enhance significant shape transformation of the DSD on the particle fall path below the melting layer. More accurate information on the vertical profile of reflectivity (VPR) given by MRR minimize the weather radar bias of ground precipitation (when the radar reflectivity must be extrapolated to the ground) (Peters et al., 2005). Also, MRR has the advantage of measuring well above drifting snow and not being much affected by wind-induced turbulence during snow precipitation, which is not the case for the other ground-based instruments such as rain gauges and disdrometers (Kneifel et al., 2011). According to Duvernoy & Gaumet (1996), Doppler radar like MRR is well suited to discrimintate rain and snow from fall velocity spectra of particles. It is also not sensitive to mist and fog. However, Kneifel et al. (2011) report large uncertainties for snow precipitation measured by MRR and highlight the dependency of radar returns to snow habit, snowflake size distribution (DSD for snow) and particle shape. This may cause deciations from the mean Z_e conversion relation. In case of snow, MRR also has limitations for the separation of snow-related low radar signal from noisy signal. Nonetheless, even if they report that MRR may overestime the total snow accumulation by 7 %, they consider that this estimation error is smaller than errors affecting estimates of snowfall intensity by the weather radar, caused by uncertain Z_e-R relationships for snowfalls. Another weakness of the MRR is the fact that it is most likely affected by the severe attenuation of the radar signal due to liquid water (especially in intense storms) for high-frequency radar (short wavelength). This leads to strong underestimation of precipitation intensities (Löffler-Mang et al., 1999; Holleman, 2006) and in contrary to weather radar, the MRR measurements are generally not corrected for atmospherical sources of error, such as for signal attenuation.

The optical disdrometer can identify many precipitation types, including mixed precipitation, and provide 2-dimensional distribution of particle size and velocity (Nemeth & Löffler-Mang, 2006; Messtechnik, O.T.T., 2009). Small drops are reliably detected (Löffler-Mang & Joss, 2000). Despite the very small volume of measurement of the disdrometer compared to the scanning weather radar, the disdrometer are used to calibrate the vertical Z-profile (VPR) at lower range gates of the MRR, which is useful for the validate the weather radar observations

(Gage et al., 2000). However, the instrument is sensitive to horizontal winds which may cause that many drops miss the sampling area of the instrument. It also has limiting detection capability (border effects, size and shape evaluation problem since only one horizontal size of the particle is retrieved). For small precipitation particles and for solid particles, such as large or fluffy snowflakes, the shape and orientation of the particle is unknown (does not follow the assumed spherical shape). This limitation increases the uncertainty on the fall velocity measurement related to the actual shape of the particles. Based on a comparison with 2D video disdrometer, the Parsivel disdrometer has a tendency to underestimate the fall speed with more than 20% and overestimate the number of small snowflakes and large particles. This leads to Z underestimation compared to radar measurement. The low differences that may be found between those two instruments are mostly due to the presence of liquid particles (Battaglia et al., 2010).

The traditional rain gauge has much lower spatial resolution (single point sampling sparsely located on the terrain) compared to the other instruments (disdrometer, MRR and weather radar). This makes the rain gauge not suitable to capture spatial variation of rainfall, especially isolated cells of intense rainfalls or fine details or precipitation events, like single light rain event (Vieux, 2013). Evaporation and the lack of sensitivity of the rain gauge affect its capacity to provide accurate and highly representative precipitation information (intensity and accumulation).

MRR, disdrometer and rain gauge provides point measurements, which represent small-area and short-interval rainfall measurements that may be combined with the weather radar for validation purpose (Richards & Crozier, 1983). However, in contrary to the weather radar station, it is difficult with those point-measurement instruments to establish a high density network which covers appropriately, in the most representative way, an area of interest.

Measurements derived from any kind of those precipitation instruments are altered or biased more or less significantly by many types of errors (Williams et al., 2005; Saltikoff et al., 2004):

1) instrument-related errors including miscalibration, sampling and processing errors

2) atmospherical and terrain-related errors (obstruction like mountains, false echoes, attenuated signal, snow melting layer of the atmosphere located at the measurement height), and
3) errors related to measurement conditions and representativity, which means incomplete sampling of the variable precipitation field (precipitation characteristics and variability, height measurement, etc.).

Some authors (Holleman, 2006; Elo, 2012; Gjertsen et al., 2003; Sanchez-Diezma et al., 2001, Saltikoff et al., 2004 and Germann et al., 2006) identify the most important errors, especially for mid to high-latitude radar instruments:

- Non-uniform vertical profile of reflectivity (VPR), caused by the movement, the evaporation or the accretion of droplets, which makes the observed Z values strongly dependent on the height measurement (range) and increases the level of uncertainty while this observed value is interpolated to the ground. This error can be large for weather radars when the sampling area is located at a certain distance, which increases significantly the height measurement.
- Attenuation of the radar energy by heavy rain, graupel and hail from the atmosphere or by the water/snow/ice layer covering the radome (weatherproof structure around the radar antenna). The type of error affects even more high-frequency radar beam, such as the MRR instrument
- Melting layer (or bright band), which is a atmospheric layer located at a uniform height range and responsible for high reflectivity measurement of melting snow particles. Since the particle phase is changing to rain while reaching the ground, the measured Z-value is far too high to represent adequately the precipitation characteristics at the ground (Figure 2.2).
- Variability (in space and in time) of the precipitation and variety of precipitation phases (rain, snow, melting snow, graupel, hail) which may be misinterpreted or misclassified, especially by single polarized radar instruments such as the the norwegian weather radar and MRR or by limiting detection capacity of the optical disdrometer for snowflakes, and leads to high variability and uncertainties in the precipitation intensity derivation since the DSD is highly variable and the Z-R relationship used (parameters A and b) not appropriate.

- Overshooting (not detected precipitation events) which occurs when precipitation is shallower than the radar sampling volume (height measurement), especially in cold climates where winter snow is usually shallower than summer rain.
- Shielding and beam blocking where the topography (particularly in Norway) and surrounding obstructing structures block the radar which leads to loss of data of the area of interest
- Anomalous propagation, caused by specific temperature or moisture differences, where the radar beam is refracted and does not follow a normal path. Also clutter, which is the radar signal that is mostly reflected by other targets than the precipitation particles, such as the ground, the atmosphere and the sea (important in Norway since all weather radar stations are located along the coast). Both sources of errors lead to the misinterpretation of the returned signal and consequently, if not corrected, to inaccurate precipitation intensity values.

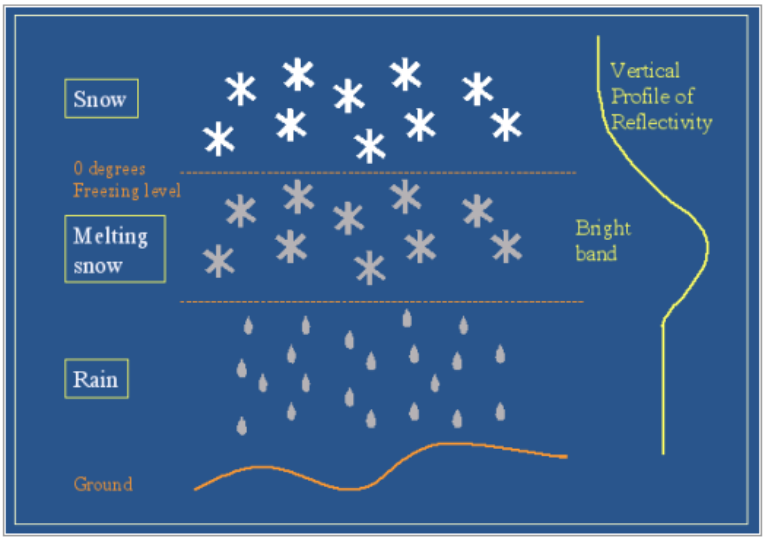

Figure 2.2 – Shematic view of the melting layer (bright band)
(extracted from radar.meteo.be,
written by the Radar and lightning detection group,
Observations Department of the
Royal Meteorological Institude of Belgium, RMI)

Some of those errors are usually corrected by an appropriate location, calibration and maintenance of the instrument and by sophisticated data post-processing (clutter, propagation, VPR, beam blockage).

According to Ulbrich & Miller (2001) and Gjertsen et al. (2003), miscalibration of the radar (especially by inaccurate determination of the antenna gain) is the main cause of the large differences found between radar-derived precipitation intensity and the ground-based precipitation measurement. Calibration of radar measurements should then be prioritized, not only by applying a correction factor based on the estimated mean radar to rain gauge ratio but also by hardware calibration of radar (mainly related to antenna).

Different levels of correction are applied to the precipitation measurement in order to provide accurate rainfall estimation. In case of radar measurement, the relevant types of correction concern (Chandrasekar & Cifelli, 2012; Gjertsen et al., 2003; Ulbrich & Miller, 2001; Germann et al., 2006):

- the extrapolation of radar measurement to the ground, considering the variable vertical profile of reflectivity (VPR),
- the removal of calibration biases or miscalibration of the radar antenna
- the minimization of beam averaging contamination
- the identification and removal of ground and other false echoes close to the radar sampling area by means of clutter mask and Doppler filtering
- the correction of missing radar echo (or beam blockage).

When the rain gauge measurement errors are assumed smaller than the radar bias, the improvement of radar predicted rainfall affected by range-dependent bias through rain gauge adjustment (considered as true rainfall and compared to the radar estimated rainfall) may be part of this correction process (Huang et al., 2010; Gjertsen et al., 2003; Germann et al., 2006). Not only the rain gauge, but also the optical Parsivel disdrometer may contribute to the validation of radar measurement. Löffler-Mang & Blahak (2001) report that DSD measured by Parsivel for snowfall in winter and alpine regions may be compared to the C-band radar estimated Z_e in order to interpret the radar results.

2.3 Estimation of Z-R relationship

Z-R relationships to estimation precipitation rate at ground level are either assumed and extrapolated to the ground (at a certain distance from the weather radar station) or developed

locally from DSD observations (from MRR or disdrometer instruments for example) or from a combination of radar and rain gauge observations (Dutta et al., 2012). Many authors (Dutta et al., 2012; Vieux & Bedient, 1998; Gjertsen et al., 2003) confirm that the combined observations radar-rain gauge improves the estimation of rainfall rate from the weather radar (lower RMSE and bias for radar estimated precipitation intensities).

Weather radars measure the radar reflectivity from the total backscattered power of all scatterers (including precipitation particles) within the scanned volume. Using the Rayleigh approximation, the backscattered signal received from individual particles, assumed spherical raindrops, are deduced from the dielectric properties of the water particles. The following equation represents the radar reflectivity factor measured at the weather radar station:

$Z_e = \lambda^4 \eta / \pi^5 |K_w|^2$ where λ is the wavelength of the radar beam

η is the backscattered power divided by the scanned volume it represents

K_w is the dielectric factor for water (rain) as a scatterer.

Knowing that the radar reflectivity (Z) is proportional to the sixth power of the diameter of each type of droplets present in the scanned volume, the relationship between Z and the droplet size and number (DSD) can be expressed as followed:

$Z = \int N(D)\, D^6\, dD$ where N(D) and D represent all drop sizes in the scanned volume (DSD).

Precipitation intensity (R) can be inferred from fall velocity of raindrops using a certain V-D relationship on DSD values (N(D) and D).

In case of the weather radar, the reflectivity Z is calculated by assuming DSD from Marshall-Palmer precipitation model ($Z=0{,}08\ N_o D_o^7$ where $N=N_o e^{-\wedge D}$, for which N_o, $\wedge$ and D_o values are given for specific types of precipitation, including snow). The standard Z-R relationship, based on Marshall-Palmer assumed DSD, comes from both calculated Z and R values from this DSD ($Z=0{,}08\ N_o D_o^7$ and $R= N_o D_o^{14/3}/4026$). It is known that for snow Z_e increased more rapidly with R than for rain (Vieux, 2013; Löffler-Mang & Blahak, 2001; Holleman, 2006; Smith, 1984). The standard Z-R relationship is expressed in power law form ($Z=AR^b$) and is selected by each weather radar among a variety of Z-R relationships presented in the literature representing different types of rainfall and geographical locations. The selection of the parameters A (between 100-500) and b (between 1,2 and 1,7) is the result of compromizing

between Z-R relations for stratiform and for thunderstorm rain, hence it represents an average type of rainfall (Ulbrich & Lee, 1999; Holleman, 2006). Some weather radar may use double Z-R relationship, for example $Z=300R^{1,4}$ for convective rain and $Z=200R^{1,6}$ for stratiform rain (Sanchez-Diezma et al., 2001). However, other authors (Richards & Crozier, 1983) consider that the use of different Z-R relationships for different types of rainfall do not really improve the accuracy of radar measurements and is not advised on real-time basis.

In case of DSD instruments, such as MRR and the disdrometer, the Z-R relationship is derived using their own calculations of reflectivity and intensity values:

1) For the OTT Parsivel (Löffler-Mang & Blahak, 2001; Ulbrich & Lee, 1999), the Z-DSD equation ($Z = \int N(D)\, D^6\, dD$) is evaluated by calculating the sum over discrete measured size classes:

   $Z_{measured\ DSD} = \Sigma_i\, n_i D_i^6 / tFv_i$ where n_i is the number of measured drops in class i during time t

   D_i is the mean diameter in class i

   F is the measuring area in the disdrometer

   v_i is the mean velocity of drops in class i.

   DSD measured by Parsivel (N(D) and D) depends on the measurement area and time.

   The precipitation intensity (R) is derived from the measurement of the particle speed and the duration of signal. From the fall velocity of raindrops of diameter D, the intensity is calculated as followed:

   $R=\pi/6 \int N(D)\, D^3\, v(D)\, dD$

2) For MRR (Maahn & Kollias, 2012; Löffler-Mang et al. 1999), the reflectivity Z is derived from the particle-size distribution N(D), such as for OTT Parsivel ($Z = \int N(D)\, D^6\, dD$) where N(D) is derived from the observed Doppler spectral η converted to Doppler velocity and to particle diameter from η(D) using the Mie theory. The calculation of N(D) implies the assumption of a terminal fall velocity-raindrop diameter (v-D) relationship.

   In case of precipitation rate (R), it is also derived from N(D) and the particle velocity v(D), such as for OTT Parsivel ($R=\pi/6 \int N(D)\, D^3\, v(D)\, dD$).

For both DSD instruments, the R estimates, when there is no turbulence and the precipitation is mostly rain, are generally more accurate than those estimated by the weather radar using an unknown DSD value. However, in case of snow precipitation, both Z and R derived from DSD instruments are highly biased and require adjustments (measurement post-processing), since the size-fall velocity relationship assumed by those instruments is quite different in case of snow and turbulence may have large effects on this velocity (Maahn & Kollias, 2012). According to Dutta et al. (2012), rain estimates by weather radar improves significantly by using locally developed Z-R relations, such as from DSD instruments.

The differences in Z-R relationships derived either from weather radar or from DSD instruments are mainly due to local and temporal variability in DSD values, since climatological conditions and precipitation types vary in time and space. In terms of spatial differences, we talk about variations of atmospherical conditions and precipitation type (affecting the Z values) with height (including possible bright band contamination of the measured Z), either caused by the distance to the weather radar or the height-range differences in MRR measurement. Even when using one of those Z-R derivation method (Z-R relation obtained from DSD measurements for example), the scatter of data around the obtained Z-R curve implied that there are deviations related to individual events. Those deviations may be as large as 50 % (Holleman, 2006; Sanchez-Diezma et al., 2001; Williams et al., 2005).

Radar estimates of rainfall is highly dependent on the Z-R relationship used to transform radar reflectivity to rainfall intensity (Ulbrich & Miller, 2001). According to Richars & Crozier (1983), for making best use of radar measurements and improve radar estimates, Z-R relationship should be refined so it represents the prevailing rainfall climatology of the measurement area. By applying an optimized space and time smoothing of the data (spatial average over the radar beam sampling volume and temporal average of DSD measured from the disdrometer), the values of R and Z are calculated from mean measured DSD, which according to the authors represent more realistically the radar sampling volume and measurement cell. The same authors report also that Z-R relationship derived only from the disdrometer data shows better goodness-of-fit than the one from the Z-R relationship calculated from both the radar (for Z_e-values) and the disdrometer (for R-values). They also confirmed that when the radar measurements are corrected for bias (rain-gauge adjusted, corrected by appropriate radar calibration), the derivation of Z-R relationship from the radar-

measured reflectivity (Z) and the measured DSD is comparable to the only disdrometer-derived Z-R relationship. This is also the conclusion of Ulbrich & Miller (2001) and Ulbrich & Lee (1999), but those authors attribute the large differences found between the weather radar estimated intensities and the surface rain gauge not primarily to the variations in Z-R parameters that may be used, but to the miscalibration of the radar. They hence recommend to perform more accurate calibration of the radar, by focussing especially on the antenna gain.

Huang et al. (2010) discuss the effect of snow precipitation on the derivation of Z-R relationship. In order to improve the relationship particle fall speed-diameter, they propose new matching algorithm using 2D video disdrometers looking at the same particle falling through the measurement area. They derive Z_e-SR relationship where SR represents the liquid equivalent snow rate in order to apply it to snowfall using the calibrated weather radar. They found optimal parameters estimated by minimizing the difference between radar-measured reflectivity and the disdrometer calculated Z. Their conclusions are interesting: the Z_e-SR relationship they derived is similar to conventional Z_e-R relations and is less affected by errors related to variable DSD or size distribution than those Z_e-R relations.

Variations in Z-R parameters may lead to large differences between radar-derived rainfall rates and rain gauge precipitation measurements. According to Ulbrich & Lee (1999), the standard Z-R relation at the weather radar WSR-88D in U.S. ($Z=300R^{1,4}$) underestimates stratiform rain intensities by 25 % and overestimates the thunderstorm rain intensities by 33 %. When the weather radar-measured reflectivities are compared to those derived from the disdrometer, the authors found out that the radar underestimates the Z-values by more than 3,5 dBZ. They explain this difference mainly by radar calibration offset. Löffler-Mang & Blahak (2001) confirm this difference between weather radar and disdrometer Z-values (from 0 to 5 dBZ, not exceeding 10 dBZ). As part of the explanation for this difference, they point out that the sampling method of the two instruments is quite different (point measurement for the disdrometer compared to volume measurement for the weather radar). They notice that the disdrometer Parsivel have tendency to underestimate Z_e and they attribute this to non-graupel-like particles. In case of convective event, the disdrometer overestimates those Z_e-values. Richards & Crozier (1983) compared precipitation rates from the weather radar, the tipping bucket rain gauge and the disdrometer, using Z-R relations determined by the disdrometer, and confirmed that radar systematically underestimate R-values.

3 MATERIALS AND METHODS

3.1 Study site and time period

Precipitation measurements are provided by three ground-based instruments (the vertical pointing radar MRR, the laser-based optical disdrometer OTT Parsivel and the tipping bucket rain gauge), located at the Risvollan hydrological station, south of Trondheim (N 63 ° 23' 55.3", E 10° 25' 22.1", 84 masl). This station is operated since 1986 by the municipality of Trondheim, NTNU and the Norwegian Water and Energy Directorate (NVE). The Risvollan station (# 68230), which is also part of the Norwegian Meteorological Institute's weather station network, provides air temperature data. About two kilometers north-east of the Risvollan station, the Voll station (# 68860, N 63 ° 24' 38.2", E 10° 27' 14.0", 127 masl) provides hourly air temperature data in order to fill missing temperature data at Risvollan (see sub-chapter 3.3).

The weather radar station operated by the Norwegian Meteorological Institute is located at Olsøyheia, a 600m-height mountain in the municipality of Rissa (N 63 ° 41' 25.9", E 10° 12' 13.5"). Its scanning area covers the Trøndelag region and parts of the Norwegian Sea (including the Risvollan station). The location of the study site (ground-based instruments) and the regional weather radar station is showed in Figure 3.1. The reflectivity (Z) measurement of the Rissa weather radar (at a tilt angle of $0{,}5^0$) over the Risvollan station, which is located at about 35 km from the radar station, occurs at a height of 900 m, since the radar beam axis is 900 m above the ground at this site (Figure 3.2).

All data cover a period of two years, from January 1st, 2012 to December 31st, 2013.

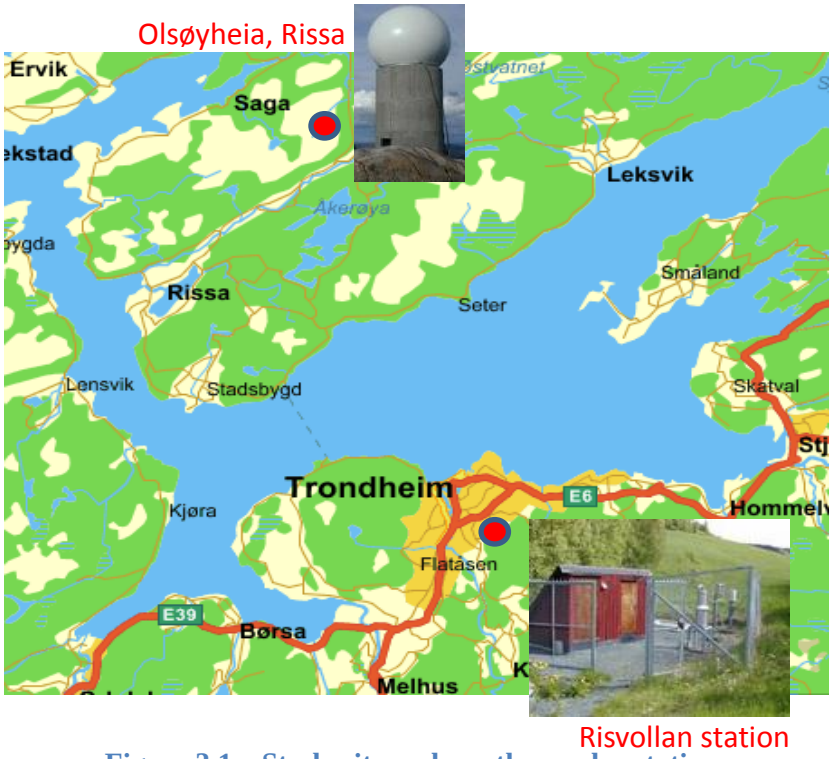

Figure 3.1 – Study site and weather radar station

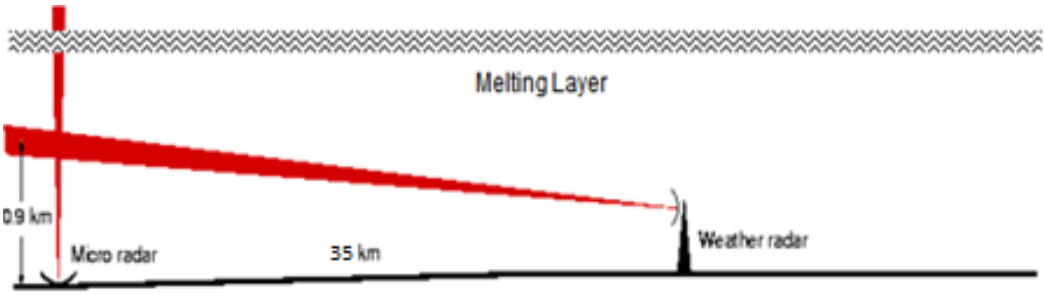

Figure 3.2 – Radar height measurement about the study site (modified from www.metek.de)

3.2 Description of instruments and variables

In this project, data from five different instruments are used:

1) Weather radar at Rissa (Figure 3.3a)
2) Vertical pointing radar MRR at Risvollan (Figure 3.3b)
3) Optical disdrometer OTT Parsivel at Risvollan (Figure 3.3c)
4) Lambrecht tipping bucket rain gauge at Risvollan (Figure 3.3d)
5) Air temperature Aanderaa sensor at Risvollan (Figure 3.3e)

(a)

(b)

(c)

(d)

(e)

Figure 3.3 - Five different instruments used in this project
(a) Weather radar at Rissa (www.met.no), (b) Vertical pointing radar MRR (www.metek.de), (c) Optical disdrometer OTT Parsivel (www.hachhydromet.com), (d) Heated Lambrecth tipping bucket rain gauge (www.ivt.ntnu.no/ivm/risvollan), (e) Air temperature Aanderaa sensor (www.ivt.ntnu.no/ivm/risvollan)

The specifications and the measurement variables selected from each instrument are presented in Table 3.1 (Peters et al., 2001; Savina et al., 2012; Messtechnik O.T.T., 2009; Battaglia et al., 2010; Kneifel et al., 2011).

3.3 Data preprocessing

Prior to the detection and identification of precipitation events, a series of data preprocessing steps are required:

1) Time shifts of the date/time recorded in norwegian winter time (UTC+1h) to UTC time for:

- Air temperature at Risvollan and Voll stations
- Precipitation at the tipping bucket rain gauge

2) Time shifts of the date/time recorded in norwegian local time (UTC+1h in winter/+2h in summer) for:
    - Optical disdrometer OTT Parsivel

Table 3.1 - Instrument specifications and selected measurement variables

	Weather radar station	**Vertical pointing radar MRR**	**Optical disdrometer OTT Parsivel**	**Lambrecht tipping bucket rain gauge (heated)**	**Air temperature Aanderaa sensor (shielded)**
Location	Olsøyheia at Rissa	Risvollan station	Risvollan station	Risvollan station	Risvollan and Voll stations
Height above the ground	6 m	10 m	1 m	2 m	2 m
Measurement surface/height	Scanned volume variable with distance to the station 1^0 (beam width)	Variable with height, 35 m (height resolution) $1,5^0$ (beam width)	54 cm^2	200 cm^2	
Sampling time resolution	7,5 and 15 minutes	1 min	10 seconds	10 min	1 min (Risvollan) 1 hour (Voll)
Selected measurement variable(s)	Reflectivity	Reflectivity Prec. intensity	Reflectivity Prec. intensity Prec. phase	Prec. accum.	Temperature
Minimum detection (R, D, v, T^0)	0,005 mm/h (R)	0,1 mm/h (R) 0,25 mm (D) 0 m/s (v)	0,001 mm/h (R) 0,2 mm (D) 0,2 m/s (v)	0,1 mm/tip (R)	$0,9^0$
Time in operation	Since 2003			Since 2004	
Producer	Gematronik GmbH	Metek	OTT Messtechnik GmbH	Lambrecht	Aanderaa Data Instruments

3) Timing checks between the vertical pointing radar MRR or the optical disdrometer OTT Parsivel, taking separately, and the tipping bucket rain gauge:
    - If there is/are systematic and significant delay(s) lasting for at least few months, a time shift corresponding to the maximum correlation between the two data series is applied.
    - In case of the MRR instrument, two time shifts have been applied:

- 8528 minutes forward from August 28th 2012 14:49 to January 1st 2013 00:00 due to errors in date recording after a breaking period.
- 43 minutes forward from September 27th 2012 19:33 to January 23rd 2013 10:45 based on a visual detection of the delay when comparing the times series of MRR and of the rain gauge.

- No delay has been detected between the OTT Parsivel and the rain gauge.

4) Validation of the missing periods for the disdrometer OTT Parsivel and exclusion of timesteps that are most likely affected by the instrument instability just before and just after down periods at the instruments (no datalogging due to instrumental errors). In total, only 417 325 timesteps have reliable records of precipitation drops at the disdrometer over the whole two-years study period (6 315 840 timesteps, i.e. (366+365) days * 24 hours * 60 minutes * 6 10-seconds periods per minute), which represents only 6,6 % valid data retained over the whole time period.
5) Filling up the missing temperature values at Risvollan rain gauge:
    - If the gap is smaller or equal to 60 minutes, new temperature values interpolated by approximation fill up the missing period.
    - If the gap is longer than 60 minutes, missing temperatures at Risvollan station are replaced by hourly values (constant hourly value for each minute) calculated by one of the two following least-squares regressions between natural logarithm of hourly average temperatures at Risvollan station and natural logarithm of hourly recorded temperatures at Voll station, giving the minimum differences just before and just after the missing period:
        - Regression on the whole time period (from January 1st, 2012 to December, 31st 2013)
        - Regression on seasonal periods corresponding to the missing periods (from January to March 2013, from October to December 2012, from January to March 2013 and from October to December 2013)

    As an example, for the missing period January 27th 2012 07:00 to January 28th 2012 10:00 (gap=28 hours), the regression on the whole time period between hourly average temperature at Risvollan station and hourly recorded temperature at Voll station is $(T_{Risvollan}+30)=0{,}7128*(T_{Voll}+30)^{1{,}0942}$, with a correlation coefficient of $R^2=0{,}94$. The regression on the 2012 winter period (from January 1st 2012 00:00 to March 31st 2012 23:00) is

$(T_{Risvollan}+30)=0{,}9605*(T_{Voll}+30)^{1{,}0269}$, with a correlation coefficient of $R^2=0{,}91$. Squared differences between each of the two regression-calculated temperatures and the observed temperatures at Risvollan just before and after the missing period are calculated. Those differences are then compared to find the minimum difference and select the most appropriate regression-calculated temperatures. The details on those calculations are showed in Table 3.2. Both before and after the missing period, 2012 winter period regression gives lowest squared differences (1,09 before and 2,23 after). This means that the seasonal regression is applied to fill up missing temperature values for Risvollan (7^{th} column in Table 3.2).

Table 3.2 - Example of replacement of missing temperature values at Risvollan

Timestep (yyyymmdd hh00)	**T_{Voll}**	**Mean $T_{Risvollan}$**	**T_{Voll}+30**	**Mean $T_{Risvollan}$+30**	**$T_{Risvollan}$** calculated by regression on the whole time period	**$T_{Risvollan}$** calculated by regression on the 2012 winter period	**Diff.^{2}** between calculated and observed temp. (whole time period)	**Diff.^{2}** between calculated and observed temp. (2012 winter period)
20120127 0600	0.3	2.9422	30.3	32.9422	29.7800	31.8991	9.9997	1.0879
20120127 0700	0.4	NA	30.4	NA	29.8875	32.0073		
20120127 0800	0.4	NA	30.4	NA	29.8875	32.0073		
20120127 0900	0.2	NA	30.2	NA	29.6724	31.7910		
20120127 1000	-0.1	NA	29.9	NA	29.3500	31.4668		
20120127 1100	0	NA	30	NA	29.4575	31.5749		
20120127 1200	0.1	NA	30.1	NA	29.5649	31.6829		
[...]								
20120128 0500	-1.2	NA	28.8	NA	28.1706	30.2786		
20120128 0600	-1.6	NA	28.4	NA	27.7428	29.8469		
20120128 0700	-1.8	NA	28.2	NA	27.5291	29.6310		
20120128 0800	-2	NA	28	NA	27.3156	29.4153		
20120128 0900	-2.1	NA	27.9	NA	27.2088	29.3074		
20120128 1000	-2.1	NA	27.9	NA	27.2088	29.3074		
20120128 1100	-2	0.9095	28	30.9095	27.3156	29.4153	12.9163	2.2328

3.4 Definition of event classes

By visualizing the time series of 15-min C-band weather radar images passing over the Risvollan station (right side of Figure 3.4), it is possible to detect the starting and ending times of precipitation events and to identify the type of event by considering the patterns and evolution of clouds together with the magnitude and variation of the reflectivity value (Z). According to Steiner et al. (1995), when the reflectivity is equal or exceeds 40 dBZ, the precipitation event can be considered with good confidence as convective.

In the case showed in Figure 3.4, the large compact cloud passing over Risvollan corresponds to a stratiform event (when reflectivity values are mostly below 40 dBZ). The starting and ending times of this event can be confirmed in the vertical Z-profile from the MRR instrument (left side of the figure) where the yellow-green colored area corresponds to the time period where reflectivity values are larger than 10 dBZ. Some convective air masses (with reflectivity values near and at certain time exceeding 40 dBZ) can develop and move within the stratiform pattern cloud, as showed in Figure 3.5 (red colored area in the MRR vertical Z-profile). Convective cells formed in patches (Figure 3.6) is another type of precipitation pattern that can be seen in the C-band weather radar images and confirmed by the MRR vertical Z-profile (red colored area).

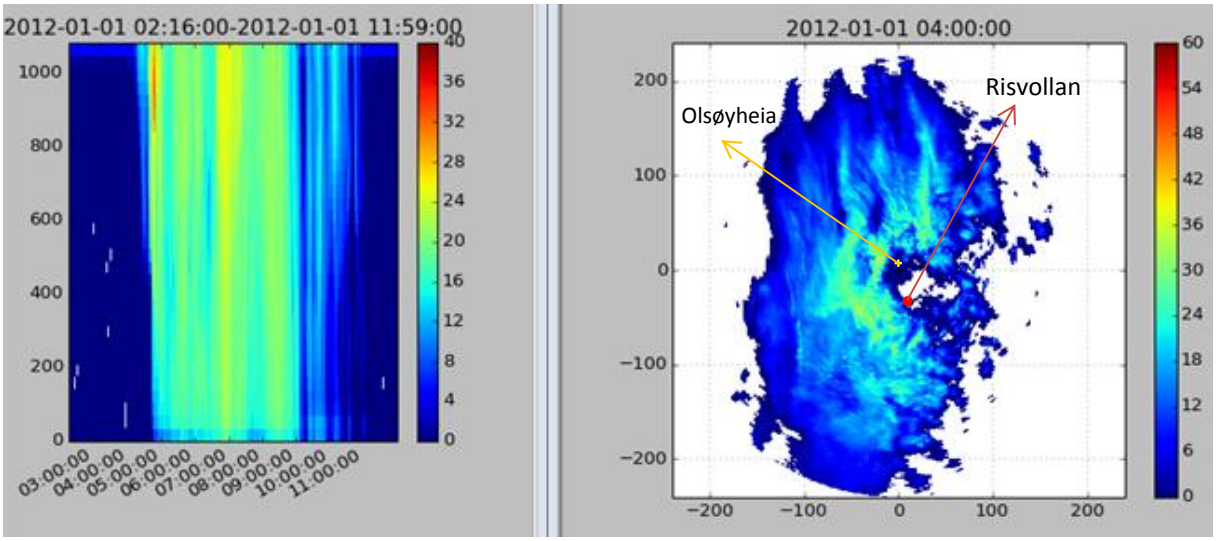

Figure 3.4 – Stratiform event passing over Risvollan station
(color values correspond to reflectivity in dBZ)

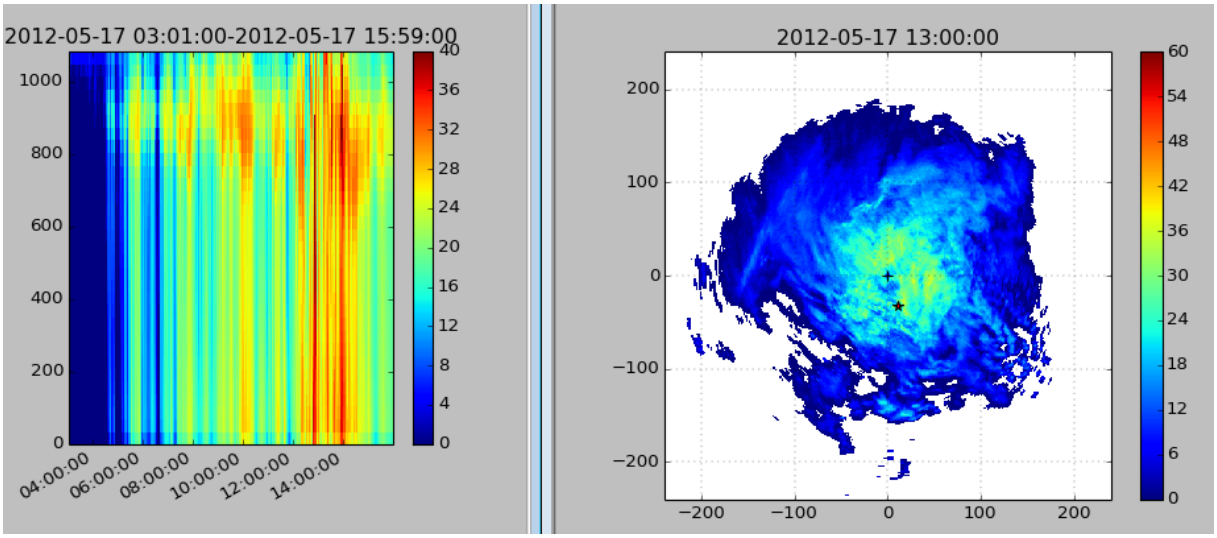

Figure 3.5 – Convective air masses within a stratiform event passing over Risvollan station
(color values correspond to reflectivity in dBZ)

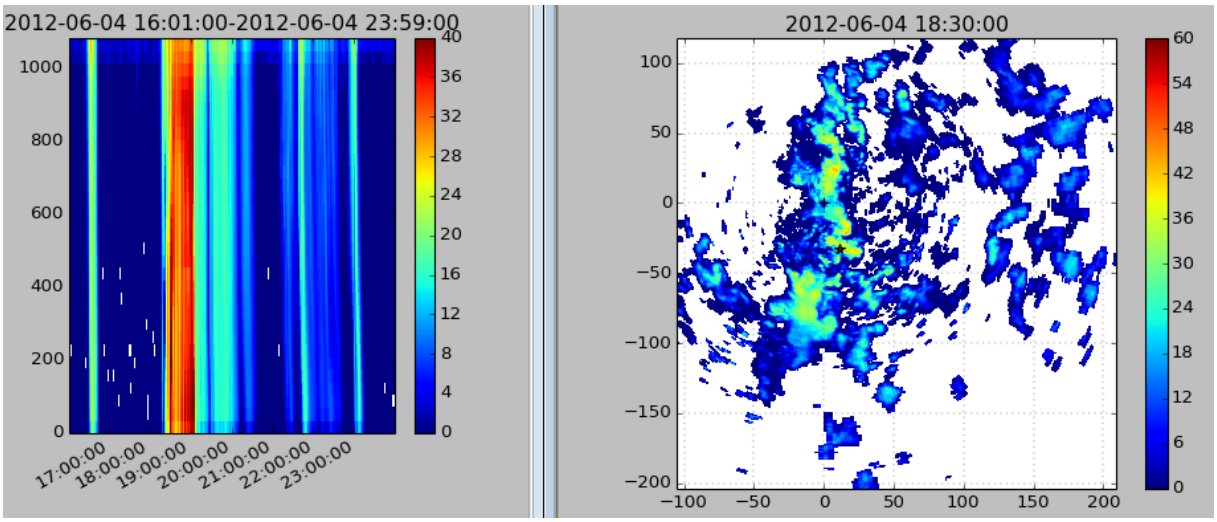

Figure 3.6 – Convective patches passing over Risvollan station
(color values correspond to reflectivity in dBZ)

In order to avoid stratiform outliers in rainfall rates (R) derived from the MRR instrument, they have been filtered out by retaining only R-values equal or below 20 mm/h, while the reflectivity (Z-value) is below 40 dBZ (stratiform).

During the visualization of the MRR vertical Z-profiles for the whole time period, the presence of bright bands at the measurement heigth (4th range gate of the MRR, i.e. 140 m above ground) have been registered and later excluded from the precipitation event classification. Bright band (high Z-values at a limited height range, corresponding to the layer

where snow melts to rain) is visible for example in Figure 3.5 at 900-m height between 9:00 and 10:00 (orange horizontal layer).

Concerning the convective periods (convective air masses and convective patches), they have first been automatically detected based on the Z-values (equal or exceeding 40 dBZ) and validated by visualizing and comparing the corresponding C-band weather radar images and MRR vertical Z-profile. The validation of automatically detected convective periods either removed those periods, in case of outliers or bright band contamination, or eventually extended it over a longer period of time, in case of an identified event where Z-values are relatively high (orange-red area in the MRR Z-profile) but are not necessarly always equal or exceeding 40 dBZ during the whole convective event.

Besides the type of event (stratiform, convective air mass, convective patches), another variable is included in the event classification at Risvollan: the precipitation phase. This variable was extracted from two different sources: 1) the air temperature sensor at Risvollan and 2) the weather code recorded at the OTT Parsivel disdrometer. From the first source, three criteria based on statistics on precipitation phase at Sagelva station (south-east of Risvollan) over a 2-year period (Figure 3.7) were applied on air temperature data:

- If $T_{air} < -1\ ^{0}C$, non-zero precipitation recorded at Risvollan (from MRR, OTT Parsivel or rain gauge) is considered as SNOW
- If $T_{air} > 3{,}5\ ^{0}C$ or in summer months (June, July, August) no matter the air temperature, non-zero precipitation recorded at Risvollan (from MRR, OTT Parsivel or rain gauge) is considered as RAIN
- If $-1\ ^{0}C < T_{air} < 3{,}5\ ^{0}C$, non-zero precipitation recorded at Risvollan (from MRR, OTT Parsivel or rain gauge) is considered as MIXED

From the second source, precipitation phase were derived from NWS weather codes recorded at the disdrometer which were aggregated in the following way:

- SNOW comprises snow (weather codes S-, S and S+) and snow grains (weather code SG)
- RAIN comprises drizzle (weather codes L-, L and L+) , drizzle with rain (weather codes RL-, RL and RL+) and rain (weather codes R-, R and R+)

- MIXED comprises rain and drizzle with snow (weather codes RLS-, RLS and RLS+) , freezing rain (weather code SP) and hail (weather code A).

All precipitation phase contradictions between the two sources (air temperature at Risvollan and weather codes recorded at the disdrometer) were excluded from the event classification. Also, there was no classification of the precipitation event at timesteps where no significant precipitation were recorded both at the disdrometer (weather code N) and the MRR instruments (R=0 mm/h).

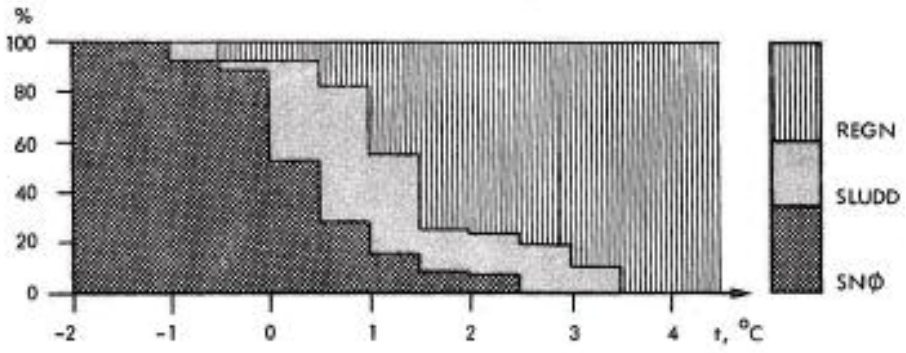

Fig. 3.16 Fordeling av nedbørstype som hhv. regn, sludd og snø for nedbør ved Ø. Jervan falt i temperaturintervallet -2 → +4 °C. Data fra perioden 1/1 73 - 31/12 75.

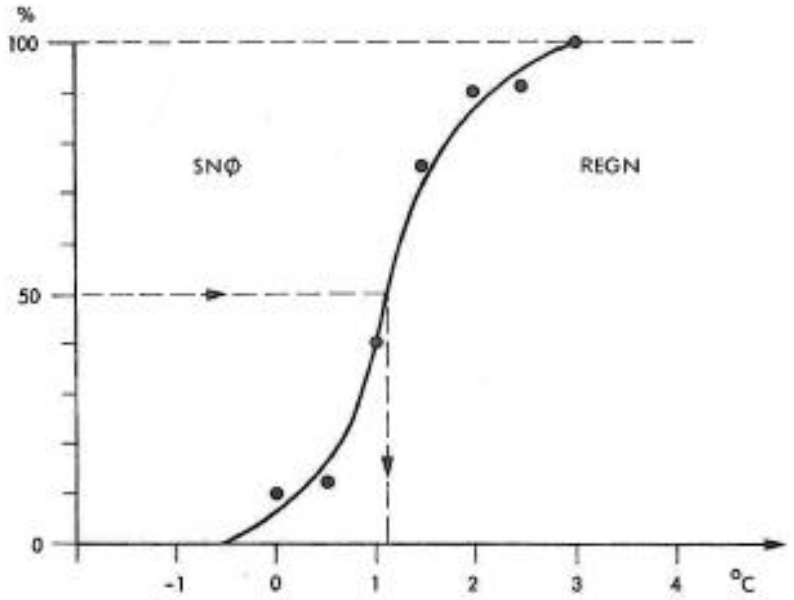

Fig. 3.17 Kumulativ fordeling av nedbørstype, snø eller regn. Øvre Jervan, data for perioden 1/1 73 - 31/12 75.

Figure 3.7 – Statistics on precipitation phase at Sagelva station from January 1st, 1973 to December 31st, 1975 (extracted from Killingtveit, 1976). Precipitation is 100% snow (SNØ) for air temperature below -1 ^{0}C and 100% rain (REGN) for air temperature over 3,5 ^{0}C.

Based on the identification of event types and precipitation phases as described above, seven precipitation event classes were created:

1) RSt (Rain - Stratiform)
2) SSt (Snow – Stratiform)
3) MSt (Mixed - Stratiform)
4) RCA (Rain – Air mass convection)
5) RCP (Rain – Convective patches)
6) MCA (Mixed – Air mass convection)
7) MCP (Mixed – Convective patches)

There were no convective snow in the two-years period.

3.5 Estimation of Z-R parameters

Z-R parameters of the power law form ($Z=AR^b$) can be derived from Z- and R-values deduced by both MRR and OTT Parsivel instruments from measured DSD. Each Z- and R-value used to derive the local Z-R relationship from both instruments has previously been time-checked with the rain gauge at Risvollan (see sub-chapter 3.3) in order to insure that those input values (Z,R) represent the exact same timesteps.

In order to use the most reliable Z- and R-values from both instruments in the derivation of the Z-R parameters, the two following criteria have been applied:

1) In order to take account of the minimum precipitation intensity that each instrument can detect with confidence, only the R-values above 0,1 mm/h were considered.
2) Among the timesteps classified as stratiform (rain, snow or mixed), only the stratiform periods lasting for at least 30 minutes were considered. This criterium permits to avoid very short stratiform periods with low precipitation accumulation. Since convective periods normally last not that long and they are not in sufficient number to make a selection (much lower occuring frequency compared with stratiform periods), this event duration criterium was not applied for convective periods.

In order to fit a linear regression equation between Z- and R-values from each instrument, the power law form of the Z-R relation can be transformed using natural logarithm:

$Z = AR^b$ where R is in mm/h and Z in mm^6/m^3

$$\ln(Z) = \ln(AR^b) = \ln(A) + b * \ln(R) \quad (1)$$

Since R (precipitation rate) needs to be estimated from Z (reflectivity factor), Z becomes the independent variable. The equation (1) is reorganized to express R in function of Z:

$$\ln(R) = \ln(Z) / b - \ln(A) / b \quad (2)$$

Equation (2) can be simplified by introducing two new intermediate/temporary parameters:

$$\ln(R) = b' \ln(Z) + A' \quad (3)$$

where $b' = 1 / b$ and $A' = - \ln(A) / b$

Since Z-values derived from the two instruments are expressed in dBZ, the equation (3) is modified to convert the input Z-values in mm^6/m^3:

$$\ln(R) = b' \ln(10) / 10 * Z_{dBZ} + A' \quad (4)$$

where $\ln(Z) = \ln(10) / 10 * Z_{dBZ}$

$= 0{,}23\ Z_{dBZ}$

since $Z_{dBZ} = 10 * \log(Z)$

$\log(Z) = Z_{dBZ} / 10$

$Z = 10^{\log(Z)} = 10^{Z(dBZ)/10}$

$\ln(Z) = \ln(10^{Z(dBZ)/10}) = Z_{dBZ} / 10 * \ln(10)$

Since the equation (4) is linear, of this type:

$y = m\ x + c$

where $y = \ln(R)$

$m = b'$

$x = \ln(Z) = 0{,}23\ Z_{dBZ}$

$c = A'$,

simple linear regression (by least squares estimator) can be calculated. The evaluation of this regression of equation (4) is then expressed in terms of:

- correlation coefficient (r^2)
- root-mean-square deviation (RMSE)
- standard errors of each intermediate parameter: SE(A') and SE(b')

According to Richards & Crozier (1983), the standard error of estimated parameters (SE(A') and SE(b')) is the absolute measure of goodness-of-fit of the regression equation to the sampled data that can quantify the unexplained variation of Z_e relative to R.

In order to express the standard errors of the real Z-R parameters (A and b), the 95 %-confidence interval on A and b was calculated. Considering that the 95 %-confidence (+/- 1,96 SE) on A' and b' are:

$$b'_{high} = b' + 1{,}96\ SE(b')$$

$$b'_{low} = b' - 1{,}96\ SE(b')$$

$$A'_{high} = A' + 1{,}96\ SE(A')$$

$$A'_{low} = A' - 1{,}96\ SE(A'),$$

the standard errors of parameters A and b can be expressed in terms of the 95 %-confidence interval on A' and b':

$$b_{low} = 1 / b'_{high}$$

$$b_{high} = 1 / b'_{low}$$

$$A_{low} = e^{- A'(high) / b'}$$

$$A_{high} = e^{- A'(low) / b'}$$

From those calculations, those two plots are generated for each instrument:

- ln(R) vs ln(Z)
- corresponding plots Z vs R, providing the Z-R parameters A and b.

Different Z-R relationships were derived from each instrument separately (MRR and OTT Parsivel) and analyzed according to one of the four specific situations each Z-R relationship represent:

- based on the whole data series (covering the two-years time period, no matter the precipitation class, event or season),
- based on each precipitation event class (storm type and precipitation phase),
- based on each event (many possible classes within an event),
- based on the month of the year.

In order to evaluate the stability and reliability of the Z-R parameters, the following three plots are generated for each situation or type of analysis:

- A vs b,
- A+/-SE(A) vs class, event or month (depending on the type of analysis),
- b+/-SE(b) vs class, event or month (depending on the type of analysis).

Quantitative precipitation estimates from both local DSD-measurement instruments (using the locally defined Z-R relationships) and the weather radar station (using the standard Z-R relationship) were also compared.

3.6 Comparative analysis of ground precipitation instruments

In order to compare the quantitative precipitation measured at Risvollan from different point-sampling instruments having different sampling conditions (vertical pointing radar MRR, optical disdrometer OTT Parsivel and tipping bucket rain gauge), accumulated precipitation (using R-values) over 30-minutes periods during the whole study period (from January 1st, 2012 to December 31st, 2013) are calculated and compared.

From the timing check performed as a data preprocessing step (see sub-chapter 3.3), it is assumed that all data from the three instruments covers exactly the same timesteps. Two other preprocessing steps prior to the calculation of accumulated precipitation were performed:

1) To avoid accumulation of noise, R-values below 0,1 mm/h were not accumulated, such as proposed by Holleman (2006).
2) To make sure that only timesteps with valid data from all three instruments are considered, all timesteps where at least one instrument has missing R-values are excluded from the calculation of accumulated precipitation.

The 30-minutes aggregation of the three instruments was first applied on the whole two-years period data, considering the missing R-values (i.e. there is no calculation of 30-minutes aggregation when at least one R-value in each 30-minutes period is missing).

In order to analyze the impact of the precipitation type, the 30-minutes accumulated precipitation was also calculated for each precipitation class, taken separately. Since the precipitation event classification previously performed for the estimation of Z-R parameters was excluding some valid R-values for different reasons (contradiction in the precipitation phases between instruments, high R-values for stratiform class, etc.) and that this data exclusion may have a significant impact on the accumulated precipitation over the whole time period (some wet timesteps not considered), another type of precipitation classification must be performed here. The following criteria, based only on the air temperature at the rain gauge,

were applied to classify the precipitation phase (the storm type was not part of this classification):

- If $T_{air} < -1\ ^0C$, the precipitation recorded at Risvollan (from MRR, OTT Parsivel or rain gauge) is considered as SNOW
- If $T_{air} > 4{,}5\ ^0C$, the precipitation recorded at Risvollan (from MRR, OTT Parsivel or rain gauge) is considered as RAIN
- If $-1\ ^0C < T_{air} < 4{,}5\ ^0C$, the precipitation recorded at Risvollan (from MRR, OTT Parsivel or rain gauge) is considered as MIXED

This type of classification, only based on air temperature, insures that all valid R-values over the whole two-years period is considered. The temperature threshold of $4{,}5^0$ insures to exclude possible bright band contamined measurements that were not pre-filtered.

In addition to precipitation accumulations, reflectivity and intensity values derived from both DSD instruments are also compared.

4 RESULTS

This chapter presents the most relevant results of the processing and analysis of the precipitation measurements.

The sub-chapter 4.1 concerns details and statistics about the different precipitation events detected and classified according to the method described in the sub-chapter 3.4. These identified events constitute the basic data for the following analysis. In the sub-chapter 4.2, estimates of Z-R parameters from the MRR and OTT Parsivel instruments for the different types of analysis (according to precipitation type, event and season) and their level of variability are presented in form of Z-R plots, plots of A-b parameters and standard error of those parameters. Also, precipitation estimates from those local Z-R relationships are compared to estimates from the weather radar, using the standard Z-R relationship. The last sub-chapter (4.3) focuses on the compared accumulated precipitation amounts from the three local instruments (tipping bucket rain gauge, vertical pointing radar MRR and optical disdrometer OTT Parsivel).

4.1 Detection and classification of precipitation events

From the visualization of C-band weather radar images together with the MRR vertical Z-profiles, 727 different precipitation events were detected. Each of these events contain one or more precipitation class(es). Table 4.1 presents the details of each precipitation class among those 727 events. The number of events characterized by only one precipitation type (class) is showed in the last column of the table 4.1.

4.2 Estimation of Z-R parameters

The Z-R relationship for the whole two-years period (all classified and not classified timesteps, all events, all seasons) is presented in Figure 4.1 for each instrument taken separately (vertical radar MRR and disdrometer OTT Parsivel). The two instruments may not cover the same time periods, since this estimation is based on the available data for each instrument. Since the number of timesteps with valid measurements is relatively low for the

disdrometer (only 6,6 % of the total timesteps), selecting only MRR timesteps that match with OTT Parsivel timesteps would have reduced significantly the representativity of the MRR data in the calculation of Z-R relationship. Statistics about the regression calculation and the variability of the Z-R parameters are also included in Figure 4.1.

Table 4.1 - Identified precipitation events and classes

Precipitation event classes	Nb. timesteps (min.) in all events	Nb. events where this class is present (av 727)	Nb. events characterized by only one class (precipitation type)
Rain – Stratiform (RSt)	101 842	547	256
Snow – Stratiform (SSt)	9 589	67	22
Mixed – Stratiform (MSt)	33 371	202	42
Rain – Air mass convection (RCA)	477	17	14
Rain – Conv. patches (RCP)	339	18	13
Mixed – Air mass convection (MCA)	27	3	1
Mixed – Conv. patches (MCP)	40	4	1
TOTAL classified	145 685	697	349
TOTAL not classified	168 818	30	30
TOTAL for the whole two-year period	314 503	727	727

Table 4.2 shows the quantitative precipitation differences that may occur between local instruments (using Z-R relationship derived locally) and weather radar (using the standard Z-R relationship), considering all available data.

4.2.1 Z-R relationships for different precipitation classes and instruments

The Z-R relationship for each precipitation class related to storm type and precipitation phase (RSt, SSt, MSt, RCA, RCP, MCA, MCP), considering all events, is presented in Figures 4.2 (stratiform classes) and 4.3 (convective classes) for each instrument taken separately. The two instruments may not cover the same time periods, since this estimation is based on the available data for each instrument. Statistics about the regression calculation and the variability of the Z-R parameters are also included in those figures.

(a) (b)

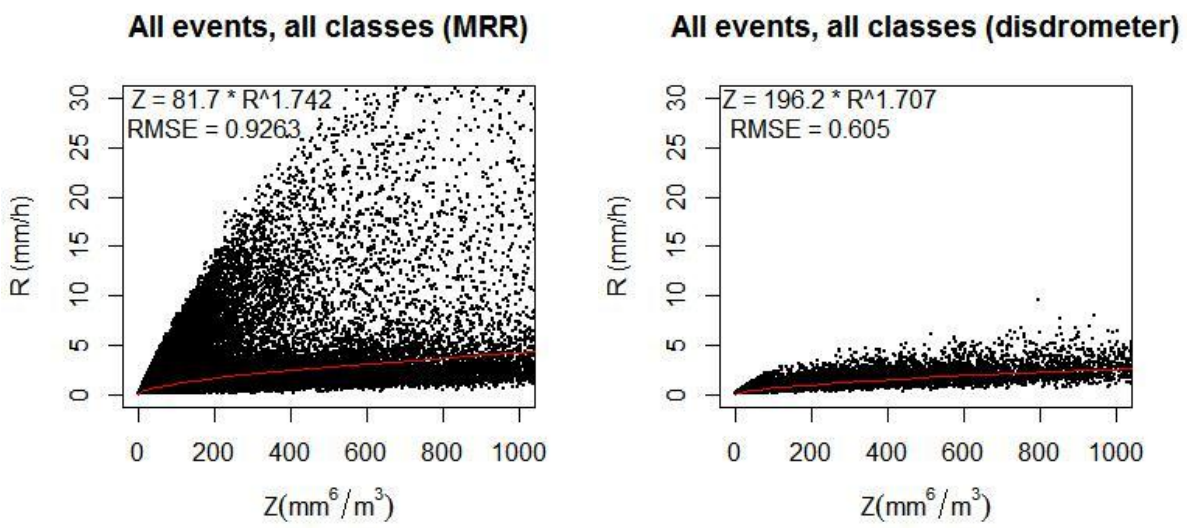

A=81,7 (A_{max}= 83,4/A_{min}=80,1)
b=1,742 (b_{max}= 1,750/b_{min}=1,733)
N=122851
RMSE=0,9263
r^2=0,5761

A=196,2 (A_{max}= 200,0/A_{min}=192,4)
b=1,707 (b_{max}= 1,714/b_{min}=1,700)
N=29949
RMSE=0,6050
r^2=0,8814

Figure 4.1 - Z-R relationship for the whole two-years period (all classified and not classified timesteps, all events, all seasons) (a) MRR (b) OTT Parsivel

Table 4.2 - Estimated R (in mm/h) from the Z-R relationships, all available data
(% compared with standard Z-R relationship)

ALL DATA	Z=10 dBZ or 10 mm^6/m^3	Z=20 dBZ or 100 mm^6/m^3	Z=30 dBZ or 1000 mm^6/m^3	Z=40 dBZ or 10000 mm^6/m^3	Z=50 dBZ or 100000 mm^6/m^3
Standard Z-R A=200 b=1,6	0,15	0,65	2,73	11,53	48,62
Z-R from MRR A=81,7 b=1,6	0,30 (+ 95 %)	1,12 (+ 73 %)	4,21 (+ 54 %)	15,79 (+ 37 %)	59,23 (+ 22 %)
Z-R from OTT A=196,2 b=1,707	0,17 (+ 14 %)	0,67 (+ 4 %)	2,60 (- 5 %)	10,00 (- 13 %)	38,55 (- 21 %)

(a)

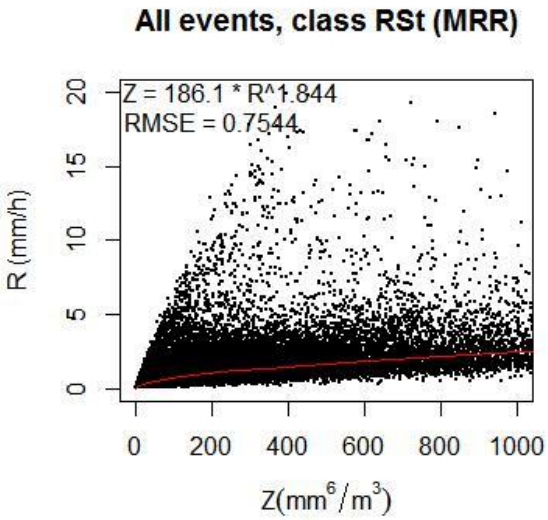

A=186,1 (A_{max}= 190,0/A_{min}=182,3)
b=1,844 (b_{max}= 1,852/b_{min}=1,835)
N=70612
RMSE=0,7544
r^2=0,7101

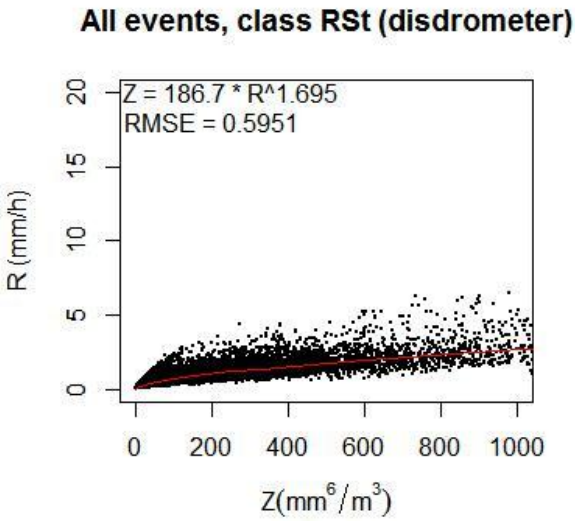

A=186,7 (A_{max}= 191,8/A_{min}=181,8)
b=1,695 (b_{max}= 1,705/b_{min}=1,685)
N=16057
RMSE=0,5951
r^2=0,8680

(b)

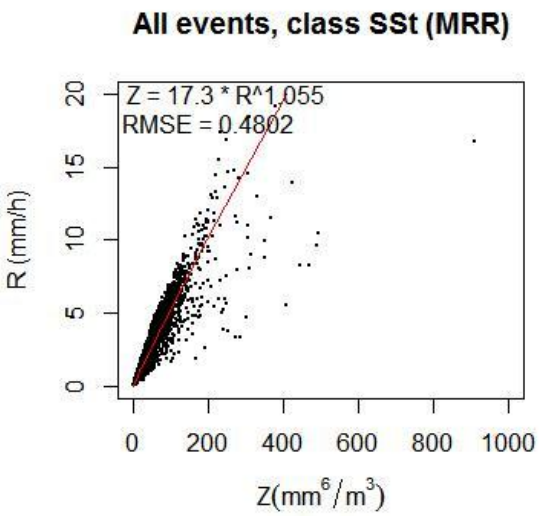

A=17,3 (A_{max}= 17,5/A_{min}=17,0)
b=1,055 (b_{max}= 1,060/b_{min}=1,050)
N=7488
RMSE=0,4802
r^2=0,9582

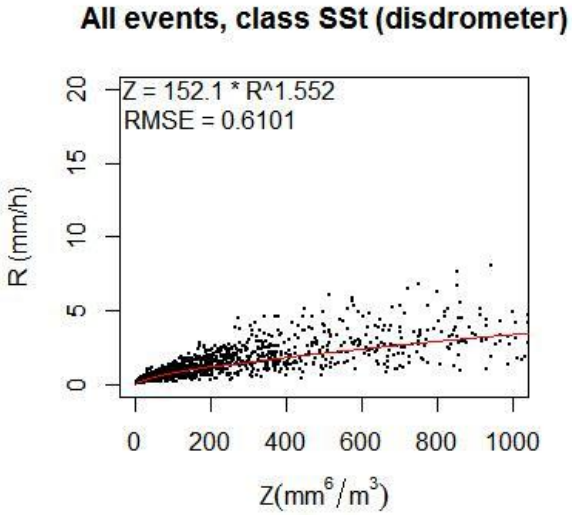

A=152,1 (A_{max}= 163,2/A_{min}=141,7)
b=1,552 (b_{max}= 1,575/b_{min}=1,529)
N=2317
RMSE=0,6101
r^2=0,8805

Figure 4.2 - Z-R relationship for each stratiform class and each instrument:
(a) rain (RSt) (b) snow (SSt)

(c)

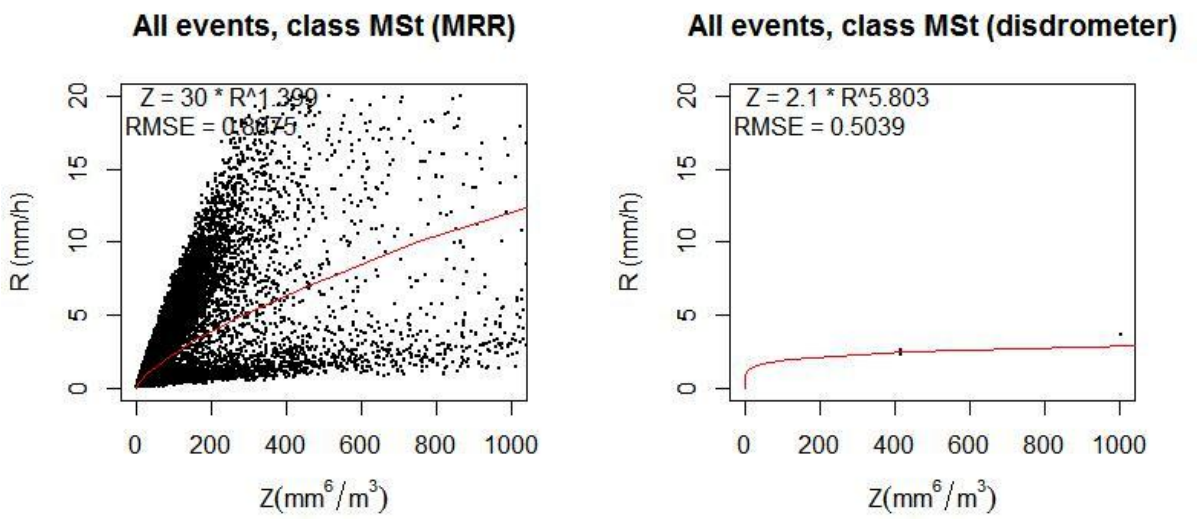

A=30,0 (A_{max}= 30,9/A_{min}=29,0)
b=1,399 (b_{max}= 1,411/b_{min}=1,387)
N=24741
RMSE=0,8675
r^2=0,6816

A=2,1 (A_{max}= 2536,4/A_{min}=2,1)
b=5,803 (b_{max}= 114,372/b_{min}=2,977)
N=5
RMSE=0,5039
r^2=0,5870

Figure 4.2 (continued) Z-R relationship for each stratiform class and each instrument:
(c) mixed (MSt)

(a)

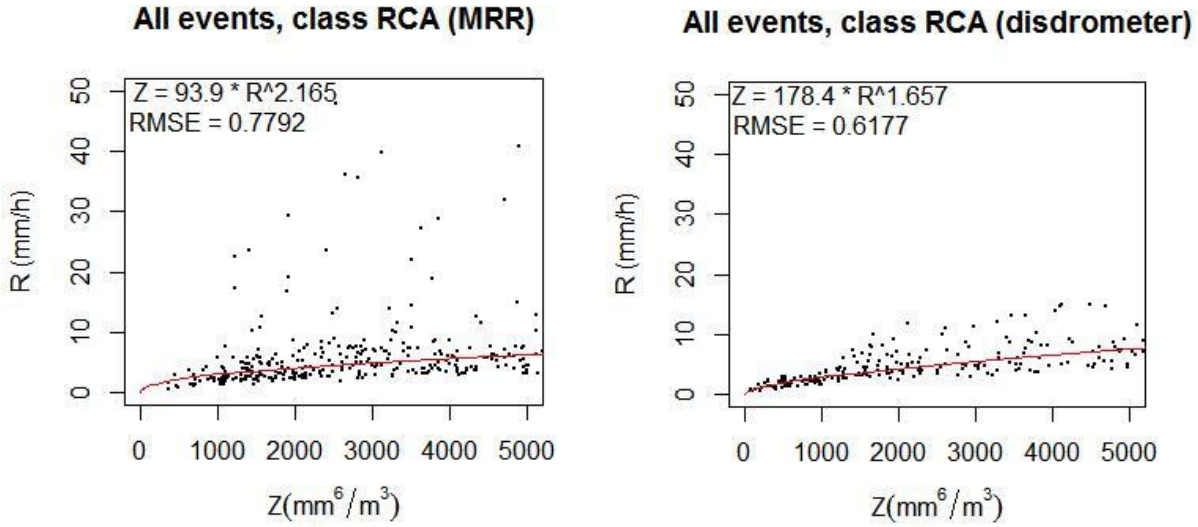

A=93,9 (A_{max}= 302,6/A_{min}=29,1)
b=2,165 (b_{max}= 2,522/b_{min}=1,897)
N=477
RMSE=0,7792
r^2=0,2874

A=178,4 (A_{max}= 307,0/A_{min}=103,6)
b=1,657 (b_{max}= 1,778/b_{min}=1,551)
N=289
RMSE=0,6177
r^2=0,7419

Figure 4.3 - Z-R relationship for each convective class and each instrument:
(a) rain - air mass convection (RCA)

(b)

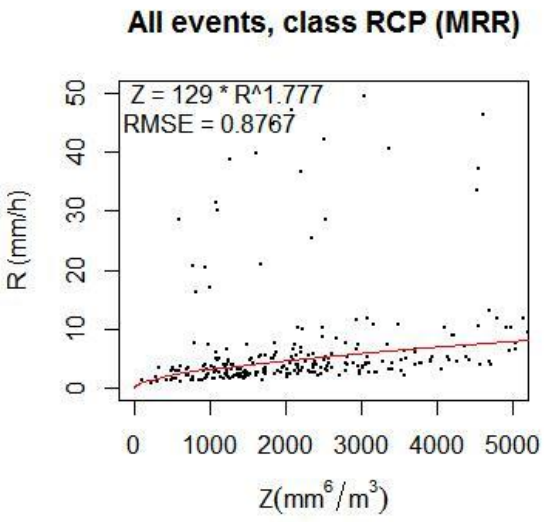

A=129,0 (A_{max}= 479,7/A_{min}=34,7)
b=1,777 (b_{max}= 2,131/b_{min}=1,524)
N=339
RMSE=0,8767
r^2=0,2930

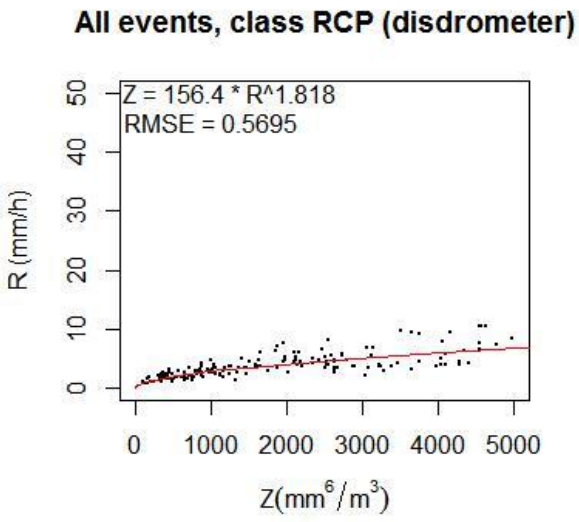

A=156,4 (A_{max}= 263,0/A_{min}=93,0)
b=1,818 (b_{max}= 1,950/b_{min}=1,703)
N=208
RMSE=0,5695
r^2=0,8023

(c)

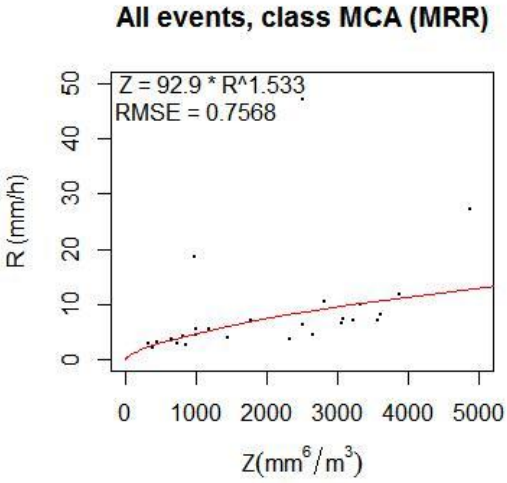

A=92,9 (A_{max}= 2095,3/A_{min}=4,1)
b=1,533 (b_{max}= 2,634/b_{min}=1,081)
N=27
RMSE=0,7568
r^2=0,4678

(d)

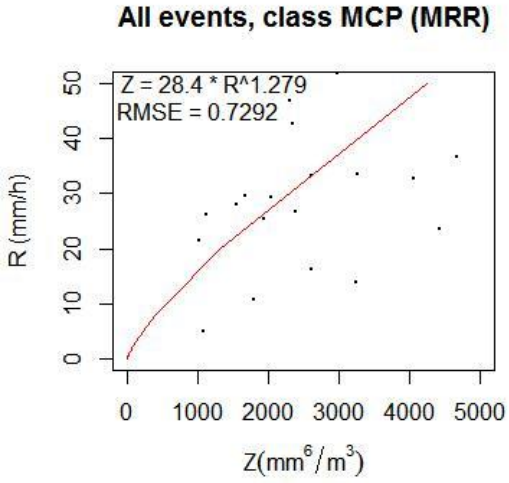

A=28,4 (A_{max}= 453,0/A_{min}=1,8)
b=1,279 (b_{max}= 1,935/b_{min}=0,955)
N=40
RMSE=0,7292
r^2=0,468

Figure 4.3 (continued) Z-R relationship for each convective class and each instrument:
(b) rain – convective patches (RCP) (c) mixed – air mass convection (MCA)
(d) mixed – convective patches (MCP)
Note: no valid Z-R relationship for mixed precipitation from the disdrometer

Table 4.3 shows the differences in precipitation estimates between local instruments (using Z-R relationship derived locally) and weather radar (using the standard Z-R relationship), considering each precipitation class separately.

Table 4.3 - Estimated R (in mm/h) from the class-related Z-R relationships
(% compared with standard Z-R relationship)

Class-related data		Z=10 dBZ or 10 mm^6/m^3	Z=20 dBZ or 100 mm^6/m^3	Z=30 dBZ or 1000 mm^6/m^3	Z=40 dBZ or 10^4 mm^6/m^3	Z=50 dBZ or 10^5 mm^6/m^3
Standard Z-R A=200 b=1,6		0,15	0,65	2,73	11,53	48,62
Z-R for RAIN-STRATIFORM	MRR A=186,1 b=1,844	0,20 (+ 33 %)	0,71 (+ 10 %)	2,49 (- 9 %)	8,68 (- 25 %)	30,24 (- 38 %)
	OTT A=186,7 b=1,695	0,18 (+ 16 %)	0,69 (+ 7 %)	2,69 (- 2 %)	10,47 (- 9 %)	40,73 (- 16 %)
Z-R for SNOW-STRATIFORM	MRR A=17,3 b=1,055	0,59 (+ 287 %)	5,28 (+ 714 %)	46,78 (+ 1611 %)	414,92 (+ 3498 %)	3679,88 (+ 7468 %)
	OTT A=152,1 b=1,552	0,17 (+ 13 %)	0,76 (+ 18 %)	3,36 (+ 23 %)	14,84 (+ 29 %)	65,41 (+ 35 %)
Z-R for MIXED-STRATIFORM	MRR A=30,0 b=1,399	0,46 (+ 197 %)	2,36 (+ 265 %)	12,26 (+ 348 %)	63,58 (+ 451 %)	329,72 (+ 578 %)
	OTT A=2,1 b=5,803	1,31 (+ 751 %)	1,95 (+ 200 %)	2,89 (+ 6 %)	4,30 (- 63 %)	6,40 (- 87 %)
Z-R for RAIN-AIR MASS CONVECTION	MRR A=93,9 b=12,165	0,36 (+ 131 %)	1,03 (+ 59 %)	2,98 (+ 9 %)	8,64 (- 25 %)	25,02 (- 49 %)
	OTT A=178,4 b=1,657	0,18 (+ 14 %)	0,71 (+ 9 %)	2,83 (+ 3 %)	11,36 (- 1 %)	45,58 (- 6 %)
Z-R for RAIN-CONVECTIVE PATCHES	MRR A=129,0 b=1,777	0,24 (+ 54 %)	0,87 (+ 34 %)	3,17 (+ 16 %)	11,57 (+ 0 %)	42,27 (- 13 %)
	OTT A=156,4 b=1,818	0,22 (+ 43 %)	0,78 (+ 21 %)	2,77 (+ 1 %)	9,85 (- 15 %)	34,94 (- 28 %)
Z-R for MIXED-AIR MASS CONVECTION	MRR A=92,9 b=1,533	0,23 (+ 52 %)	1,05 (+ 62 %)	4,71 (+ 72 %)	21,16 (+ 83 %)	95,02 (+ 95 %)
	OTT	NA	NA	NA	NA	NA
Z-R for MIXED-CONVECTIVE PATCHES	MRR A=30,0 b=1,399	0,44 (+ 188 %)	2,68 (+ 313 %)	16,19 (+ 492 %)	97,98 (+ 750 %)	592,94 (+ 1119 %)
	OTT	NA	NA	NA	NA	NA

4.2.2 Z-R relationships for different events and instruments

All Z-R relationships calculated for each precipitation event, considering all classes (387 events), is presented in Figure 4.4 (each instrument taken separately). Figure 4.5 shows all event-related Z-R relationships considering each precipitation class separately (each instrument taken separately). In both figures, the standard Z-R relationship is showed as a reference (red line). The variability of those class-related Z-R relationships is also presented in Figure 4.6 (for all classes and each class) in form of A-b parameter plots. Figure 4.7 shows event-related A-b standard error plots for stratiform classes (derived from MRR). The A and b-value are represented in purple, +SE(A) and +SE(b) corresponding to A_{max} and b_{max} are in red, while -SE(A) and -SE(b) corresponding to A_{min} and b_{min} are represented in green.

(a) (b)

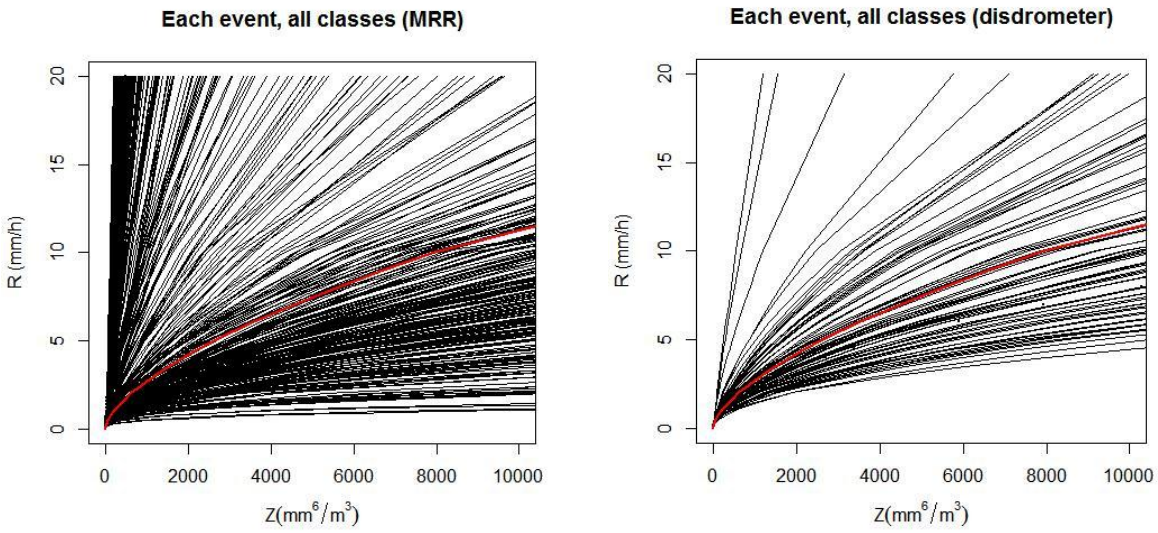

Figure 4.4 - Z-R relationships for each event, all precipitation classes (a) MRR (b) OTT Parsivel
Red line represents the standard Z-R relationship (Marshall-Palmer: $Z=200R^{1,6}$)

(a)

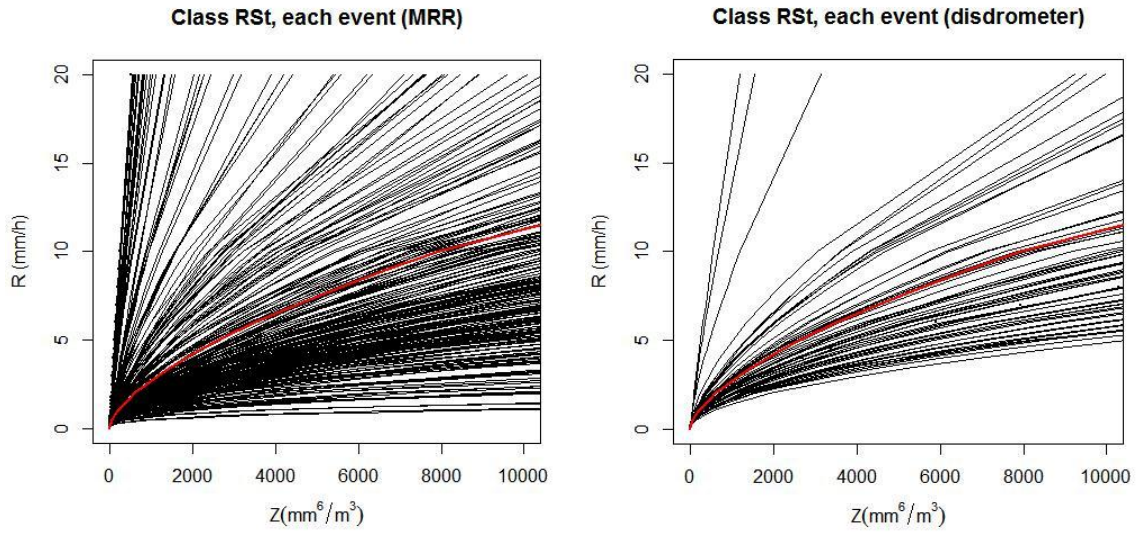

(b)

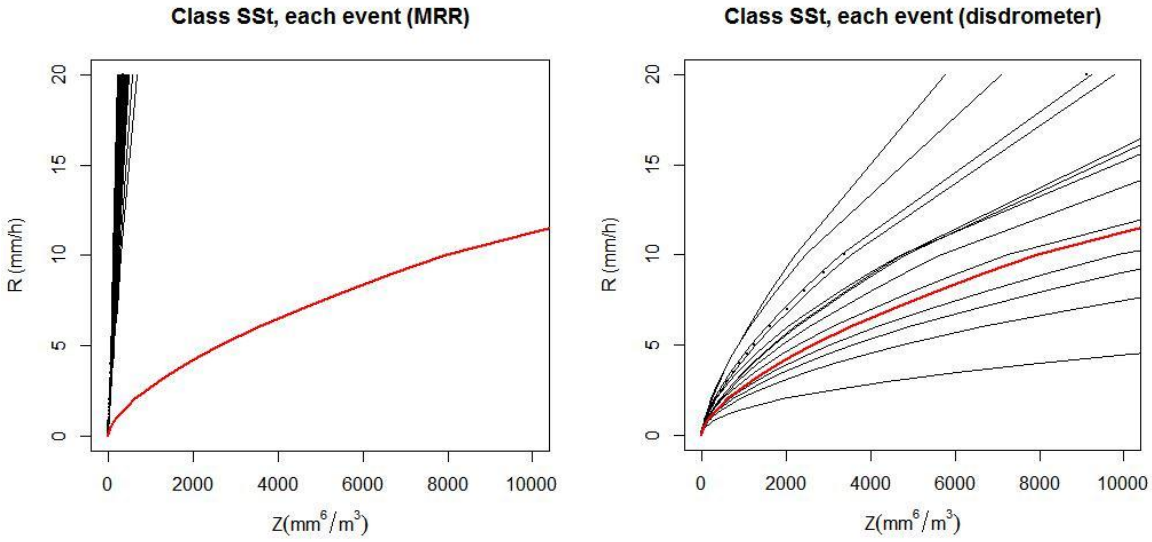

Figure 4.5 - Z-R relationships for each event, each class and each instrument:
(a) RSt (b) SSt
Red line represents the standard Z-R relationship (Marshall-Palmer: $Z=200R^{1,6}$)
Note: no valid Z-R relationship for mixed precipitation (stratiform and convective) from both instruments

(c)

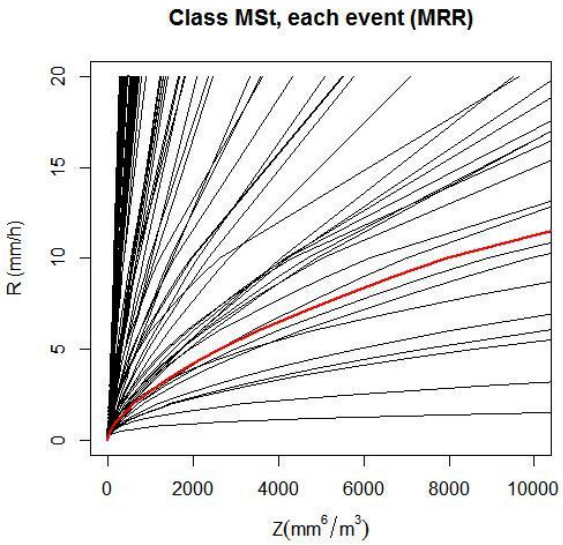

(d)

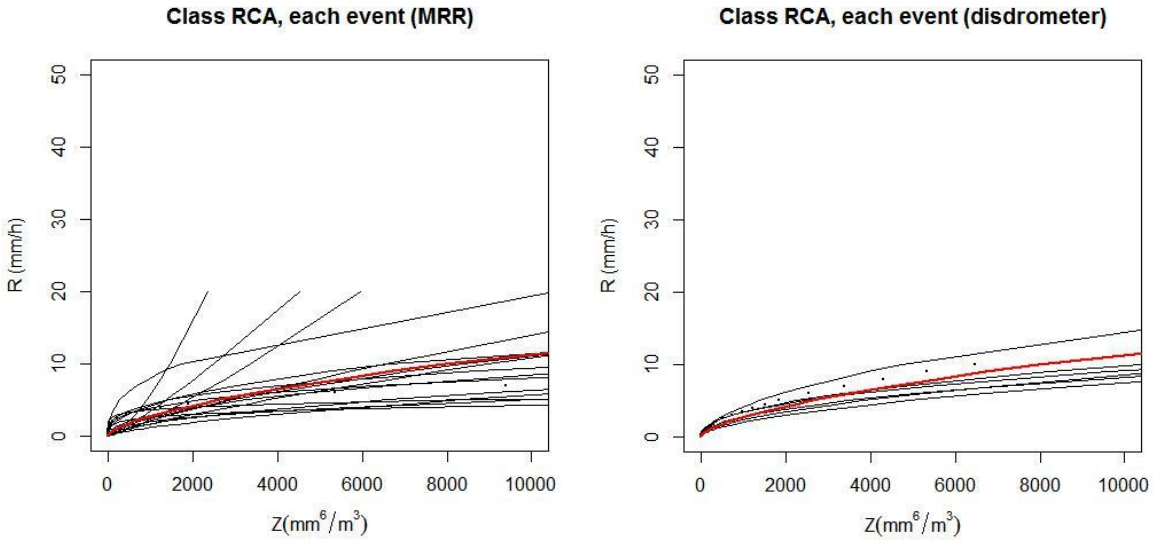

Figure 4.5 (continued) Z-R relationships for each event, each class and each instrument:
(c) MSt (d) RCA
Red line represents the standard Z-R relationship (Marshall-Palmer: $Z=200R^{1,6}$)
Note: no valid Z-R relationship for mixed precipitation (stratiform and convective) from both instruments

(e)

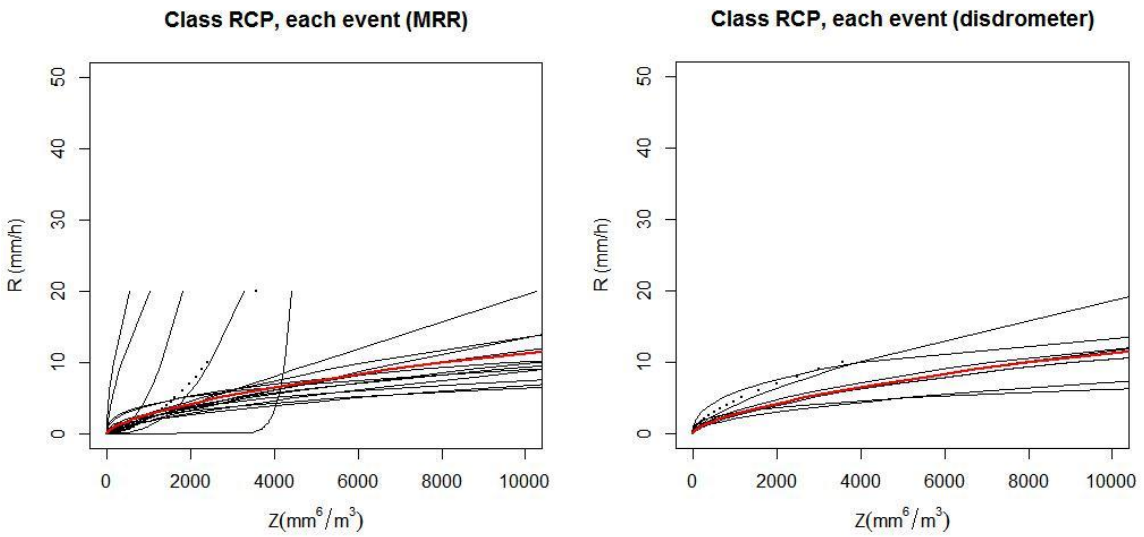

Figure 4.5 (continued) Z-R relationships for each event, each class and each instrument: (e) RCP
Red line represents the standard Z-R relationship (Marshall-Palmer: $Z=200R^{1,6}$)
Note: no valid Z-R relationship for mixed precipitation (stratiform and convective) from both instruments

(a)

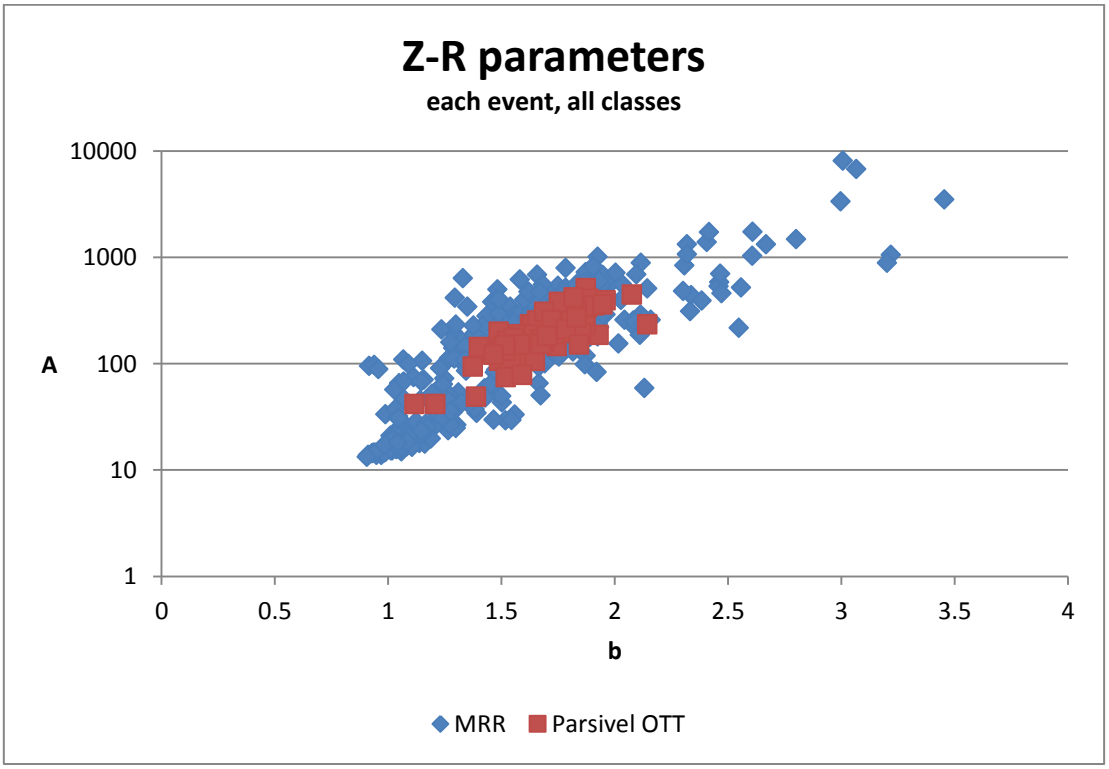

Figure 4.6 - A-b plots for each event and each instrument: (a) all classes
(red squares: A,b from OTT Parsivel; blue diamonds: A,b from MRR)

(b)

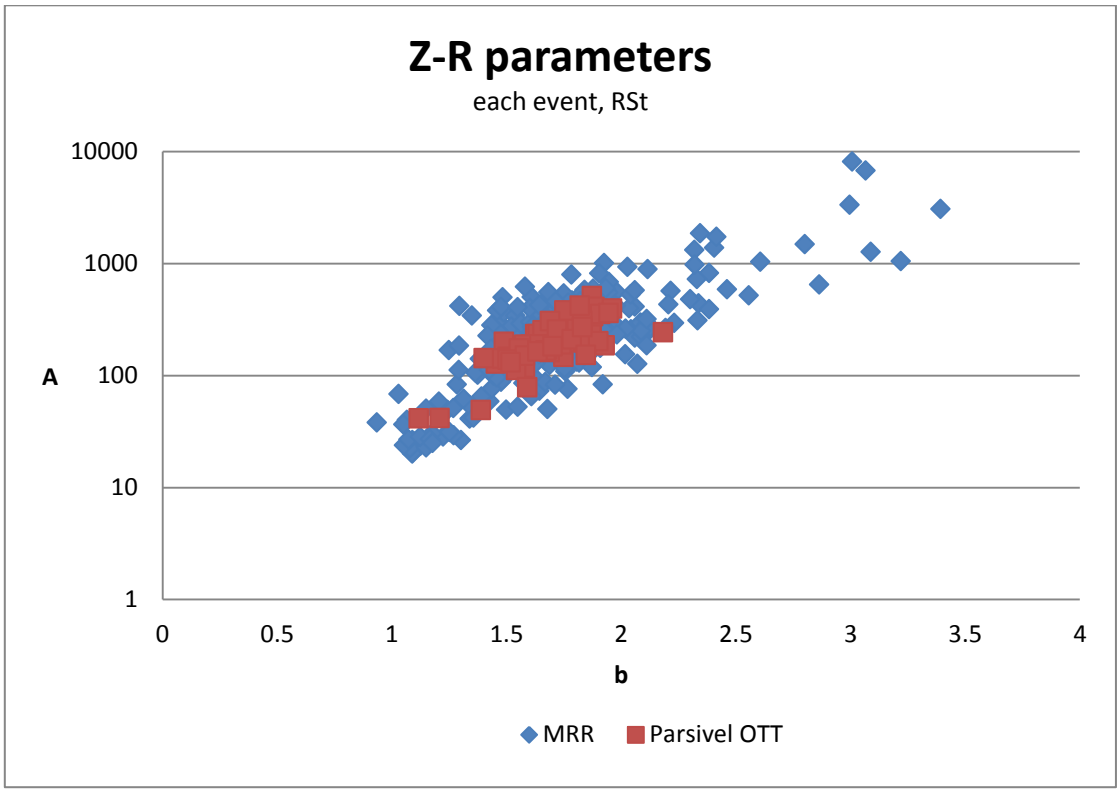

(c)

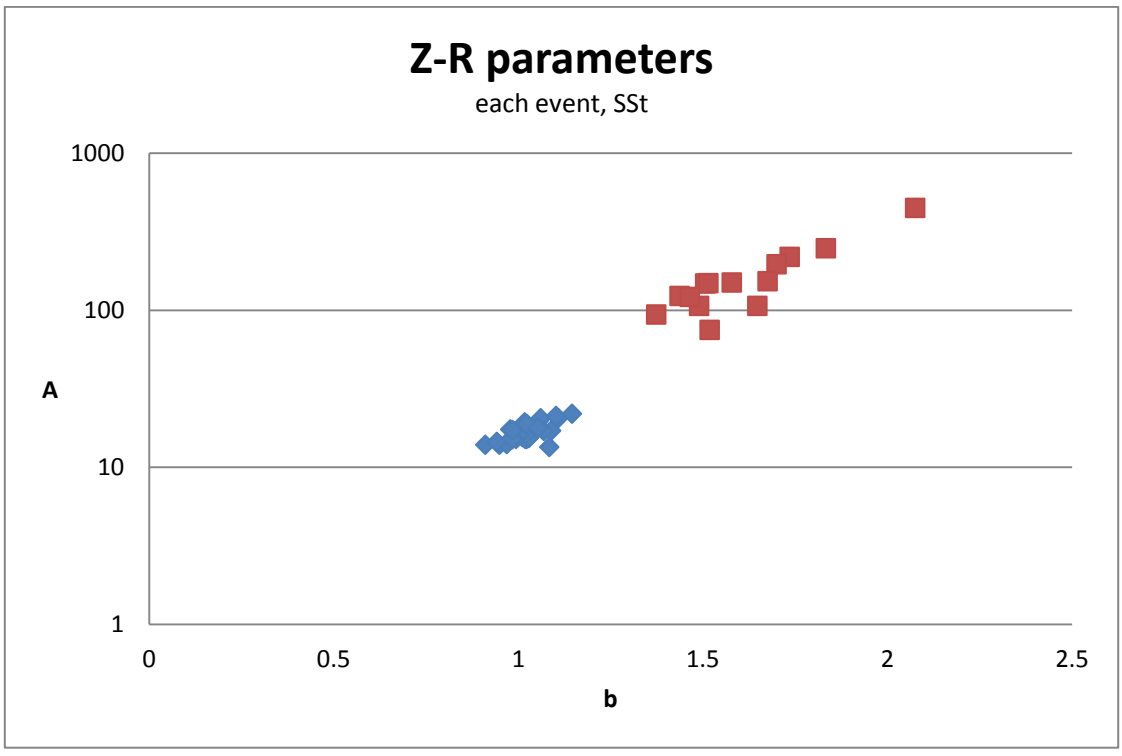

Figure 4.6 (continued) A-b plots for each event and each instrument: (b) RSt (c) SSt (red squares: A,b from OTT Parsivel; blue diamonds: A,b from MRR)

(d)

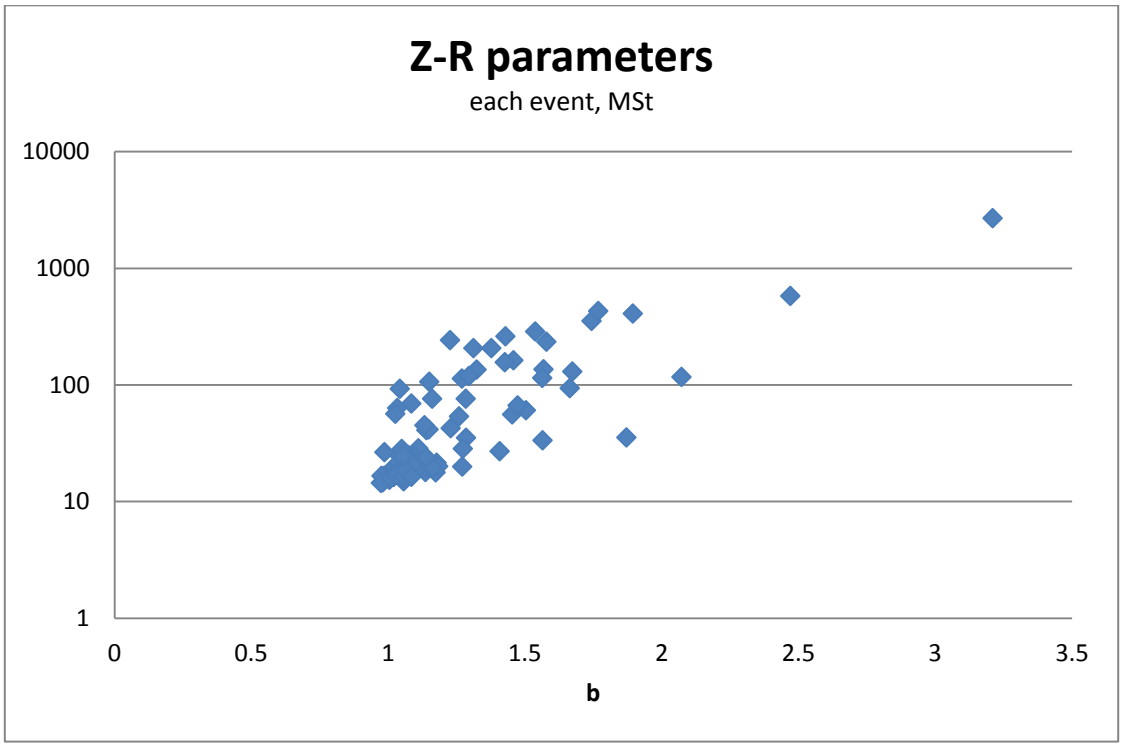

(e)

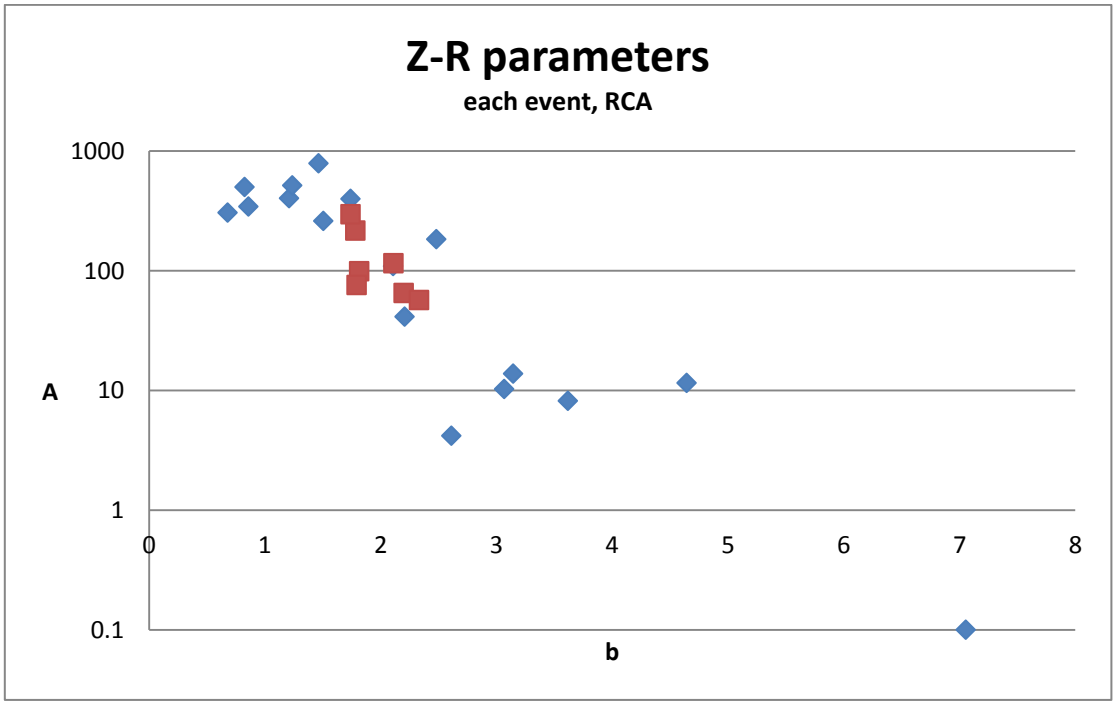

Figure 4.6 (continued) A-b plots for each event and each instrument: (d) MSt (e) RCA (red squares: A,b from OTT Parsivel; blue diamonds: A,b from MRR)

(f)

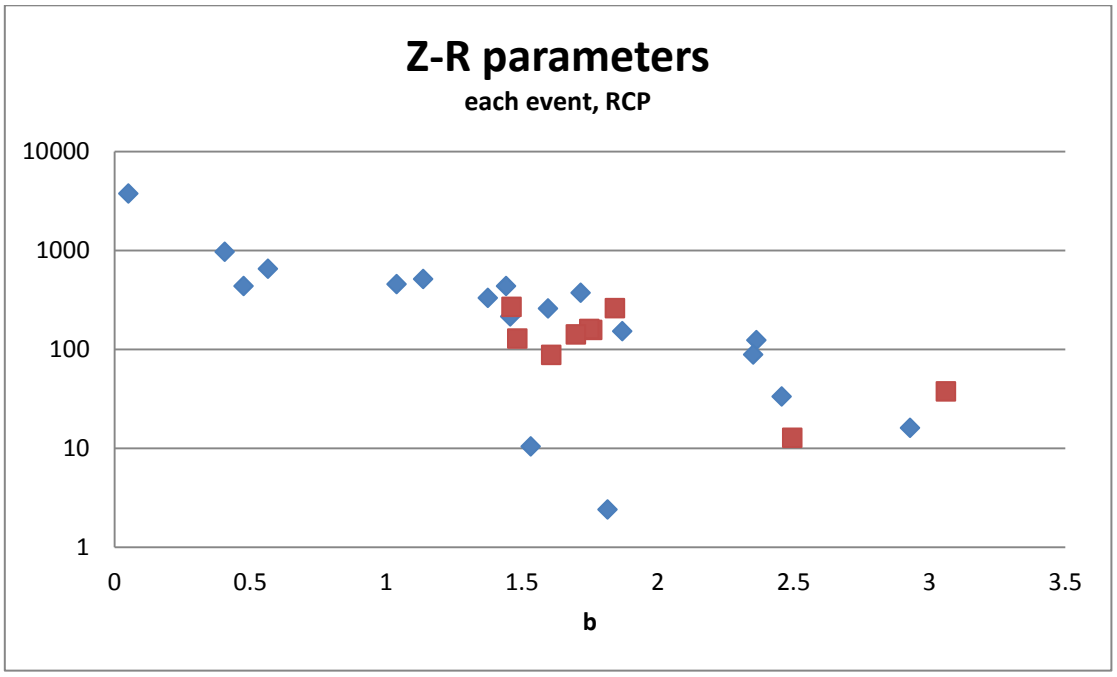

Figure 4.6 (continued) A-b plots for each event and each instrument: (f) RCP (red squares: A,b from OTT Parsivel; blue diamonds: A,b from MRR)

(a)

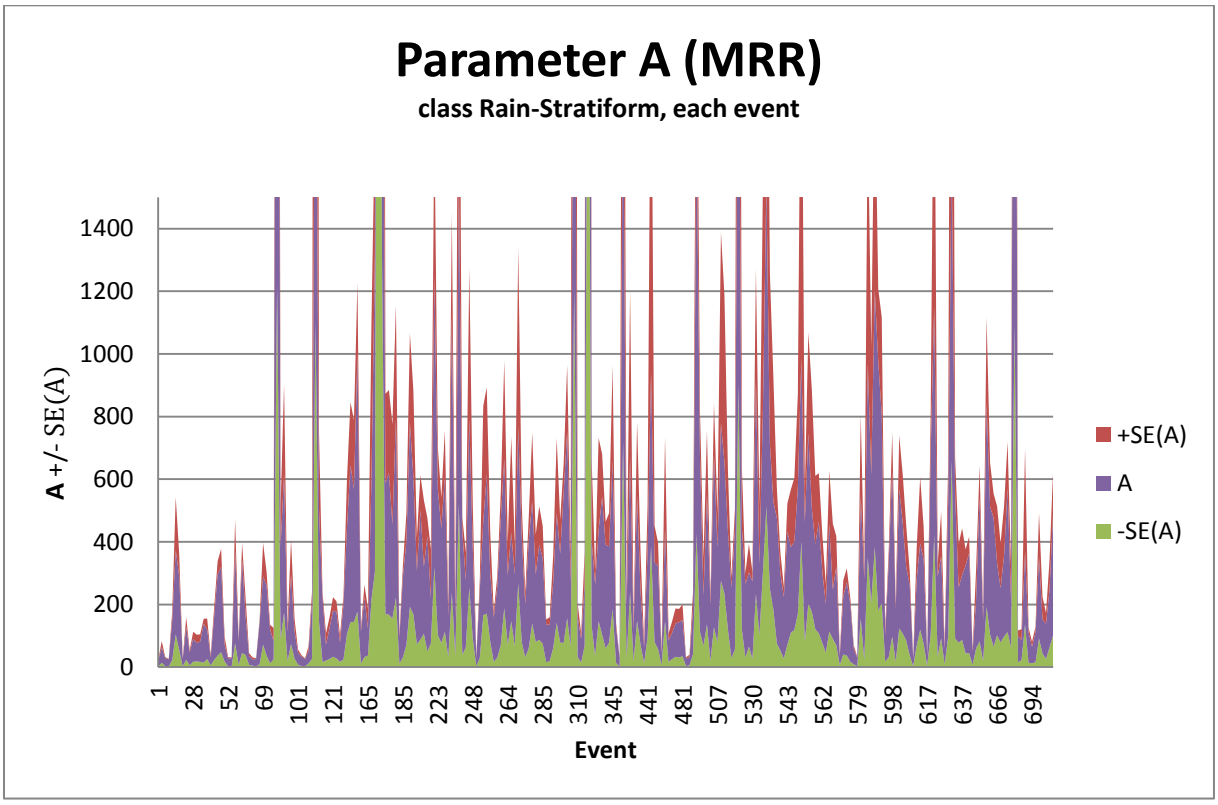

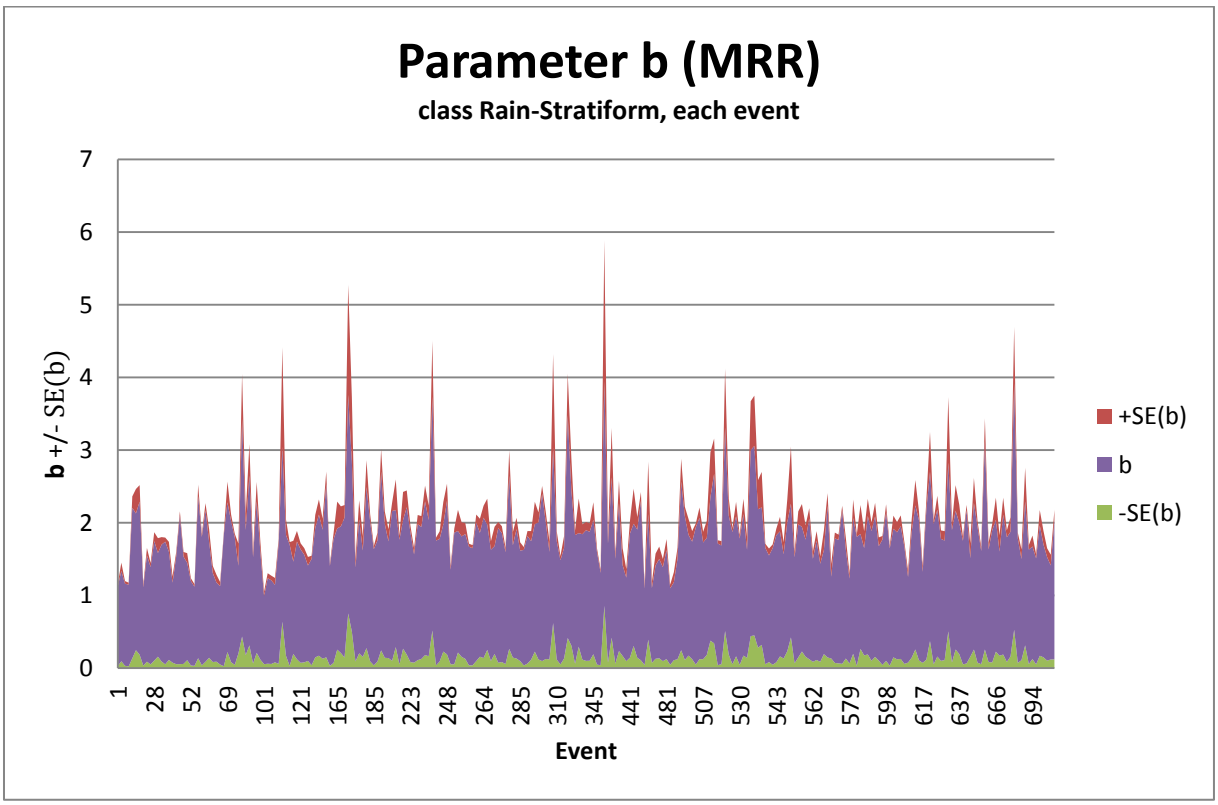

Figure 4.7 - SE(A), SE(b) plots for stratiform classes: (a) rain
(Purple: A or b-value, Red: +SE(A) or +SE(b) corresponding to A_{max} or b_{max}, Green: -SE(A) or -SE(b) corresponding to A_{min} or b_{min})

(b)

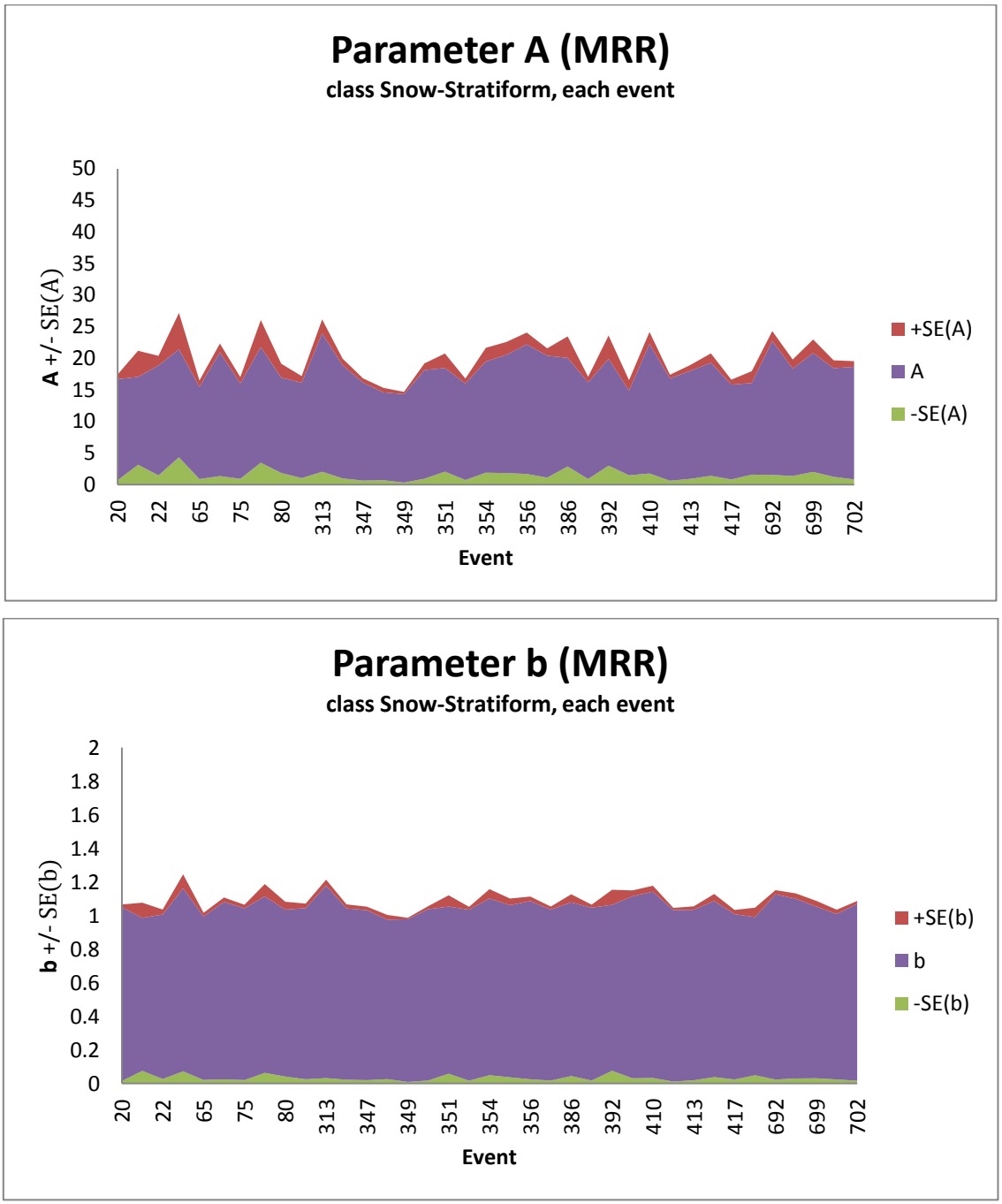

Figure 4.7 (continued) SE(A), SE(b) plots for stratiform classes: (b) snow
(Purple: A or b-value, Red: +SE(A) or +SE(b) corresponding to A_{max} or b_{max}, Green: -SE(A) or -SE(b) corresponding to A_{min} or b_{min})

(c)

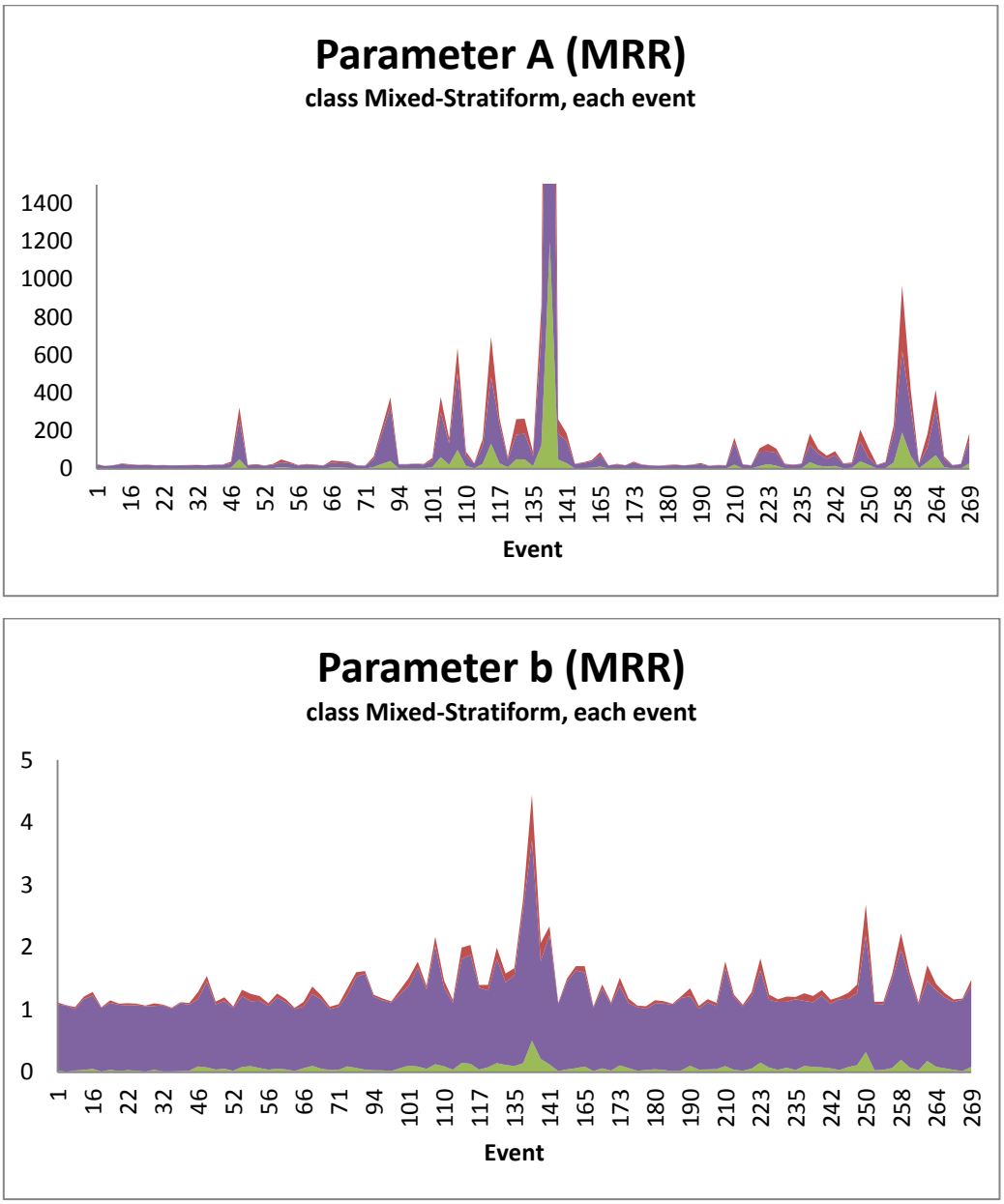

Figure 4.7 (continued) SE(A), SE(b) plots for stratiform classes: (c) mixed (Purple: A or b-value, Red: +SE(A) or +SE(b) corresponding to A_{max} or b_{max}, Green: -SE(A) or -SE(b) corresponding to A_{min} or b_{min})

Also, the Z-R parameters generated by both instruments are compared for two single events, one of the type Rain-Stratiform including air mass convection (the two classes are processed separately) and one of the type Snow-Stratiform. Z-R relationships are derived separately for each precipitation class in each of those two events. Figure 4.8 shows those event-related Z-R relationships with regression statistics (RMSE, r^2, standard errors of both parameters). The first event (# 638) occurs between October 6th, 2013 20:20 and October 7th, 2013 13:42 and consists of stratiform rain periods interspersed with six short air mass convection periods

lasting from 2 to 27 minutes. The stratiform snow event (# 387) occurs on February 1st, 2013 between 01:42 and 12:32.

(a)

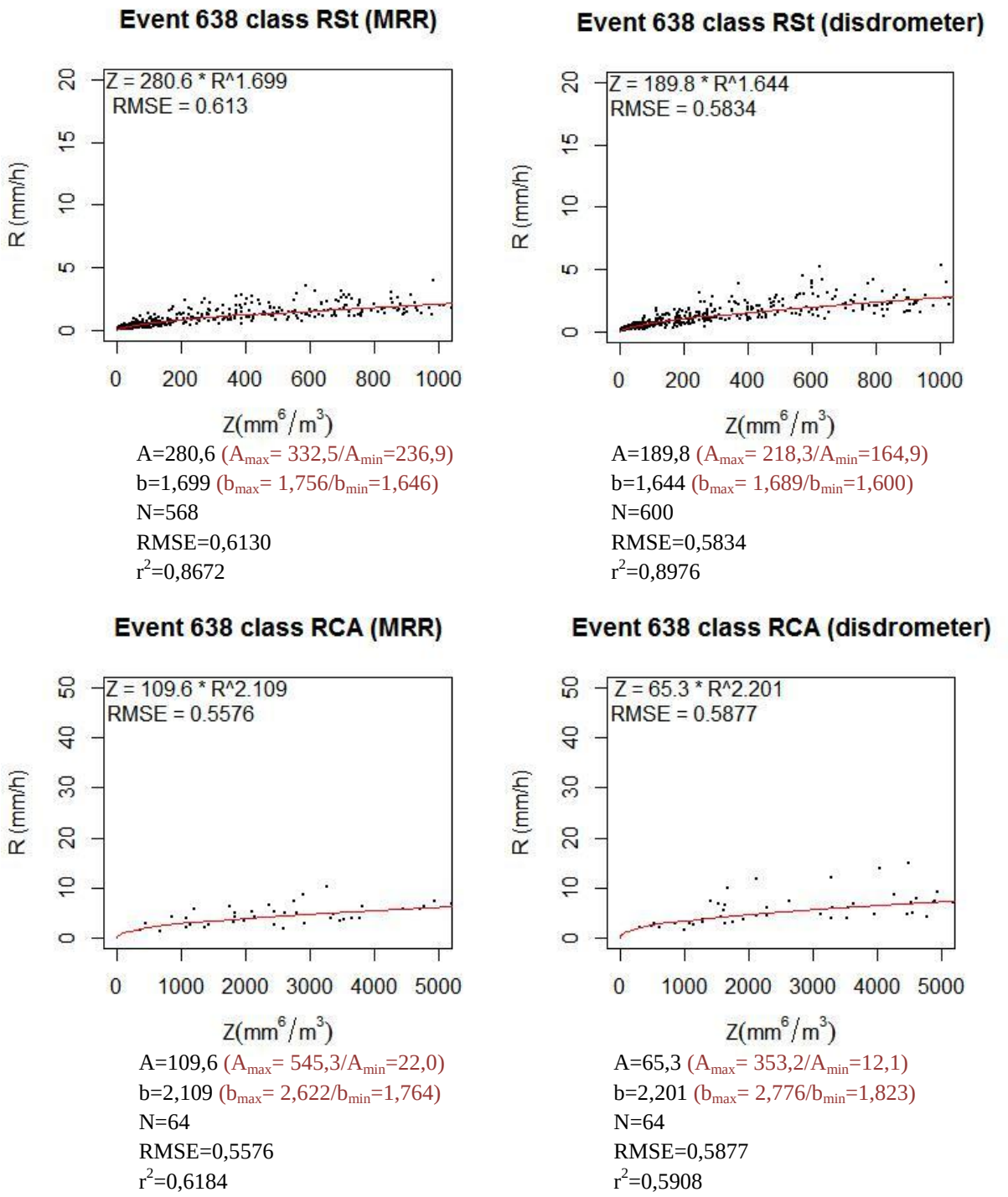

Figure 4.8 - Z-R relationships derived from MRR and OTT Parsivel within two events:
(a) Rain-Stratiform with air mass convection (event # 638), each class processed separately
Note: Timesteps do not necessarily cover the same time periods for each instrument. Only stratiform periods lasting for at least 30 minutes are considered (no such restriction for air mass convection periods).

(b)

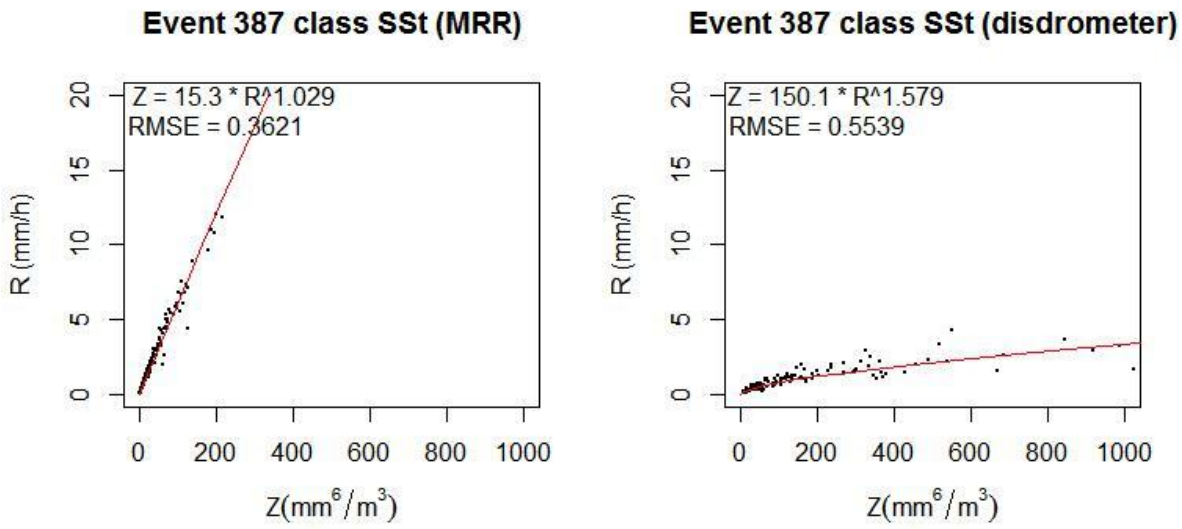

A=15,3 (A_{max}= 16,2/A_{min}=14,4)
b=1,029 (b_{max}= 1,047/b_{min}=1,011)
N=154
RMSE=0,3621
r^2=0,9879

A=150,1 (A_{max}= 188,7/A_{min}=119,4)
b=1,579 (b_{max}= 1,663/b_{min}=1,502)
N=175
RMSE=0,5539
r^2=0,900

Figure 4.8 (continued) Z-R relationships derived from MRR and OTT Parsivel within two events: (b) Snow-Stratiform (event # 387)
Note: Timesteps do not necessarily cover the same time periods for each instrument. Only stratiform periods lasting for at least 30 minutes are considered (no such restriction for air mass convection periods).

Table 4.4 shows the estimated precipitation intensities (R) derived from both instruments for those two events and three precipitation classes (event-related Z-R relationships for each class) compared with the R-estimates 1) from the standard Z-R relationship and 2) from the class-related Z-R relationships. These estimates comparison gives information 1) on the magnitude of the precipitation intensity variance that is expected locally during a specific event and 2) on the variability differences between events of the same type (class) and within those two events. By comparing Table 4.2 (together with Z-R plots in Figure 4.1) and Table 4.4 (together with the Z-R plots in Figure 4.2), it is also possible to comment generally on the variability differences between events of any type (all data) and within events of the same type.

Table 4.4 - Estimated R (in mm/h) for two specific events covering three types of precipitation classes (in bold)

Z-R relationships derived separately for each of those events and each of those classes, comparison between the R-estimates from the standard and class-related Z-R relationships
(% compared with standard Z-R relationship)

Class-related events		Z=10 dBZ or 10 mm^6/m^3	Z=20 dBZ or 100 mm^6/m^3	Z=30 dBZ or 1000 mm^6/m^3	Z=40 dBZ or 10^4 mm^6/m^3	Z=50 dBZ or 10^5 mm^6/m^3
All classes	Standard Z-R A=200 b=1,6	0,15	0,65	2,73	11,53	48,62
Rain stratiform (all events)	MRR A=186,1 b=1,844	0,20 (+ 33 %)	0,71 (+ 10 %)	2,49 (- 9 %)	8,68 (- 25 %)	30,24 (- 38 %)
	OTT A=186,7 b=1,695	0,18 (+ 16 %)	0,69 (+ 7 %)	2,69 (- 2 %)	10,47 (- 9 %)	40,73 (- 16 %)
Rain stratiform (event # 638)	**Z-R from MRR A=280,6 b=1,699**	**0,14 (- 9 %)**	**0,54 (- 16 %)**	**2,11 (- 23 %)**	**8,19 (- 29 %)**	**31,77 (- 35 %)**
	Z-R from OTT A=189,8 b=1,644	**0,17 (+ 9 %)**	**0,68 (+ 4 %)**	**2,75 (+ 0 %)**	**11,15 (- 3 %)**	**45,24 (- 7 %)**
Rain air mass convection (all events)	MRR A=93,9 b=12,165	0,36 (+ 131 %)	1,03 (+ 59 %)	2,98 (+ 9 %)	8,64 (- 25 %)	25,02 (- 49 %)
	OTT A=178,4 b=1,657	0,18 (+ 14 %)	0,71 (+ 9 %)	2,83 (+ 3 %)	11,36 (- 1 %)	45,58 (- 6 %)
Rain air mass convection within stratiform event (event # 638)	**Z-R from MRR A=109,6 b=2,109**	**0,32 (+ 109 %)**	**0,96 (+ 48 %)**	**2,85 (+ 4 %)**	**8,50 (- 26 %)**	**25,33 (- 48 %)**
	Z-R from OTT A=65,3 b=2,201	**0,43 (+ 177 %)**	**1,21 (+ 87 %)**	**3,45 (+ 26 %)**	**9,83 (- 15 %)**	**28 (- 42 %)**
Snow stratiform (all events)	MRR A=17,3 b=1,055	0,59 (+ 287 %)	5,28 (+ 714 %)	46,78 (+ 1611 %)	414,92 (+ 3498 %)	3679,88 (+ 7468 %)
	OTT A=152,1 b=1,552	0,17 (+ 13 %)	0,76 (+ 18 %)	3,36 (+ 23 %)	14,84 (+ 29 %)	65,41 (+ 35 %)
Snow stratiform (event # 387)	**Z-R from MRR A=15,3 b=1,029**	**0,66 (+ 330 %)**	**6,20 (+ 856 %)**	**58,10 (+ 2025 %)**	**544,46 (4622 %)**	**5102,50 (+ 10394 %)**
	Z-R from OTT A=150,1 b=1,579	**0,18 (+ 17 %)**	**0,77 (+ 19 %)**	**3,32 (+ 22 %)**	**14,29 (+ 24 %)**	**61,41 (+ 26 %)**

4.2.3 Z-R relationships for different months and instruments

The Z-R relationships for each month generated by each instrument, considering all precipitation classes, are presented in Figure 4.9. Figure 4.10 shows the Z-R relationships for each month and each precipitation class. The two instruments may not cover the same time periods, since this estimation is based on the available data for each instrument.

(a) (b)

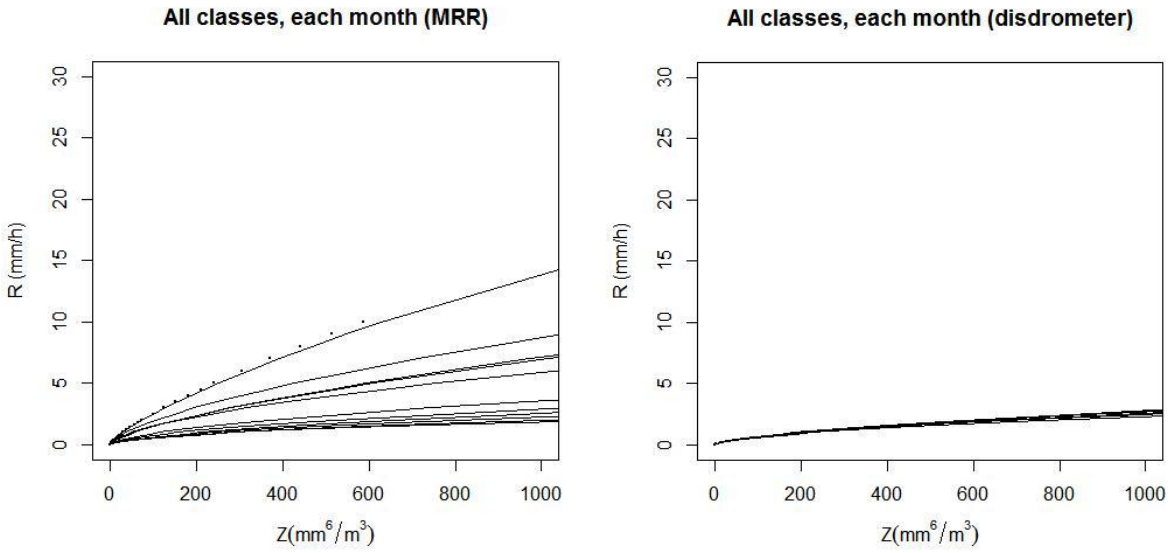

Figure 4.9 - Z-R relationships for each month, all precipitation classes: (a) MRR (b) OTT Parsivel

(a)

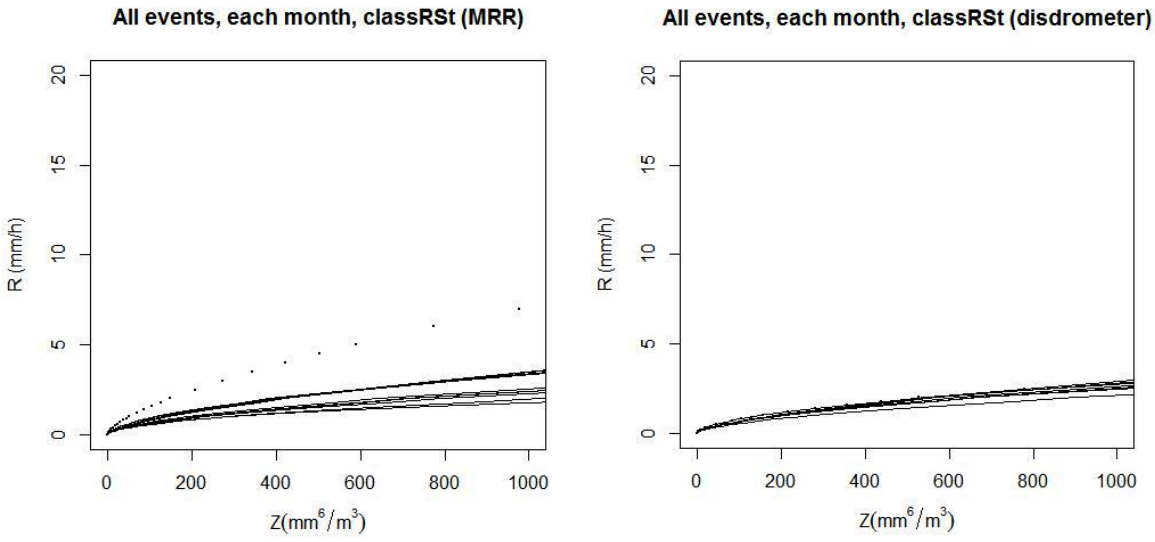

Figure 4.10 - Z-R relationships for each month, each precipitation class, each instrument: (a) RSt

(b)

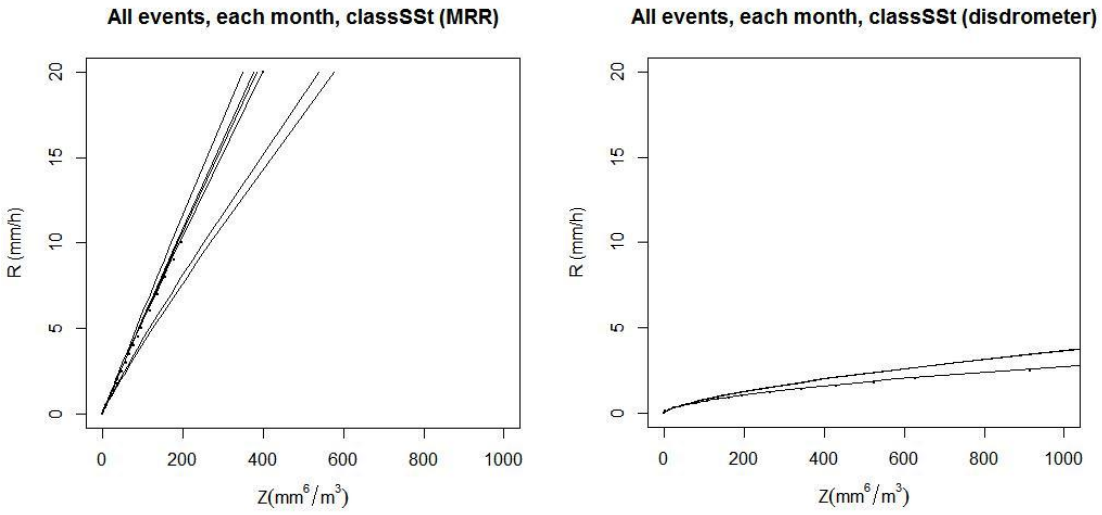

(c)

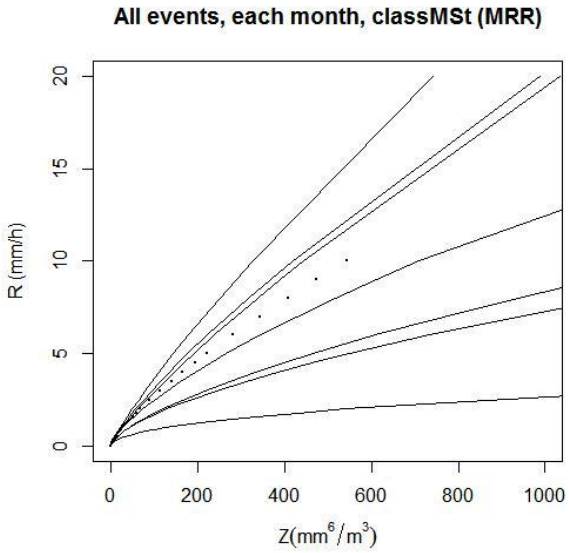

Figure 4.10 (continued) Z-R relationships for each month, each precipitation class, each instrument: (b) SSt (c) MSt

(d)

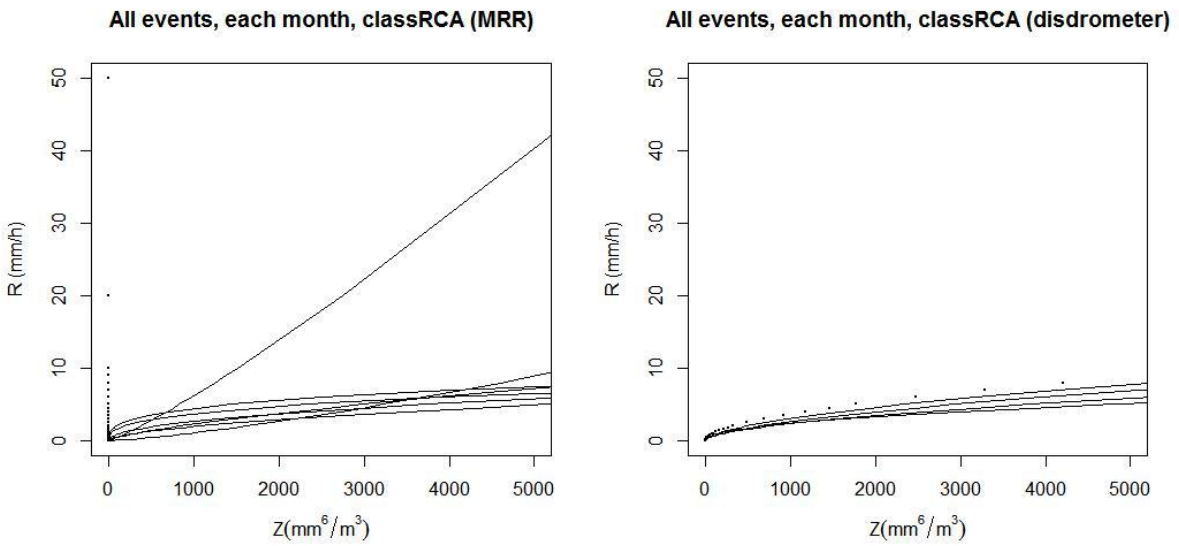

(e)

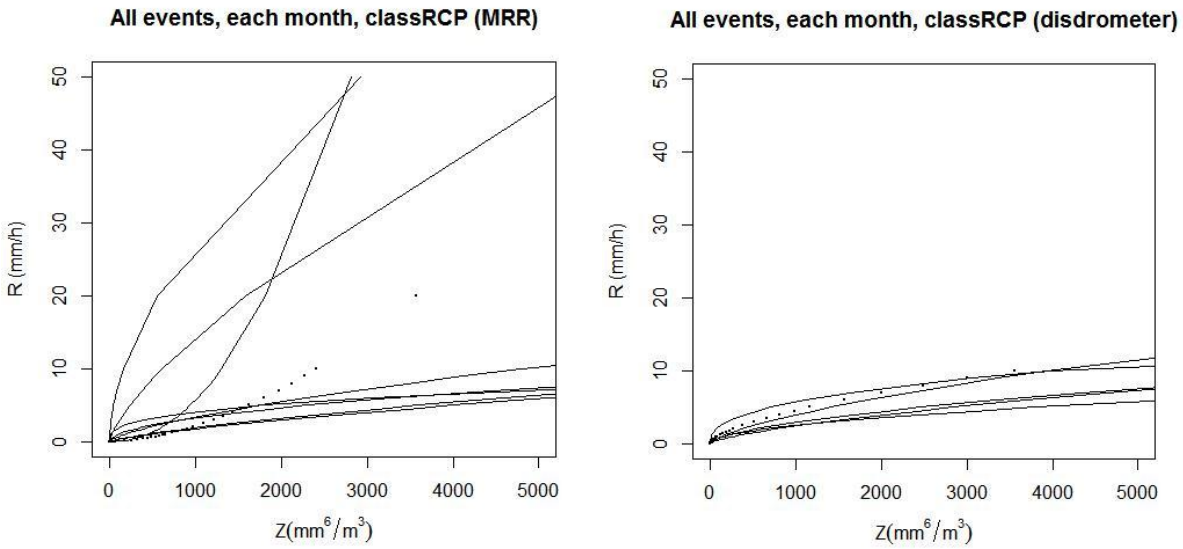

Figure 4.10 (continued) Z-R relationships for each month, each precipitation classes and each instrument: (d) RCA (e) RCP

4.3 Comparative analysis of precipitation measurement instruments

In order to compare the precipitation measurement of the three local instruments (MRR, OTT Parsivel and tipping bucket rain gauge), this sub-chapter presents:

1) cumulative plots of precipitation accumulations over a period of 30 minutes in function of the precipitation intensity (R) for the three instruments and for the whole time period and for each precipitation phase (sub sub-chapter 4.3.1)

2) 2D histograms comparing radar reflectivity (Z) and/or precipitation intensity (R) from the three instruments, compared by pairs: MRR vs Disdrometer, MRR vs rain gauge, Disdrometer vs rain gauge (sub sub-chapter 4.3.2).

4.3.1 Cumulative plots of precipitation accumulations

Figure 4.11 shows accumulations over 30-minute periods considering all available data, in function of precipitation intensity for the three instruments. Figure 4.12 presents the same cumulative plots for each precipitation class (rain, snow, mixed).

(a)

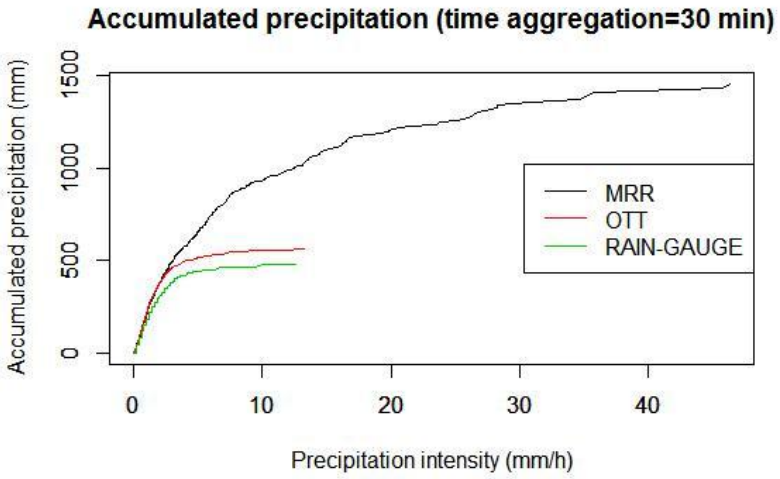

(b)

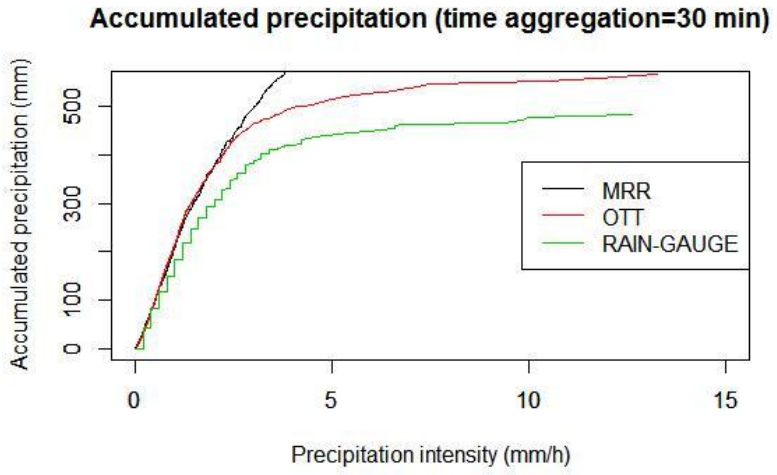

Figure 4.11 - Precipitation accumulations (30 minutes of time aggregation) vs precipitation intensity for MRR, Parsivel OTT and rain gauge (all data): (a) overview (b) at larger scale

(a)

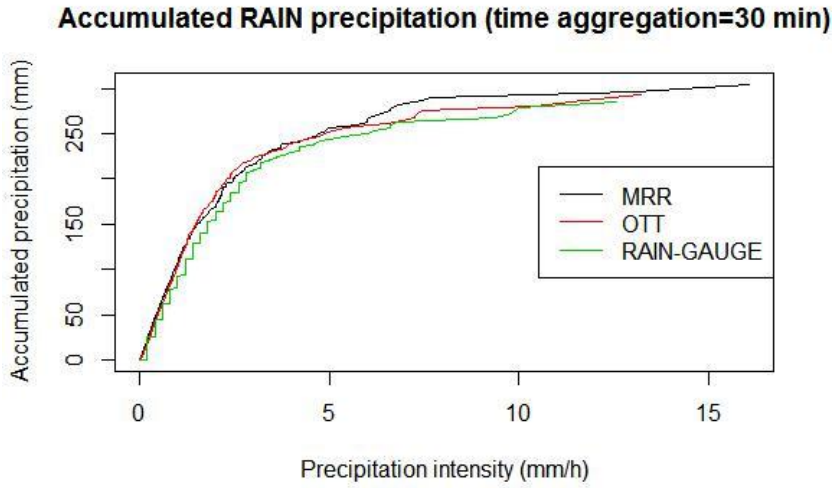

(b)

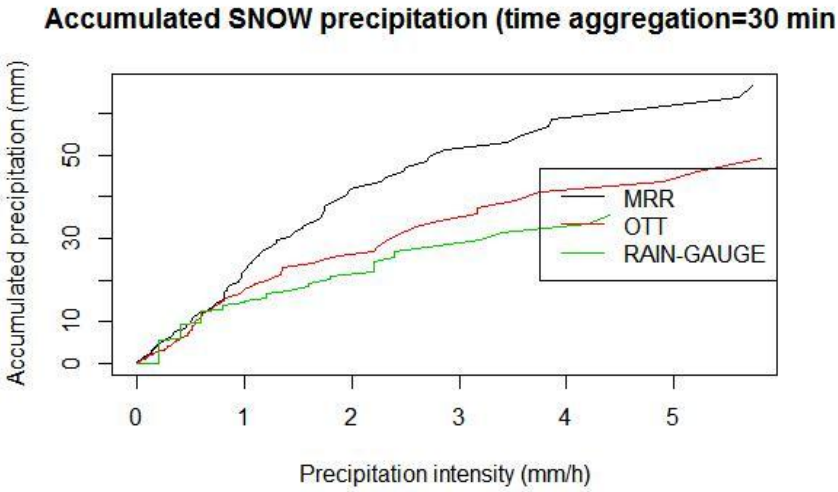

Figure 4.12 - Precipitation accumulations for each precipitation class (30 minutes of time aggregation) vs precipitation intensity for MRR, Parsivel OTT and rain gauge:
(a) rain (b) snow

(c)

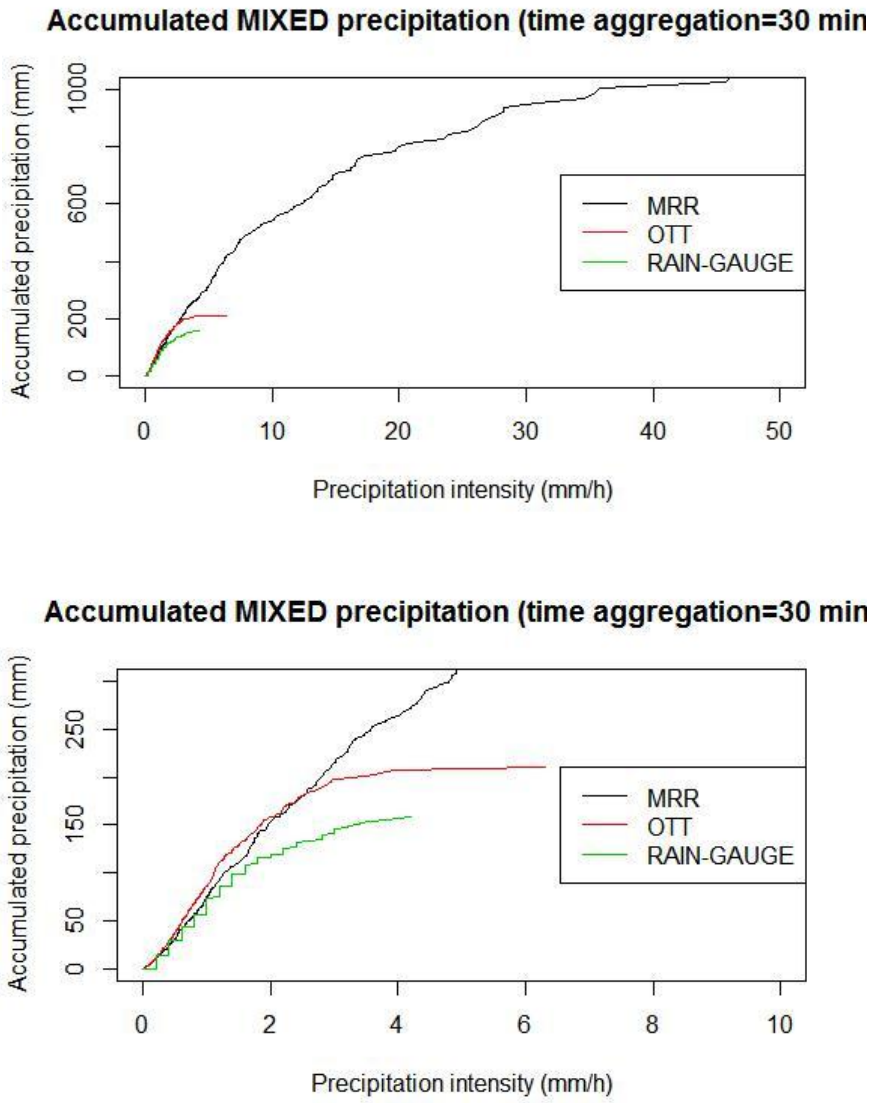

Figure 4.12 (continued) Precipitation accumulations for each precipitation class (30 minutes of time aggregation) vs precipitation intensity for MRR, Parsivel OTT and rain gauge: (c) mixed (overview and at larger scale)

4.3.2 2D histograms comparing accumulations, intensities and reflectivities

Figures 4.13 and 4.14 present compared 30-minute accumulations for each pair of instruments (MRR/OTT Parsivel, MRR/rain gauge and OTT Parsivel/rain gauge): considering all data (Figure 4.13) and for each precipitation class (Figure 4.14). Figure 4.15 compares intensity (R) and reflectivity (Z) values between the MRR and the disdrometer.

(a)

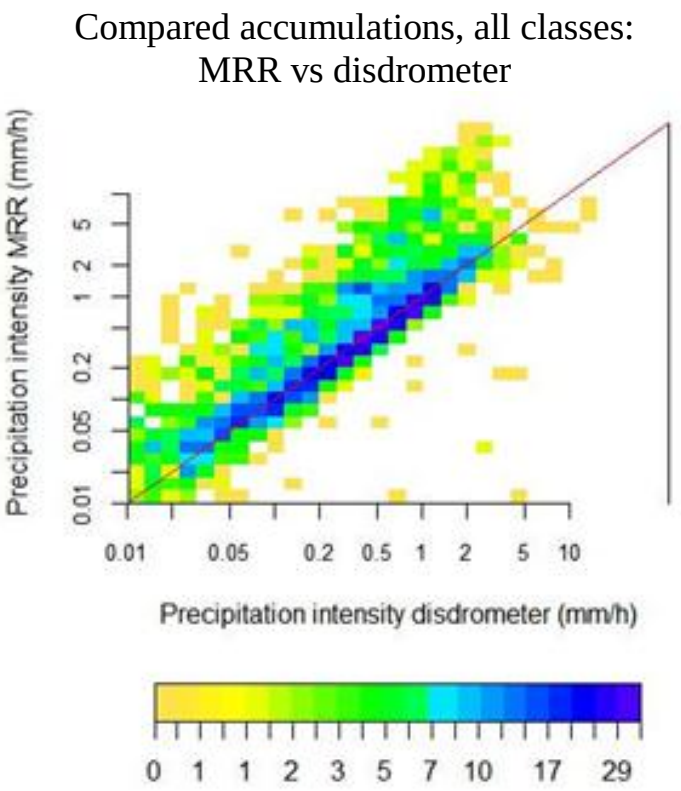

(b)

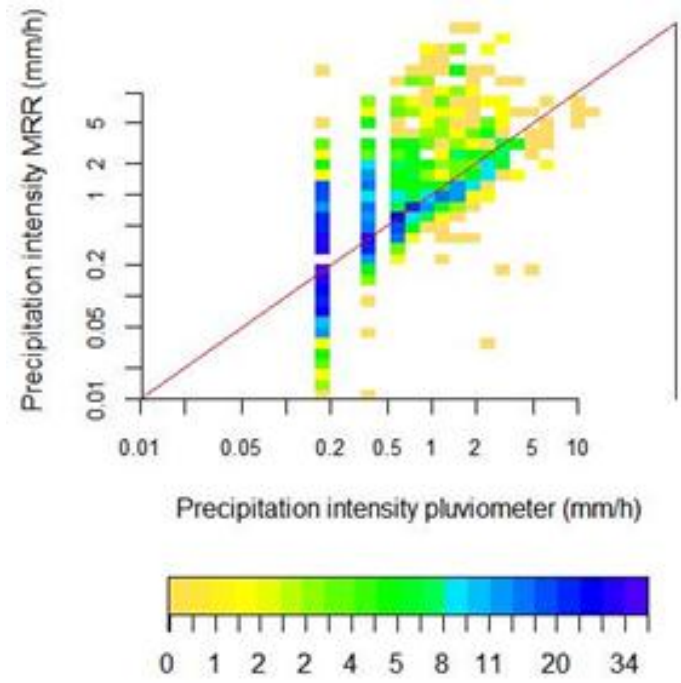

Figure 4.13 - Compared 30-minute accumulations, all classes
(a) MRR/OTT Parsivel (b) MRR/rain gauge

(c)

Compared accumulations, all classes:
disdrometer vs rain gauge

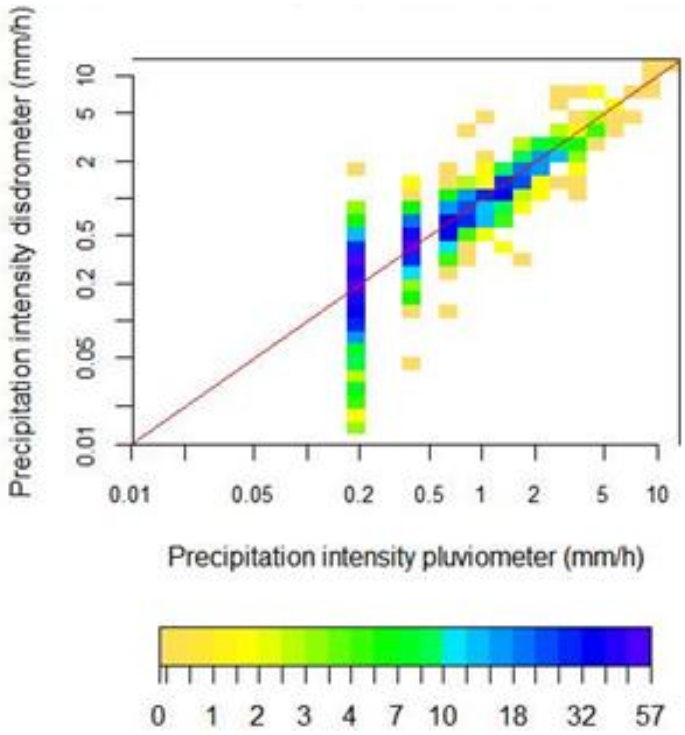

Figure 4.13 (continued) Compared 30-minute accumulations, all classes:
(c) OTT Parsivel/rain gauge

(a)

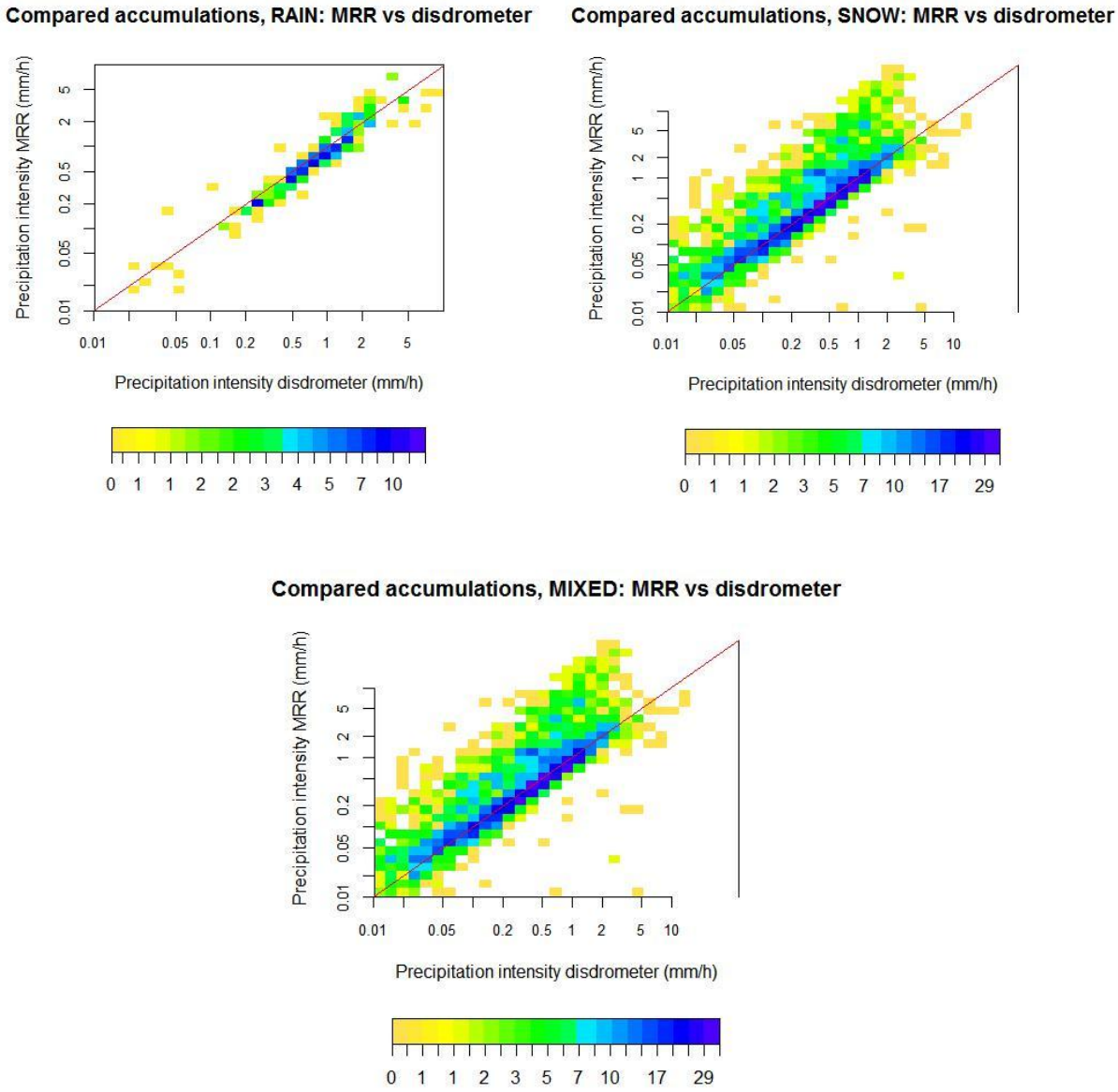

Figure 4.14 - Compared 30-minute accumulations, each class (rain, snow, mixed):
(a) MRR/OTT Parsivel

(b)

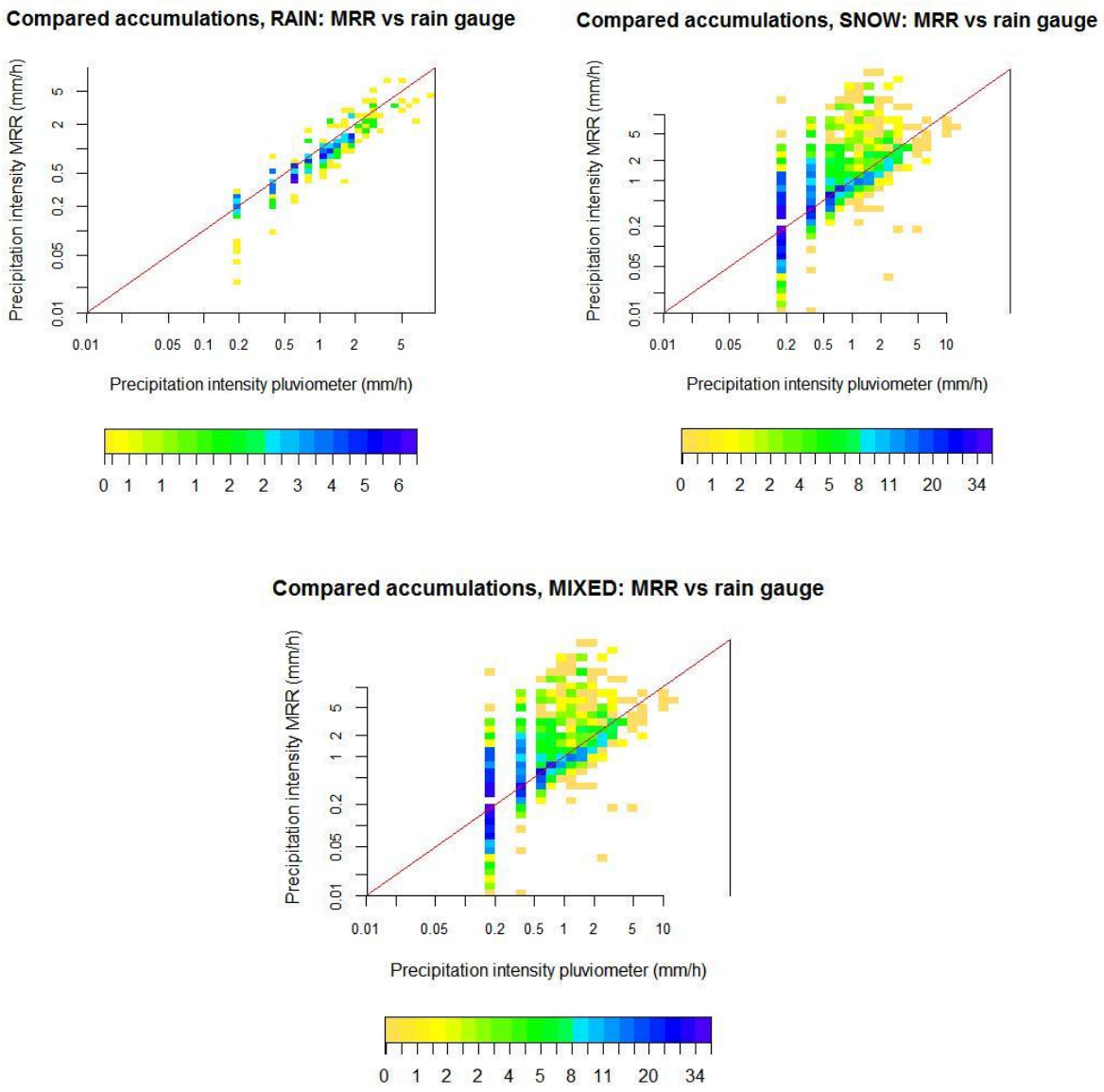

Figure 4.14 (continued) Compared 30-minute accumulations, each class (rain, snow, mixed): (b) MRR/rain gauge

(c)

Compared accumulations: disdrometer vs rain gauge

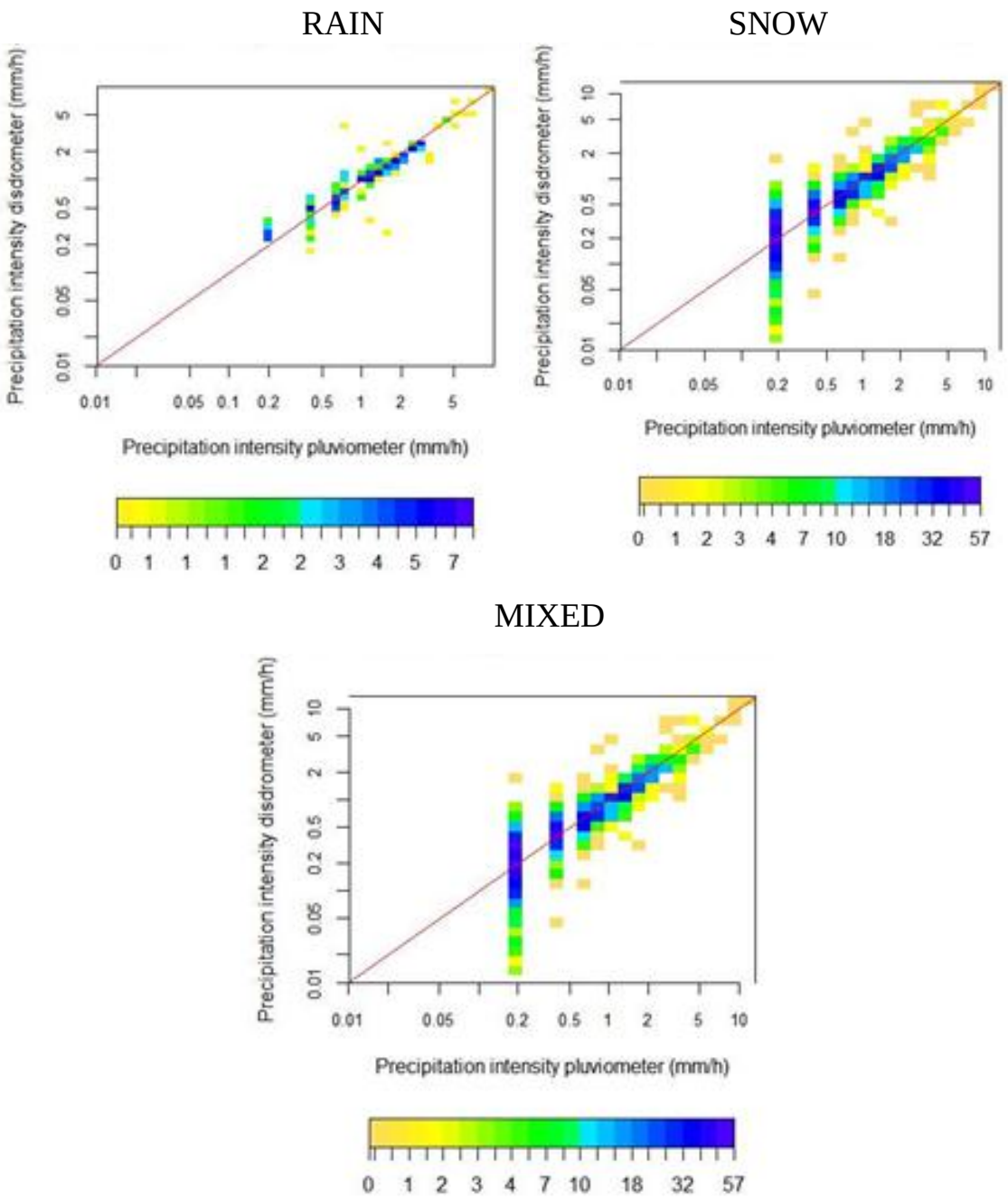

Figure 4.14 (continued) Compared 30-minute accumulations, each class (rain, snow, mixed): (c) OTT Parsivel/rain gauge

(a)

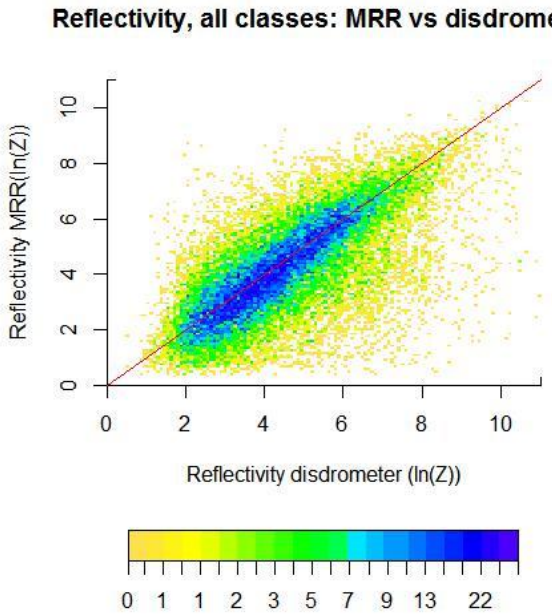

(b)

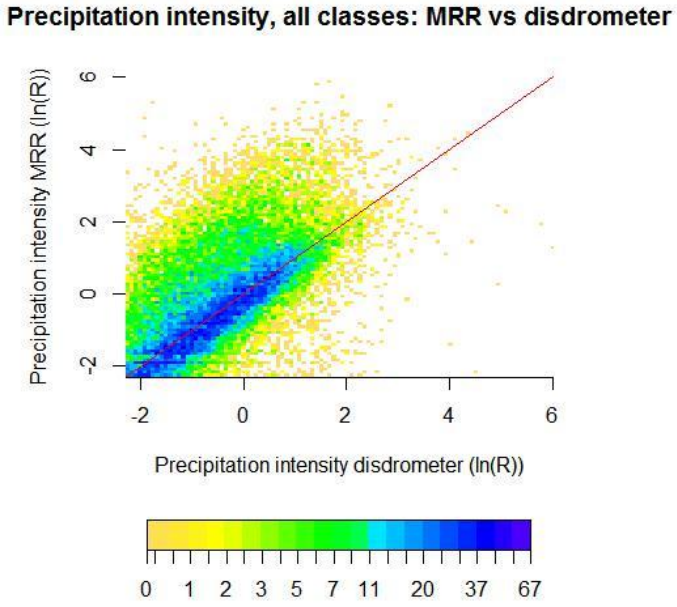

Figure 4.15 - Compared Z and R, all data, MRR vs OTT Parsivel:
(a) reflectivity (b) precipitation intensity

5 DISCUSSION

In this chapter, the estimated Z-R relationships derived from local DSD instruments, together with their variability, as presented in the previous chapter, are discussed and compared with the standard Z-R relationship ($Z=200R^{1,6}$). This comparison highlights the magnitude of the difference that is expected locally when using a fixed Z-R relationship on weather radar measurements performed at a certain distance of the local station. The discussion focuses on differences in Z-R parameters related to the precipitation type or class (sub sub-chapter 5.1.1), to the events (differences between and within the events, classified or not) (sub sub-chapter 5.1.2), to the month of the year (sub sub-chapter 5.1.3) and to the instrument they are derived from (MRR and OTT Parsivel) (sub sub-chapter 5.1.4). The sub sub-chapter 5.1.5 summarizes the estimation of Z-R relationships from DSD-measurement instruments and concludes on the capacity to identify clear, unique Z-R relationships from those instruments and on their reliability and stability in different precipitation conditions.

The sub-chapter 5.2 concerns the comparative analysis of quantitative precipitation (accumulations, intensities and reflectivities) derived from three types of local instruments (conventional rain gauge, disdrometer, vertical pointing radar). Differences related to the precipitation type or class (sub sub-chapter 5.2.1) and to the instrument (sub sub-chapter 5.2.2) are discussed based on the results presented in the chapter 4. The sub-chapter 5.3 summarizes the advantages and limitations of the different instruments and proposes some conditions or situations where those instruments should be efficiently used.

5.1 Z-R parameters

The Z-R relationship plots using all valid data available for each instrument (MRR and OTT Parsivel) (Figure 4.1) shows larger variations in Z and R values for MRR compared to OTT Parsivel. This high variability increases the uncertainty on the estimation of Z-R parameters from MRR, since the calculated Z-R curve does not have the best fit to the sampled data (relatively low correlation coefficient: 0,58). Table 4.2 shows the quantitative differences that

may occur between local instruments and weather radar (using the standard Z-R relationship). For example, for the same reflectivity value (Z), the estimated precipitation intensity (R) from MRR is constantly and significantly higher than the one estimated by the standard Z-R relationship, by a factor of 2 for low Z-values.

In case of the disdrometer, the estimated Z-R curve fits best to the sampling data and corresponds also better to the standard Z-R relationship than MRR. For the same reflectivity value (Z), the estimated precipitation intensity (R) from the disdrometer is either lower (for high Z-values) or higher (for low Z-values) than the standard estimated R, but the variation does not exceed 20 % (Table 4.2).

5.1.1 Class-related differences

When Z-R relationships are derived according to the different precipitation classes (based on storm type and precipitation phase), we see that the goodness-of-fit of the regression Z-R equation is significantly improved in case of MRR (r^2=0,87 and RMSE=0,59 for rain, r^2=0,96 and RMSE=0,48 for snow), compared to the Z-R equation derived from all available data (r^2=0,58 and RMSE=0,93). In case of the disdrometer, the Z-R relationships remains nearly the same with or without class filtering. However, there is one exception for the disdrometer: it was not possible to find valid Z-R relationships for mixed precipitation, both stratiform and convective (see Figure 4.2c where there are extremely high standard error values for both A and b parameters). This is due to insufficient number of valid data (both non-zero Z and R values) to make the calculation (only few points in the Z-R plot, Figure 4.2c).

The figures 4.2 (stratiform events) and 4.3 (convective events) show clearly that the Z-R parameters derived from MRR are precipitation phase-dependent (large differences in Z-R relationships for rain, mixed and snow). It also shows high variability in Z-R values for rain and mixed, when all events are considered. The best correlated Z-R curves derived from MRR (with lowest RMSE and highest r^2) concerns the snow events. When comparing to the disdrometer-derived Z-R curves, there is no such precipitation phase-dependency and high variability such as for MRR. In the only case of rain, the Z-R relationships derived from MRR and the disdrometer are similar. Since the disdrometer does not show the same precipitation

phase-dependency than MRR, there are significant differences in derived Z-R parameters for non-rain precipitation (mixed, snow) between the two instruments.

In terms of estimated precipitation intensity (R), MRR exceeds significantly the standard estimated R for snow and mixed precipitation (Table 4.3). MRR-estimated intensities are higher for snow by a factor of 3 for low Z-values and a factor of 75 for high Z-values. They are also higher for mixed precipitation by a factor of 2 for low Z-values and a factor of 6 for high Z-values. However, MRR-estimated R for rain correspond relatively well to those estimated from the standard Z-R relationship (does not exceed +33 % for low Z-values and -38 % for high Z-values).

OTT Parsivel estimates of rain and snow intensities correspond very well to those estimated from the standard Z-R relationship. In Table 4.3, we see that for snow, R estimates are 12 % higher for low Z-values and 35 % higher for high Z-values, while for rain, they are 16 % higher for low Z-values and 16 % lower for high Z-values).

Concerning the convective events (Figure 4.3), the Z-R parameters derived from MRR are not reliable since the correlation coefficients of the Z-R curves are much too low (<0,5), RMSE are high and the standard errors of the parameters are extremely high (mainly for the parameter A). In case of the disdrometer, the Z-R curves for convective events are better correlated with the sampled data than for MRR, but the Z-R parameters are quite unstable (standard errors of the parameters are also too high). This may be due to very short and very low number of convective periods detected in the two-years period.

Based on the disdrometer-derived Z-R parameters for convective events (Table 4.3), there is no clear variance associated to the storm type (no significant differences in R-estimates for rain stratiform and convective), but the number of convective events in this analysis is probably insufficient to compare with confidence to stratiform events. Nevertheless, Richards & Crozier (1983) concluded that the Z-R relationship variability cannot be explained by the storm type.

5.1.2 Event-related differences

The Z-R regression lines calculated for each event, no matter the precipitation class (Figure 4.4) show how much the Z-R relationships vary between events. There is a very high event-to-event variability in case of MRR, while the Z-R relationships derived from the disdrometer for the different events are more stable. However, with this large variation between events while the timesteps used for the Z-R relationship calculation do not necessarly cover the same time period for both instruments, the event-to-event comparison between the instruments is risky.

When looking at the different precipitation classes (Figure 4.5), it seems that this event-to-event variability in MRR-derived Z-R relationships is related to the precipitation phase. From a visual comparison between Figures 4.4 and 4.5 for MRR, we notice that all variability patterns for rain, snow and mixed precipitation (variability within the events, especially the stratiform events) contribute to the high Z-R relationship variability between events (when the precipitation phase is not considered). Highest Z-R parameter variability for MRR concerns the rain and mixed precipitations. Such as seen in the class-related differences (sub sub-chapter 5.1.1), MRR-derived Z-R parameters for snow precipitation are best defined (least variability compared with rain and mixed). This means that snow events, when measured by MRR, depend most on a local Z-R relationship. However, when there is so high variability within some events (mixed precipitation for example), it is difficult to compare the Z-R relationship variability between the different precipitation classes.

For convective events, Z-R parameters from MRR show higher stability than for stratiform events. Outliers in Z-R parameters for rain-convective events (RCA and RCP), visible in Figures 4.5d and 4.5e, are associated to very short events (N<=12) where few points with quite different R,Z values generate steep Z-R curves (many of those curves have parameter b < 1, confirmed in Figures 4.6e and 4.6f). Most of the extremely low A-values for both convective classes come from not reliable Z-R relationships (r^2 << 0,5 and extremely high SE(A) and SE(b)). However, as mentioned earlier, the number of convective events is too low to compare to stratiform events and to eventually conclude on the influence of the storm type in the derivation of Z-R parameters.

In case of the disdrometer, the estimated Z-R parameters for the different events are, here again, independent of the precipitation phase. However, it was not possible to generate Z-R parameters for mixed precipitation, probably due to the lack of available data from the disdrometer where both Z and R values are valid. We must remind here that only 6,6 % of the disdrometer timesteps during the whole two-years study period provides valid data. This is much less than for the MRR, but it results in more stable Z-R relationships both between and within the events.

From Figure 4.6 (A-b plots for both instruments), we notice that most outliers in A,b parameters are derived by MRR. Those events with extreme Z-R parameters cannot be compared to the same events captured by the two other instruments (tipping bucket rain gauge and optical disdrometer), since there are no valid data from those instruments for the corresponding time periods. However, when we look into the characteristics of those events (precipitation phase, ground temperature, number of timesteps in the calculation of Z-R parameters), we notice that many events with very high A and b values either have a very low number of timesteps ($N < 50$) or are mixed or rain precipitation with a ground temperature below 5 ^{0}C (near the threshold between rain and mixed). In case of events with very low b parameters ($b < 1$), they are characterized by low number of timesteps ($N < 50$) and/or snow or mixed precipitation. The high number of outliers in MRR-derived Z-R parameters increase the level of uncertainty around this instrument, which may sometimes fail to represent adequately the actual precipitation event.

We may compare the Z-R parameters derived by both instruments for two single events, one of the type rain-stratiform including air mass convection (the two classes are processed separately) and one of the type snow-stratiform. Z-R relationships are derived separately for each precipitation class in each of those two events. Figure 4.8 shows those event-related Z-R relationships with regression statistics (RMSE, r^2, standard errors of both parameters). The first event (# 638) occurs between October 6th, 2013 20:20 and October 7th, 2013 13:42 and consists of stratiform rain periods interspersed with six short air mass convection periods lasting from 2 to 27 minutes. The stratiform snow event (# 387) occurs on February 1st, 2013 between 01:42 and 12:32.

When comparing Z-R relationship plots (sampled point spreading) between the events of all types (Figure 4.1) and within these two events (Figure 4.8), it is clear that the event-to-event variability in case of MRR is significantly higher than within a specific type of event. When we look at the point spreading around the Z-R curves derived for all events of the same type (Figure 4.2), we notice also a higher variability between events of the same type than within those two events (Figure 4.8). This difference is most visible for the rain-stratiform events. In case of the disdrometer, the goodness-of-fit of Z-R curves are quite the same between events and within a specific event.

However, even if event-related Z-R curves (within events) fit better to the sampled data (higher r^2, lower RMSE) than Z-R curves derived for all events (between events), the standard errors of the Z-R parameters derived for each event are much higher. For example, we see the large difference between the MRR-derived A and b values for rain-stratiform events considering all events (A=186,1; b=1,844) and those within the event # 638 (A=280,6; b=1,699). We cannot generalize the results of the comparison of Z-R relationships and R estimates based only on those two events. To do so, we should compare, for many events, the estimates of precipitation rates using both the standard Z-R relationship and the Z-R relationship derived for each event separately. This project does not include this comparison of R-values done systematically for each event.

In terms of estimated precipitation intensities for those two events (Table 4.4), the difference between locally derived R estimates and R estimated by the standard Z-R relationship is quite similar when we consider all events or those two events (of type RSt, RCA and SSt). One exception is the disdrometer-derived R estimates for the rain stratiform event (# 638) which correspond much better to the standard R estimates within this specific event (lower difference percentages by a factor of 2) than generally between events.

As confirmed in the precipitation class analysis (sub sub-chapter 5.1.1), the disdrometer-derived Z-R parameters within those two specific events correspond very well to the standard Z-R relationship, especially for stratiform precipitation (rain or snow). In case of MRR, the R estimates for snow precipitation are significantly different than those from the weather radar

and are very high compared to rain intensities. Those differences that we notice here, within those two events, confirm the conclusions from the precipitation class analysis. One exception concerns the air mass convection periods in event # 638, where the disdrometer provides R estimates far away from the weather radar for very low and very high Z-values (high difference percentages). However, as mentioned earlier, it is difficult to conclude on the performance of Z-R parameters to estimate R in convective events, since very few data were processed for these air mass convection periods (in event # 638).

5.1.3 Season-related differences

Figure 4.9 shows that MRR is much more affected by seasonal Z-R variations (monthly Z-R curves) than the disdrometer. When the precipitation phase is taken into account (Figure 4.10), we notice that the seasonal variability in MRR-derived Z-R parameters is directly related to the precipitation type. Mixed precipitation generates the highest Z-R variability for MRR, while Z-R curves vary also in case of convective events. Such as confirmed in other types of analysis (class-related and event-related), the Z-R parameters from MRR are quite different for snow and for rain precipitation.

In case of the disdrometer, the constant low variability among precipitation classes and for all monthly data shows that this instrument is seasonal independent. This may mean that the detection and identification of precipitation particles and different phases encountered through a full year do not cause any measurement errors (or outliers) in case of the disdrometer, while the MRR shows some problems to detect and measure adequately the varying precipitation phases.

5.1.4 Event-related differences

Such as seen in the previous types of analysis (by precipitation class, event and month), the Z-R parameters are instrument-dependent. Almost all Z-R relationships derived from one instrument are quite different than those derived from the other, which lead to different locally estimated precipitation. The largest difference in Z-R parameters concern the snow

precipitation, where the estimated intensity is extremely high in case of MRR and follows the standard R estimation in case of OTT Parsivel. However, one exception remains: in case of stratiform rain precipitation, both instruments provides similar Z-R relationships. Actually, the standard Z-R relationship was originally defined by this type of precipitation. In order to convert indirect measurements (DSD, radar reflectivity) to precipitation values, the processing system of each of those instruments (weather radar, MRR, OTT Parsivel) is based on the assumption of liquid precipitation and precipitation statistics where stratiform rain is overrepresented (most common precipitation type). In order to better interpret snow and mixed precipitation, specific post-processing algorithms considering the low fall velocity (easily mixed with signal noise) and particular shape of snow particles should be included.

Generally, the disdrometer provides best correlated Z-R curves and lowest RMSE, independent of the season, the precipitation phase and storm type. However, the comparative analysis between the two instruments is not based on the exact same timesteps for both instruments. This requires us to be caution in making general statements on instrument-related differences. Nevertheless, by using all available valid data from each instrument in the calculation of Z-R parameters, we may presume that we have found the most representative Z-R relationship derived from each DSD instrument.

5.1.5 Can we obtain robus Z-R parameters?

Such as found in the event-related analysis (sub sub-chapter 5.1.2), Z-R parameters are highly variable between events, mainly for MRR and less for the disdrometer. When looking at the A-b and standard errors plots (Figures 4.6 and 4.7), it is clear that those parameters derived from MRR are highly variable for rain and mixed precipitation, as well as for convective storms. In case of the disdrometer, Z-R parameters are independent of the precipitation conditions (storm type, precipitation phase, season). Generally, the b-parameter shows lower variability (better stability) between and within events than the A-parameter.

Through the different analysis, we found that the variability of Z-R parameters are highly dependent on the instrument they are derived from. The optical disdrometer provides generally more stable Z-R parameters (same variability for any storm type, precipitation

phase and month of the year) than MRR. However, MRR shows a certain stability in its derived Z-R parameters for snow precipitation.

Based on those data processing and analysis, we cannot expect that MRR can derive robust and reliable Z-R parameters for the following reasons:

- high event-related and class-related variability in Z-R parameters derived from MRR, partly explained by the varying precipitation phase, other than rain,
- large difference between R estimates from MRR and both standard and disdrometer-derived R estimates,
- high standard errors on MRR-derived A,b parameters, especially for convective and mixed precipitation (many outliers in A-b values compared to the disdrometer).

However, only one of the 31 height ranges of MRR was used in the Z-R parameter calculation (4^{th} range gate, corresponding to 140 m height). We could have spatially aggregated Z and R values from few MRR height ranges near the ground (for example 3^{rd}, 4^{th} and 5^{th} range gates, corresponding to a height range of 105 m instead of the actual 35 m) in order to test if the derived Z-R parameters could have been different. Can the spatial aggregation of MRR height measurements, by its averaging effect, reduce the importance of outliers and produce more stable and reliable Z-R parameters?

In contrary to the MRR-derived parameters, the Parsivel-derived Z-R parameters show better constancy and reliability, no matter the type of storm, the precipitation phase (except for mixed precipitation where no valid Z-R relationship was found) and the month of the year. In addition, those Z-R parameters correspond well to the standard parameters used by the weather radar, as well as the precipitation intensity estimates derived from OTT Parsivel compared the standard R estimates. On the other hand, only a small part of the disdrometer measurement was valid, due to long periods of instrument instability or breakdown. In those conditions, the derived Z-R parameters may not represent adequately the actual instrument capabilities and limitations in different time periods and/or precipitation conditions. Even if the Z-R parameters derived by the disdrometer in this project seem more robust than the MRR-derived ones, we are not completely sure that they may remain robust in other station location, precipitation conditions and time periods. Such as for MRR, we could also have tested the temporal aggregation of the Parsivel measurements in the calculation of Z-R

parameters. For example, we could have converted the highest temporal resolution of Parsivel Z and R values (10 seconds) to the lowest resolution level of the MRR instrument (1 minute). Can this temporal aggregation of Parsivel measurement to the MRR resolution level reduce the differences between the two instruments in terms of Z-R parameter values and stability?

5.2 Precipitation observed by different instruments

In order to compare the precipitation measured by the three local instruments, comparative accumulated precipitation plots and comparative precipitation reflectivity and intensity plots are produced (Figures 4.11 to 4.15). Those comparisons are analyzed according to the instrument-related differences (sub sub-chapter 5.2.1) and precipitation class-related differences (sub sub-chapter 5.2.2). The advantages and limitations of those instruments are discussed in the sub sub-chapter 5.2.3, as well as proposals on conditions of use and possible combination of those instruments.

5.2.1 Instrument-related differences

From the comparative accumulated precipitation plot using all available data (Figure 4.11), it is clear that MRR measures significantly higher accumulations than other instruments. It also detects large range of precipitation intensities (R-values) compared with OTT Parsivel and the tipping bucket gauge. For the last two instruments, the measured accumulations concern event intensities lower than 12 mm/h, which do not necessarly mean that they cannot detect high precipitation intensities, since those high intensities from short convective events were averaged, hence smoothed, over 30 minutes (longer than many convective events). We are also uncertain about the validity of high precipitation intensities measured by MRR (many non-filtered outliers were found for this instrument).

The extremely high accumulated precipitation values from MRR include R outliers (very high R-values in stratiform periods where $Z < 40$ dBZ) that could not be filtered during the data processing (averaging precipitation intensities over a certain time). Those outliers may be due to the bright-band contamined measurement range (4^{th} height range), where the radar

backscattered signal received at the MRR contains false high reflectivity values (Z) that do not represent the actual ground precipitation. Very high precipitation accumulations from MRR are also probably due to significantly high MRR-derived intensities for snow and mixed precipitation (see the next sub sub-chapter for class-related differences).

In case of the disdrometer, it provides accumulations that correspond well with the conventional rain gauge. If we make the assumption that the rain gauge, by its direct precipitation measurements, represent best the "true" precipitation, this means that the disdrometer is more likely to provide "true" precipitation values and that MRR generally overestimate the precipitation accumulations.

Since cumulative plots of precipitation accumulations may compensate for under and overestimation of accumulations occuring at certain time periods, it may be interesting to look at 2D histograms of accumulations measured at the same time by each pair of instruments (Figure 4.13) and be more aware of small and significant variations in accumulation values from one or the other instrument. The figure 4.13 confirms the findings from cumulative plots using all available data:

- MRR shows constant high values of accumulations (most points are on the MRR side of the 1:1 red line) compared with the disdrometer and the rain gauge,
- The accumulations measured by the disdrometer correspond well to those measured by the rain gauge.

When comparing reflectivity and intensity values (Z, R) from MRR and the disdrometer (Figure 4.15), there is a slight higher variability and higher values of reflectivity for the disdrometer, but a clear tendency of higher intensity values for MRR. The slight higher Z-values of the disdrometer while MRR shows clear higher R-values may be explained by the presence of non-filtered MRR outliers (very high intensities with low reflectivity that cannot represent any convective event. Those very high R-values from MRR are not corroborated by other instruments. However, when we look into the characteristics of those timesteps with very high MRR intensities (precipitation phase, ground temperature), we notice that they occur when the bright band is present in the height measurement, such as identified in the event classification step, and when there is mixed or rain precipitation with a ground

temperature below 5 ^{0}C (near the threshold between rain and mixed). Since it is most likely to find precipitation intensity outliers in MRR measurement and that it influences significantly the estimated precipitation accumulations over time, it is recommanded to filter and correct MRR measurement, prior to any precipitation estimations, for bright band contamination and very low fall velocities for snow and mixed precipitation.

5.2.2 Class-related differences

As shown in Figure 4.12a, rain accumulations derived from the three instruments correspond well together and cover the same precipitation intensity range (R<15 mm/h). Rain events are the only types of precipitation where all three ground-based instruments show a good agreement in their measurement.

From Figures 4.12b, 4.12c, 4.14a and 4.14b, it is quite clear that high accumulation values from MRR, as seen in Figure 4.11, are mainly associated to mixed precipitation and snow. The mixed precipitation accumulation plot shows the increasing differences between the instruments from relatively low R-values. In case of snow, differences are significant between OTT Parsivel, rain gauge and MRR from R>1 mm/h. Again, MRR shows highest snow accumulations, compared to the two other instruments. Based on those large differences with MRR, we may question at this point the real ability and reliability of MRR to detect, identify and quantitatively represent with good accuracy the mixed and snow accumulations. Is MRR well calibrated for this type of precipitation? We note also that rain gauge measures lowest snow accumulations. This may be explained by the fact that the rain gauge is more likely affected by high snow precipitation losses due to wind-induced turbulence around the instrument and the fact that solid precipitation needs to be melted before it can be recorded (tipped), which delay the measurement (Savina et al., 2012). The snowfall (and mixed precipitation) intensities detected by all three instruments are relatively low compared to rainfalls.

Generally, OTT Parsivel and rain gauge correspond best in terms of quantitative accumulations for all precipitation phases (Figures 4.12 and 4.14c). Concerning the large

accumulation differences with MRR, we have already seen that this instrument is more likely to produce precipitation outliers and could require more filtering and corrections prior to the precipitation calculations.

5.3 Advantages and limitation of instruments

Even if MRR cover larger event intensity values (R) than the disdrometer and the rain gauge, it is uncertain if those MRR-measured R were affected or not by the bright-band or other sources of errors, such as signal attenuation. MRR is more likely to be affected by this latter error, which may contribute to precipitation loss or uncertainties/errors in data capture. The filtering of high R-values corresponding to stratiform events (predefined threshold applied to R-values from MRR, see sub-chapter 3.4) might minimize the impact of such types of error, but we should keep in mind that radar measurement from MRR is not corrected for all kind of atmospherical errors (attenuation, clutter, bright band) as it is done for the weather radar. On the other hand, the MRR instrument is less affected by the wind near the ground than other instruments since the measurement is performed at different height ranges. In this project, only one height range was used (4^{th} range gate equivalent to 140 m above ground). As proposed in the sub sub-chapter 5.1.5, if many height ranges nearest ground (for example 3rd, 4^{th}, 5^{th} gates) were taken into account and averaged to estimate the precipitation amount and rate, the resulting values (accumulations, intensity, reflectivity, Z-R parameters) could have been different.

Another challenge with the MRR is the difficulty to identify precisely the precipitation phase. In this project, the thresholding of temperature values at the gauge, confirmed by the disdrometer's precipitation identification sensor, was the only method used to determine the precipitation phase and classify the events. With large differences in precipitation measurement for snow and mixed (sleet), the calibration of MRR for those precipitation phase becomes important and can be evaluated and adjusted, if required.

From the precipitation accumulations derived from OTT Parsivel and the tipping bucket rain gauge, we found that these two instruments show little differences in all kind of precipitation

phase. The optical disdrometer like OTT Parsivel is a precipitation identification sensor which is less affected than the rain gauge by wind-induced turbulences (the laser sensors are protected by heated heads) or any obstacle for precipitation catching (losses by evaporation, splash, etc.) (Nemeth & Löffler-Mang, 2006; Messtechnik, O.T.T., 2009). However, the optical disdrometer may present some challenges, as reported by those authors (see chapter 2). It may misinterpret (under or overestimate) precipitation (especially for snow and particles with irregular shape) at very low or very high intensity, limitating the confident use of extreme R-values.

The conventional rain gauge has the advantage of direct precipitation measurement, avoiding uncertainties related to conversion and estimation process, and cover a long term time periods (necessary for historical precipitation studies). However the rain gauge-derived precipitation may be easier biased by catch deficit (light precipitation, short single event, snow precipitation with strong wind, etc.). Since the time interval for recording precipitation is unknown, the time aggregation for comparing accumulated precipitation for the three instrument must be set to 30 minutes, even if the other instruments have better time resolution in their data recording.

As confirmed by some authors (see chapter 2), the disdrometer is more and more used to calibrate weather radar precipitation measurements. Since OTT Parsivel shows similar precipitation estimates for most precipitation types to both rain gauge and weather radar estimates, this may confirm the capability of this instrument to compensate the conventional rain gauge for precipitation losses and limited time resolution and improve the ground precipitation estimates.

6 CONCLUSION

In order to improve radar precipitation estimation from the C-band weather radars, different Z-R relationships were estimated from co-located ground-based precipitation intruments (the vertical pointing radar MRR and the optical disdrometer OTT Parsivel) based on mesured drop size distributions (DSD). Z-R parameters derived from each instrument were then evaluated for their variability and reliability as well as their dependency to different precipitation characteristics and conditions (storm type, ground precipitation phase and season). Precipitation intensity estimated based on those locally defined Z-R relationships were finally compared to the precipitation estimates from the standard Z-R relationship used at the corresponding C-band weather radar station (Rissa) covering this local weather station (Risvollan).

Four types of Z-R parameters were estimated for each DSD instrument:

1) based on all available data (not classified),
2) based on classified events related to precipitation phase (rain, snow or mixed) and to storm types (stratiform or convective of two types: air mass convection within stratiform event and convective patches),
3) based on each event (not classified) and on each event of a certain type (classified according to precipitation phase and storm type)
4) based on each month of the year.

MRR provides the most variable and uncertain Z-R parameters that are highly dependent on the precipitation phase and the month of the year. This dependency leads to high event-to-event variability of those Z-R parameters. The uncertainty around MRR-derived Z-R parameters is mainly due to the large number of outliers in Z-R parameters, associated to mixed and snow precipitation.

MRR-derived precipitation intensity estimates are constantly and significantly higher than those estimated by the standard Z-R relationship. Mixed precipitation shows the highest variability and uncertainties in terms of precipitation estimates, while snowfall intensities

exceed significantly (at maximum, by a factor of 75) the estimated intensities derived from the C-band weather radar. This precipitation phase dependency of MRR measurement explains also the high seasonal variability of estimated Z-R parameters.

The disdrometer provides the most stable and reliable Z-R parameters that are independent of the precipitation phase and the season. In contrary to MRR, there is no significant event-related variability in those Z-R parameters derived from OTT Parsivel. Z-R parameters derived from OTT Parsivel are much different in terms of variability and robustness than those from MRR. In the only case of rain events, the Z-R relationships estimated by both instruments are similar and provides similar precipitation estimates (until 38 % of differences for MRR and until 16% for OTT Parsivel), but for other types of precipitation the differences may be significant. Both the disdrometer-derived Z-R parameters and resulting precipitation estimates correspond very well to the standard Z-R relationship and precipitation estimates from the weather radar.

For any of those two instruments, there is no evident dependency of derived Z-R parameters on storm type. However, since the number of convective events was actually very low compared to stratiform events, more investigations and analysis are required to confirm or infirm this latter statement. Nonetheless, the important instrument-related differences in terms of Z-R parameters and precipitation estimates for any precipitation other than rain may influence the choice of precipitation DSD instrument that has the capability (and reliability) to validate locally the Z-R relationship. However, the disdrometer located at Risvollan was only able to provide slighlty more than 6 % of valid data during the whole two-year time period of this study.

In order to assess under which conditions the precipitation measurements from the tipping-bucket rain gauge and the local Z-R relationships determined by the MRR and OTT Parsivel instruments are reliable, a comparative analysis of quantitative precipitation values (accumulations, intensities and reflectivities) derived from the three local instruments at the same timesteps was performed. Differences associated to the instrument in use and to the precipitation type (rain, snow, mixed) were analyzed. From this, the following statements came up:

- MRR provides significantly higher precipitation values (accumulations and precipitation intensities) for snow and mixed events than those derived from the two other instruments (disdrometer and rain gauge).
- OTT Parsivel and the tipping bucket rain gauge provide relatively similar precipitation accumulations for any type of precipitation. However, the rain gauge provides the lowest snow accumulations.
- In case of rain events, the three instruments provide similar precipitation accumulations.
- Knowing that MRR radar measurements are not systematically corrected for significant atmospherical errors (signal attenuation, bright band contamination), in contrary to the weather radar station, that many outliers in precipitation intensities found during the comparative analysis originated from MRR, that MRR cannot identify clearly the precipitation phase of the measured particles and that there are large differences in precipitation values compared to the two other instruments, there remains some uncertainties around precipitation accumulations derived from MRR.
- OTT Parsivel shows robust Z-R relationships and precipitation accumulations for any type of precipitation, even if there remains some differences with the rain gauge for snow accumulations. The low number of valid data from this instrument in the two-years period of time, the representativity of those results in all precipitation conditions and time of the year is questioned. Concerning the optical disdrometer, we should also remind from the literature that the snow and precipitation particles with irregular shape can be misinterpreted at very low and very high precipitation intensity, which may lead to under and overestimation of the actual precipitation.

Due to the short periods of convective precipitation and relatively long aggregation time (30 minutes) for comparing the three instruments, it was not possible to conclude on the instrument performance in case of high-intensity events. A larger number of convective events (over a longer period than two years or with a different definition and detecting method of convective events within the time period) should have contributed to better comparison between stratiform and convective events.

Also, different data processing could have been undertaken in this project in order to systematically detect and evaluate the signification of outliers in MRR precipitation values (and eventually remove those that do not represent realistic measurements) and to compare better the different instruments by adjusting/smoothing the temporal and/or spatial scale representation of the various precipitation measurements. Among those additional data processing, there are

1) the spatial aggregation of MRR measurements over more than one height ranges (for example 3rd, 4th and 5th range gates)
2) the temporal aggregation of the disdrometer measurements to smooth the original 10-sec temporal measurement spacing to 1-min (corresponding to the temporal resolution of the MRR)
3) the selection of events and timesteps where both instruments (MRR, disdrometer) have valid Z,R measurements (for instrument-related comparison)
4) a more strict condition (for example, higher temperature threshold) to define rain events in order to exclude uncertainties about the presence of mixed precipitation
5) the detection (and eventual exclusion) of mismatched precipitation data in time series of the different instruments and the comparison with large differences found in precipitation estimates and Z-R parameters between the instruments
6) a different method to define and identify the timing and type of event in order to exclude very long events that include many sub-events of different types and start/end timesteps that were just estimated due to missing data or too long time interval between the C-band radar images
7) the verification of wind conditions at the timesteps where large differences in precipitation estimates and outliers are found

Those additional data processing could confirm or infirm the large variability in Z-R parameters estimated by MRR as well as the large differences in precipitation estimated by MRR compared to those obtained by the two other instruments. It can also confirm or infirm, despite the low number of valid data from the disdrometer, the good agreement of the OTT Parsivel-derived Z-R parameters and precipitation values to the standard Z-R relationship and estimated precipitation from both the weather radar using the standard Z-R relationship and the conventional rain gauge.

Based on the previous statements, we should be prudent in our recommandations concerning the use and/or exclusion of one or many of those local instruments for the estimation of precipitation. However, since the optical disdrometer OTT Parsivel provides relatively robust Z-R relationships for both rain and snow precipitation (it could not be confirmed for mixed precipitation) and agree relatively well with the conventional rain gauge and precipitation estimates from the weather radar, it may be used both to compensate for precipitation losses, catch deficit and low temporal resolution of the conventional rain gauge and to provide local Z-R relationships that may validate the precipitation estimates from the weather radar (in case of snow and rain). Since we did not obtain satisfying Z-R relationships from the disdrometer for mixed precipitation events and the disdrometer instability and down periods did not provide sufficient valid data, the complete replacement of the rain gauge by OTT Parsivel is not considered or recommanded at this stage of the analysis. Also, the actual low performance of MRR in providing robust Z-R relationships (without including outliers) for precipitation other than rain and in estimating precipitation accumulations that correspond well with the other ground-based instruments can not lead to a total exclusion of this instrument. More investigations and analysis is required in addition to some MRR-measurement filtering and correction in order to try to reduce the uncertainties around the Z-R parameters and precipitation estimates derived from this instrument.

7 REFERENCES

Battaglia, A., Rustemeier, E., Tokay, A., Blahak, U., & Simmer, C. (2010). PARSIVEL Snow Observations: A Critical Assessment. *Journal of Atmospheric & Oceanic Technology, 27*(2).

Chandrasekar, V., & Cifelli, R. (2012). Concepts and principles of rainfall estimation from radar: Multi sensor environment and data fusion. *Indian J. Radio & Space Phys, 41*, 389-402.

Dutta, D., Sharma, S., Kannan, B. A. M., Venketswarlu, S., Gairola, R. M., Rao, T. N., & Viswanathan, G. (2012). Sensitivity of ZR relations and spatial variability of error in a Doppler Weather Radar measured rain intensity. *Indian Journal of Radio & Space Physics, 41*, 448-460.

Duvernoy, J., & Gaumet, J. L. (1996). Precipitating hydrometeor characterization by a CW Doppler Radar. *Journal of Atmospheric and Oceanic Technology*, *13*(3), 620-629.

Elo, C.A. (2012). *Correcting and quantifying radar data*. met.no report 2/2012, met.no, January 2012.

Gage, K. S., Williams, C. R., Johnston, P. E., Ecklund, W. L., Cifelli, R., Tokay, A., & Carter, D. A. (2000). Doppler radar profilers as calibration tools for scanning radars. *Journal of Applied Meteorology*, *39*(12), 2209-2222.

Germann, U., Galli, G., Boscacci, M., & Bolliger, M. (2006). Radar precipitation measurement in a mountainous region. *Quarterly Journal of the Royal Meteorological Society*, *132*(618), 1669-1692.

Gjertsen, U., Salek, M., & Michelson, D. B. (2003). Gauge-adjustment of radar-based precipitation estimates–a review. *COST-717 working document No. WDD, 2*(200310), 1.

Holleman, I (2006). *Bias adjustment of radar-based 3-hour precipitation accumulations*. Technical Report, KNMI TR-290, 2006

Huang, G. J., Bringi, V. N., Cifelli, R., Hudak, D., & Petersen, W. A. (2010). A Methodology to Derive Radar Reflectivity–Liquid Equivalent Snow Rate Relations Using C-Band Radar and a 2D Video Disdrometer. *Journal of Atmospheric & Oceanic Technology*, *27*(4).

Huang, L., Salles, C., Tournoud, M. G., Yin, C., Carreau, J., Rodier, C., & Huang, L. (2012) Uncertainties in radar rainfall fields due to the ZR relationships adjustment schemes. *ERAD 2012 – The 7th European Conference on Radar in Meteorology and Hydrology*

Jameson, A. R., & Kostinski, A. B. (2001). What is a raindrop size distribution?. *Bulletin of the American Meteorological Society*, *82*(6), 1169-1177.

Killingtveit, Å. (1976). *En studie av vannbalansen I Sagelva hydrologiske forskningsfelt*. Series Licentiatavhandling, 432, NTNU, 279 p.

Kneifel, S., Maahn, M., Peters, G., & Simmer, C. (2011). Observation of snowfall with a low-power FM-CW K-band radar (Micro Rain Radar). *Meteorology and Atmospheric Physics*, *113*(1-2), 75-87.

Löffler-Mang, M., & Blahak, U. (2001). Estimation of the equivalent radar reflectivity factor from measured snow size spectra. *Journal of Applied Meteorology*, *40*(4), 843-849.

Löffler-Mang, M., & Joss, J. (2000). An optical disdrometer for measuring size and velocity of hydrometeors. *Journal of Atmospheric & Oceanic Technology*, *17*(2).

Löffler-Mang, M., Kunz, M., & Schmid, W. (1999). On the performance of a low-cost K-band Doppler radar for quantitative rain measurements. *Journal of Atmospheric and Oceanic Technology*, *16*(3), 379-387.

Maahn, M., & Kollias, P. (2012). Improved Micro Rain Radar snow measurements using Doppler spectra post-processing. *Atmospheric Measurement Techniques Discussions*, *5*(4), 4771-4808.

Messtechnik, O. T. T. (2009). Operating instructions: Present Weather Sensor–Parsivel.

Nemeth, K., & Löffler-Mang, M. (2006). OTT-parsivel–enhanced precipitation identifier and new generation of present weather sensor. In *4th ICEAWS Conference, Lisboa, 8p*.

Norwegian Meteorological Institute and Norwegian Broadcasting Corporation, *Weather radar* [online], available at http://www.yr.no/radar/ [consulted on May 27th 2014].

Peters, G., Fischer, B., Münster, H., Clemens, M., & Wagner, A. (2005). Profiles of raindrop size distributions as retrieved by microrain radars. *Journal of Applied Meteorology*, *44*(12).

Peters, G., Fischer, B., & Andersson, T. (2002). Rain observations with a vertically looking Micro Rain Radar (MRR). *Boreal environment research*, *7*(4), 353-362.

Peters, O., Hertlein, C., & Christensen, K. (2001). A complexity view of rainfall. *Physical review letters*, *88*(1), 018701.

Piccolo, F., Chirico, G. B., & Ferraris, L. (2005). Sampling errors in rainfall measurements by weather radar. *Advances in Geosciences*, *2*.

Richards, W. G., & Crozier, C. L. (1983). Precipitation measurement with a C-band weather radar in southern Ontario. *Atmosphere-Ocean*, *21*(2), 125-137.

Saltikoff, E., Gjertsen, U., Michelson, D., Holleman, I., Seltmann, J., Odakivi, K., ... & Haase, G. (2004). Radar data quality issues in Northern Europe. *ERAD Publication Series*, *2*, 212-215.

Sánchez-Diezma, R., Sempere-Torres, D., Creutin, J. D., Zawadzki, I., & Delrieu, G. (2001). Factors affecting the precision of radar measurement of rain. In *An assesment from a hydrological perspective. 30th Int. Conf. on Radar Meteor., Munich (Germany)* (pp. 573-575).

Savina, M., Schäppi, B., Molnar, P., Burlando, P., & Sevruk, B. (2012). Comparison of a tipping-bucket and electronic weighing precipitation gage for snowfall. *Atmospheric Research*, *103*, 45-51.

Smith, P. L. (1984). Equivalent radar reflectivity factors for snow and ice particles. *Journal of Climate and Applied Meteorology*, *23*(8), 1258-1260.

Steiner, M., Houze Jr, R. A., & Yuter, S. E. (1995). Climatological characterization of three-dimensional storm structure from operational radar and rain gauge data. *Journal of Applied Meteorology*, *34*(9), 1978-2007.

Thurai, M., Petersen, W. A., Tokay, A., Schultz, C., & Gatlin, P. (2011). Drop size distribution comparisons between Parsivel and 2-D video disdrometers. *Advances in Geosciences*, *30*.

Ulbrich, C. W., & Miller, N. E. (2001). Experimental Test of the Effects of Z–R Law Variations on Comparison of WSR-88D Rainfall Amounts with Surface Rain Gauge and Disdrometer Data. *Weather & Forecasting*, *16*(3).

Ulbrich, C. W., & Lee, L. G. (1999). Rainfall Measurement Error by WSR-88D Radars due to Variations in Z--R Law Parameters and the Radar Constant. *Journal of Atmospheric & Oceanic Technology*, *16*(8).

Vieux, B.E. (2013) Radar Rainfall Applications in Hydrology. Chapter 11 in: Bedient, P.B., Huber, W.C. & Vieux, B.E., *Hydrology and Floodplain Analysis*. Harlow, Pearson Education Limited, 5th Edition, p. 657-702.

Vieux, B. E., & Bedient, P. B. (1998). Estimation of rainfall for flood prediction from WSR-88D reflectivity: A case study, 17-18 October 1994. *Weather & Forecasting*, *13*(2).

Williams, C. R., Gage, K. S., Clark, W., & Kucera, P. (2005). Monitoring the reflectivity calibration of a scanning radar using a profiling radar and a disdrometer. *Journal of Atmospheric & Oceanic Technology*, *22*(7).